

TABLE OF CONTENTS

Volume 1, Number 2, September 2009

Direct real-time PCR examination for <i>Mycobacterium tuberculosis</i> in respiratory samples can be cost effective	
B. J. Renton, P. D. Morrell, R. P. D. Cooke, P. D. O. Davies.....	63
Electrospun nanofiber-based drug delivery systems	
D. G. Yu, M. Z. Li, K. White, C. Branford-White.....	67
An ion-based chromogenic method of detecting for inorganic phosphate in serum and milk	
C. X. Yin, J. Su, F. J. Huo, P. Yang.....	76
Serum homocysteine concentrations of Chinese intellectuals and the influential factors concerned	
Y. Hou, Y. Y. Cheng, Y. Hong, W. Q. Chen, D. L. Wang.....	83
A comparison study of two breathing exercise techniques in tetraplegics	
S. J. Winsler, J. George, P. Stanley, G. Tharion.....	88
Evaluation of the inclusive payment system based on the diagnosis procedure combination with respect to cataract operations in Japan —A comparison of lengths of hospital stay and medical payments among hospitals	
K. Nawata, M. Ii, H. Toyama, T. Takahashi.....	93
Ceruloplasmin levels in human sera from various diseases and their correlation with patient's age and gender	
V. Lopez-Avila, W. H. Robinson, K. Lokits.....	104
Non-invasive foetal heartbeat rate extraction from an underdetermined single signal	
R. Acharyya, N. L. Scott, P. D. Teal.....	111
Comparison between static and dynamic warm-up exercise regimes on lower limb muscle power	
J. Shelton, G. V. P. Kumar.....	117
Pattern recognition of surface electromyography signal based on wavelet coefficient entropy	
X. Hu, Y. Gao, W. X. Liu.....	121

HEALTH

Journal Information

SUBSCRIPTIONS

The *HEALTH* (Online at Scientific Research Publishing, www.SciRP.org) is published quarterly by Scientific Research Publishing, Inc., USA.

E-mail: service@scirp.org

Subscription rates: Volume 1 2009

Print: \$50 per copy.

Electronic: free, available on www.SciRP.org.

To subscribe, please contact Journals Subscriptions Department, E-mail: service@scirp.org

Sample copies: If you are interested in subscribing, you may obtain a free sample copy by contacting Scientific Research Publishing, Inc at the above address.

SERVICES

Advertisements

Advertisement Sales Department, E-mail: service@scirp.org

Reprints (minimum quantity 100 copies)

Reprints Co-ordinator, Scientific Research Publishing, Inc., USA.

E-mail: service@scirp.org

COPYRIGHT

Copyright© 2009 Scientific Research Publishing, Inc.

All Rights Reserved. No part of this publication may be reproduced, stored in a retrieval system, or transmitted, in any form or by any means, electronic, mechanical, photocopying, recording, scanning or otherwise, except as described below, without the permission in writing of the Publisher.

Copying of articles is not permitted except for personal and internal use, to the extent permitted by national copyright law, or under the terms of a license issued by the national Reproduction Rights Organization.

Requests for permission for other kinds of copying, such as copying for general distribution, for advertising or promotional purposes, for creating new collective works or for resale, and other enquiries should be addressed to the Publisher.

Statements and opinions expressed in the articles and communications are those of the individual contributors and not the statements and opinion of Scientific Research Publishing, Inc. We assumes no responsibility or liability for any damage or injury to persons or property arising out of the use of any materials, instructions, methods or ideas contained herein. We expressly disclaim any implied warranties of merchantability or fitness for a particular purpose. If expert assistance is required, the services of a competent professional person should be sought.

PRODUCTION INFORMATION

For manuscripts that have been accepted for publication, please contact:

E-mail: health@scirp.org

Direct real-time PCR examination for *Mycobacterium tuberculosis* in respiratory samples can be cost effective

Bryan Joseph Renton¹, Patricia Denise Morrell², Richard Peter Davidson Cooke², Peter David Owen Davies¹

¹Department of Respiratory Medicine, University Hospital Aintree, Liverpool; Correspondence author: bjrenton@doctors.net.uk

²Department of Clinical Microbiology, University Hospital Aintree, Liverpool

Received 5 June 2009; revised 15 July 2009; accepted 18 July 2009.

ABSTRACT

Aim: To assess whether the use of direct real-time polymerase chain reaction (PCR) on smear-positive sputa can be cost-effective, by speciating mycobacteria earlier than current methods and thereby preventing unnecessary screening tests as part of the contact tracing process.

Methods: A retrospective study of all patients with smear-positive sputa in a Liverpool teaching hospital between 2004 and 2007. All the PCRs performed on these patients were reviewed and compared them with their mycobacterial culture results. Unit costs for PCR, chest X-ray (CXR), tuberculin skin test (TST), interferon-gamma (IFN- γ) and medical/nursing time were conservatively estimated at £50, £11, £10, £40 and £30 respectively. The total PCR costs were compared with the costs of unnecessary follow up of patients, negative for *Mycobacterium tuberculosis* (MTB) by PCR, subsequently confirmed to be MTB culture negative.

Results: 203 smear-positive patients underwent direct PCR testing. 126 (62%) patients grew *Mycobacterium tuberculosis* (MTB), 74 (37%) had environmental mycobacterial infection (EMI) and 3 (1%) were culture negative. Of the 126 patients' culture positive MTB patients, 123 were PCR positive and 3 PCR negative. Of the 77 patients that were culture negative for MTB, 75 were PCR negative and 2 PCR positive. The sensitivity, specificity, positive and negative predictive values for direct PCR versus MTB culture were 98%, 96%, 98% and 97% respectively. Total costs of all PCRs performed amounted to £10,150. The cost of contact procedures for PCR-negative and MTB culture-negative index cases was estimated at £19,650. This equated to a total saving of £9,500 in con-

tact tracing costs.

Conclusions: Direct PCR examination testing of smear-positive patients can be cost-effective in areas where there is a high incidence of EMI.

Keywords: Tuberculosis; PCR and Cost Effective

1. INTRODUCTION

Current national guidelines for diagnosing active pulmonary tuberculosis (TB) recommends performing a posterior-anterior chest X-ray (CXR) and obtaining at least 3 sputum samples (with one early morning sample), which are then sent for TB microscopy and culture. [1] These sputum smears are initially stained for acid-fast bacilli (AFB), but as *Mycobacterium tuberculosis* (MTB) and environmental mycobacteria have a similar microscopic appearance, it is not possible to differentiate between them at this stage. Mycobacterial culture and subsequent speciation is therefore required but is often not available until several weeks after specimen collection.

In patients suspected of active TB, which is usually based on a smear-positive sputum or bronchoalveolar lavage (BAL), a contact tracing process is initiated early to prevent potential further spread. Screening is usually offered to household and other close contacts. Typically, most contacts will have a chest X-ray and a tuberculin skin test (TST), with a significant proportion of contacts also going on to have an interferon-gamma (IFN- γ) test. However, in areas where there is a high incidence of environmental mycobacterial infection (EMI), this can result in a large proportion of contacts being unnecessarily screened. Indeed, in the study carried out by Corless *et al.*, 51% of smear positive patients did not have TB. This resulted in 31% of contacts of patients being screened who either cultured environmental organisms, or had negative cultures. The median number of contacts traced per index case was 11 for patients culturing MTB and 4 for patients culturing environmental organisms or with negative cultures. This report highlighted the cur-

rent inefficiencies that exist in the contact tracing procedures. The authors felt that there are clear grounds for using rapid tests to identify and type mycobacteria more quickly than current solid or liquid media methods; thereby avoiding extra unnecessary screening costs. [2] This would certainly seem to be applicable to areas with a high incidence of lung disease caused by EMI, but unfortunately there still remains no published national database on this topic. However, a further review of mycobacterial isolates cultured from respiratory samples in Merseyside 2000 – 2008 has again confirmed the high proportion (approximately 50%) of smear positive sputum that yield environmental mycobacteria.

Polymerase chain reaction (PCR) allows for more rapid identification of MTB, but is not routinely recommended, principally due to cost implications. Current national guidance advises its use only if rapid confirmation of a TB diagnosis in a sputum smear-positive person would alter their care (e.g. exclusion of non-tuberculosis mycobacteria in immunocompromised patients), or before conducting a large contact tracing initiative (e.g. in a school or hospital). [3] In this study, we aimed to assess whether the use of direct PCR on smear-positive sputa can be cost-effective, by speciating mycobacteria earlier than current methods, and therefore preventing unnecessary screening tests as part of the contact tracing process.

2. MATERIALS AND METHODS

This retrospective study was carried out at a large teaching hospital in Liverpool (University Hospital Aintree). All AFB smear-positive respiratory specimens underwent direct PCR testing for MTB and *Mycobacterium avium-intracellulare complex*. PCR testing on smear-positive sputa has been routine practice in this hospital for the last 4 years, initially on a weekly basis, and due to increasing clinical demand, is now performed twice-weekly. On receiving the smear-positive sample, the average time to issue a PCR result is between 48-72 hours. Once this result is available, the responsible clinician is notified immediately.

All the direct PCRs performed on patients with smear-positive sputa between 2004 and 2007 were reviewed and compared with their mycobacterial culture results.

A real-time PCR assay (Real Art™ Mycobac. Diff. LC PCR kit, artus Biotech USA) was used for the detection of MTB complex (human MTB, *M. bovis*, *M. africanum*, *M. microti*, *M. cannetti*) and *Mycobacterium avium-intracellulare complex*. A region of the mycobacterial 16S DNA, conserved in all members of MTB complex, was amplified and detected by the specific melting point temperature of the fluorescent probe used [4].

The assay system contains, in one master mix, all reagents and enzymes for the specific amplification and

detection of a 163 base pair region of the MTB genome. The kit also provides a dilution series of external positive MTB controls for precise quantification of the MTB complex load. PCR inhibitors are also to be detected to prevent the generation of false negative results. An internal control, co-amplified with the specific target DNA in the same capillary, is therefore included in the assay kit. This internal control does not influence the sensitivity or specificity of the MTB PCR. If the internal control is added to the sample before the nucleic acid isolation process, it can also be used to control the efficiency of the DNA extraction procedure.

Unit costs for PCR, CXR, TST and IFN- γ were estimated at £50, £11, £10 and £40 respectively. We also conservatively estimated a further minimum cost of £30 per patient, which incorporated district nurse, TB control nurse and medical time. We aimed to compare the total PCR costs with the costs of unnecessary follow up of PCR negative patients, who subsequently proven to be MTB culture negative.

The cost of contact procedures for PCR-negative and MTB-culture negative index cases was based on the assumption that there were 4 contacts traced per index case for patients with EMI. [2]

3. RESULTS

A total of 203 smear-positive patients underwent direct PCR testing. 126 (62%) patients grew MTB, 74 (37%) had EMI and 3 (1%) were culture negative. Of the 126 patients that were culture positive for MTB, 123 were PCR positive and 3 PCR negative. Of the 77 patients that were culture negative for MTB, 75 were PCR negative and 2 PCR positive (**Table 1**). The sensitivity, specificity, positive and negative predictive values for direct PCR versus MTB culture were 98%, 96%, 98% and 97% respectively.

Table 1. Comparison of PCR and culture results for 203, AFB smear-positive sputa.

	MTB Culture		
	+	-	
+	123	2	125
MTB* PCR	3	75	78
-			
	126	77	203

MTB: *Mycobacterium tuberculosis*

PCR: Polymerase chain reaction

*Sensitivity: 98%

Specificity: 96%

Positive predictive value: 98%

Negative predictive value: 97%

Table 2. Breakdown of estimated costs for PCR tests and contact tracing procedures for PCR / M. tuberculosis culture negative index cases.

TST	CXR	INF- γ test	Medical/nursing	Contact tracing	PCR	Savings
£3,000	£1,650	£6,000	£9,000	£19,650	£10,150	£9,500

TST : Tuberculin skin test

CXR : Chest xray

INF- γ : Interferon-gamma

PCR : Polymerase chain reaction

The following costs per index case was identified:

Number of PCR-negative/MTB culture-negative cases (i.e. unnecessarily screened) = 75

Number of contact cases per index case with EMI = 4

Total cost for TST = $75 \times 4 \times £10 = £3,000$

Total cost for INF- γ (approximately 50% of contacts go on to get this) = $75 \times 2 \times £40 = £6,000$

Total cost for CXR (at least 50% of contacts require this) = $75 \times 2 \times £11 = £1,650$

Total cost for medical/nursing time = $75 \times 4 \times £30 = £9,000$

Total costs of all PCRs performed amounted to £10,150 ($£50 \times 203$). The cost of contact procedures for PCR-negative and MTB culture-negative index cases was estimated at £19,650. This equated to a total saving of £9,500 in contact tracing costs (**Table 2**).

4. DISCUSSION

Previous studies looking at the cost effectiveness of PCR have focused primarily on the savings due to averted isolation, drug treatment, in-patient beds saved and further investigations. [5-7] To our knowledge, there have been no studies that have specifically looked at the cost-effectiveness of PCR in avoiding unnecessary contact tracing costs. We estimated that direct PCR use in this population of patients with smear-positive sputa, resulted in an overall net saving of £9,500 in contact tracing costs. Whilst this seems a relatively modest amount over a 3-year time period, it is nevertheless, a saving, and justifies the expenditure on PCR (£10,150). We also should not underestimate the other benefits that an early diagnosis will have. In our study, over a third of patients who had smear-positive sputa did not have MTB, which is in keeping with previous data in this area. [2] Currently, all smear-positive patients should be commenced on anti-tuberculosis treatment. In a population such as ours, this will result in a significant number of patients being incorrectly treated. Also, there are significant adverse effects that are associated with anti-TB therapy, [8] so these decisions should not be taken lightly. Prompt diagnosis using direct PCR may therefore also save on unnecessary treatment costs and adverse events

which were not included in the costing model. Furthermore, from a psychological perspective, an early diagnosis will save a lot of patients' close contacts going through the stress of being subjected to a number of unnecessary tests to establish that they don't have MTB.

Whilst our study showed a saving in contact tracing costs of £9,550, this is likely to be a very conservative estimate. Once a person has been diagnosed with active TB, the diagnosing physician should inform relevant colleagues so that the need for contact tracing can be assessed without delay. [1] This contact tracing process usually begins with a TB health visitor interviewing the patient. Screening is then offered to household and any other close contacts, which usually involves a visit to the TB screening clinic. After a TST, contacts will need a further visit to have the result read and if testing is inconclusive, they should be referred to a TB specialist. [1] All this equates to a significant amount of medical, health visitor and nursing time and it may well be that £30 per contact is a gross underestimate. Without a diary analysis of this time spent screening contacts, it was however, difficult to formally assess this. Overall, our estimate of £9,550 saved in contact tracing costs shows that PCR virtually pays for itself.

Microscopically, 5,000-10,000 AFB ml⁻¹ must be present for smear-positivity, compared to 10-100 AFB ml⁻¹ that are required for culture positivity. Therefore, a smear-positive respiratory sample signifies a high bacterial load and an increased risk of infectivity. In a mini review of available nucleic acid amplification tests (NAAT) for the detection of MTB in clinical specimens (21 studies), the mean sensitivity in smear-positive specimens was 94.5%. [9] The positive-predictive value and sensitivity of the PCR in our study was 98%, which is in-keeping with previous data on this particular real-time PCR assay (100% sensitivity). [4] In view of this, and the fact that PCR is expensive, we feel that performing PCR on only one of the three smear positive specimens should be enough to aid diagnosis and decide which patients' contacts do and do not need to be screened. In contrast, NAAT sensitivity on smear-negative specimens was much lower, at 69.3%. [10] However, as smear-negativity signifies a low bacterial load, these patients are likely to have a low risk of infectivity, so

contact tracing becomes less of an urgent issue. As rapid liquid culture takes approximately 8-10 days in our hospital, we therefore felt that routine use of PCR in this group of patients would be unlikely to be cost-effective.

In a recent article by Taegtmeier *et al.*, the authors found that PCR had a direct impact on clinical management in one third of smear-positive patients in whom it was used. This included patients for whom treatment was changed and situations in which contact tracing exercises were either commenced or stopped. PCR significantly reduced the time to identification of the mycobacteria and detection or exclusion of rifampicin resistance, which allowed prompt alterations in management when needed. They concluded that there would be additional clinical benefit from PCR being applied to all smear-positive specimens in low prevalence settings. [10] We would concur with this, and believe that our study illustrates that direct PCR testing of all smear-positive patients can also be cost-effective.

In conclusion, although current national guidance on direct PCR recommends its use principally to confirm true MTB before a large contact tracing exercise is undertaken, our results suggest that it may have a useful and cost-effective role in routine clinical practice on smear-positive respiratory samples, particularly in areas with a high incidence of EMI. Whilst there are reports suggesting that the incidence of EMI has increased over the past few decades, this observation has not been conclusively established due to the lack of a comprehensive surveillance system. [11] This data would be particularly helpful in deciding which areas in the UK may benefit from direct PCR testing on all smear-positive respiratory specimens. Such an approach should be reflected in the National Institute of Clinical Excellence (NICE) guidelines when they are next revised.

REFERENCES

- [1] CG33 Tuberculosis – National Institute of Clinical Excellence (NICE) guidelines. March 2006.
- [2] Corless, J.A., Stockton, P.A., Davies, P.D. (2000) Mycobacterial culture results of smear-positive patients with suspected pulmonary tuberculosis in Britain. *Eur Respir J*, **16**: 976-9.
- [3] National Collaborating Centre for Chronic Conditions: clinical diagnosis and management of tuberculosis and measures for its prevention and control. (2006). London, Royal College of Physicians.
- [4] Cramer, S.O., Matinmehr, F., Hillemann, D. (2004) Fast and sensitive detection of the Mycobacterium tuberculosis complex by real-time PCR, *Clinical Microbiology and Infection*, **10**(3), 418.
- [5] Drobniewski, F.A., Watterson, S.A., Wilson, S.M., Harris, G.A. (2000) A clinical, microbiological and economic analysis of a national service for the rapid molecular diagnosis of tuberculosis and rifampicin resistance in Mycobacterium tuberculosis. *J Med Microbiol*, **49**:271-8.
- [6] Dowdy, D.W., Maters, A., Parrish, N., Beyrer, C., Dorman, S.E. (2003) Cost-effectiveness analysis of the Gen-Probe amplified Mycobacterium tuberculosis direct test as used routinely on smear-positive respiratory specimens. *J Clin Microbiol*, **41**(3), 948-953.
- [7] van Cleeff, M., Kivihya-Ndugga, L., Githui, W., Ng'ang'a L., Kibuga, D., Odhiambo, J., *et al.* (2005) Cost-effectiveness of polymerase chain reaction versus Ziehl-Neelsen smear microscopy for diagnosis of tuberculosis in Kenya. *Int J Tuberc Lung Dis*, **9**:877-83.
- [8] Zalekis, R. (2005) Side-effects of Tuberculosis treatment. *Breathe*, **2**(1), 69-73.
- [9] Piersimoni, C. and Scarparo, C. (2003) Minireview–Relevance of commercial amplification methods for direct detection of Mycobacterium tuberculosis complex in clinical samples. *J Clin Microbiol*, **41**(12), 5355-5365.
- [10] Taegtmeier, M., Beeching, N.J., Scott, J., Seddon, K., Jamieson, S., Squire, S.B., Mwandumba, H.C., Miller, A.R.O., Davies, P.D.O., Parry, C.M. (2007) The Clinical impact of nucleic acid amplification tests on the diagnosis and management of tuberculosis in a British hospital. Thorax Online.
- [11] Griffith, D.E., Aksamit, T., Barbara, A., *et al.* (2007) American thoracic society guidelines: Diagnosis, treatment and prevention of nontuberculous mycobacterial diseases. *Am J Resp and Crit Care Med*, **175**, 367-417.

Electrospun nanofiber-based drug delivery systems

Deng-Guang Yu¹, Li-Min Zhu^{1*}, Kenneth White², Chris Branford-White²

¹College of Chemistry, Chemical Engineering and Biotechnology, Donghua University, Shanghai, China

²Institute for Health Research and Policy, London Metropolitan University, London, UK

Received 15 May 2009; revised 8 June 2009; accepted 11 June 2009.

ABSTRACT

Electrospinning is a very simple and versatile process by which polymer nanofibers with diameters ranging from a few nanometers to several micrometers can be produced using an electrostatically driven jet of polymer solution or polymer melt. Significant progress has been made in this process throughout the past few years and electrospinning has advanced its applications in many fields, including pharmaceuticals. Electrospun nanofibers show great promise for developing many types of novel drug delivery systems (DDS) due to their special characteristics and the simple but useful and effective top-down fabricating process. The current state of electrospun nanofiber-based DDS is focused on drug-loaded nanofiber preparation from pharmaceutical and biodegradable polymers and different types of DDS. However, there are more opportunities to be exploited from the electrospinning process and the corresponding drug-loaded nanofibers for drug delivery. Additionally, some other related challenges and the possible resolutions are outlined in this review.

Keywords: Electrospinning; Nanofibers; Drug Delivery Systems; Controlled Release

1. INTRODUCTION

Electrospinning, firstly reported in 1934, has been used for more than 60 years, and yet is under developed in studying the fabrication of continuous nanofibers. The term “electrospinning”, derived from “electrostatic spinning”, was coined relatively recently. Since 1980s and especially in recent years, the electrospinning process has regained more attention probably due in part to a surging interest in nanotechnology, as ultrafine fibers or fibrous structures of various polymers with diameters in the submicron/nanometer range can be easily fabricated using this process. A survey of open publications and

patents related with electrospinning in the past several years is given in **Figure 1**. The data were obtained from Elsevier ScienceDirect, Wiley InterScience and the Dewent Innovations Index, and clearly demonstrates that electrospinning has attracted increasing attention in recent times. [1-3]

A schematic diagram demonstrating the process of electrospinning of polymer nanofibers is shown in **Figure 2**. There are basically three components: a high voltage supplier, a capillary tube with a pipette or needle of small diameter, and a metal collecting screen. In electrospinning a high voltage is used to create an electrically charged jet of polymer solution or melt out of the pipette. Before reaching the collecting screen, the solution jet evaporates or solidifies, and is collected as an interconnected web of small fibers. One electrode is placed into the spinning solution/melt and the other attached to the collector. In most cases, the collector is simply grounded. The electric field is applied across the end of the capillary tube that contains the solution fluid held by its surface tension. This induces a charge on the surface of the liquid. Mutual charge repulsion and the contraction of the surface charges to the counter electrode create a force directly opposite to the surface tension. As the intensity of the electric field is increased, the hemispherical surface of the fluid at the tip of the capillary tube elongates to form a conical shape known as the Taylor cone. Further increasing the electric field, a critical value is attained with which the repulsive electrostatic force overcomes the surface tension and the charged jet of the fluid is ejected from the tip of the Taylor cone. The discharged polymer solution jet undergoes an instability and elongation process, which allows the jet to become very long and thin. Meanwhile, the solvent evaporates, leaving behind a charged polymer fiber. In the case of the melt the discharged jet solidifies when it travels in the air *stream*. [2-12]

Electrospinning appears to be affected by the following parameters and variables: 1) system parameters such as molecular weight, molecular weight distribution and architecture (branched, linear, etc.) of the polymer, and polymer solution properties (viscosity, conductivity, dielectric constant, and surface tension, charge carried by the spinning jet) and 2) process parameters such as

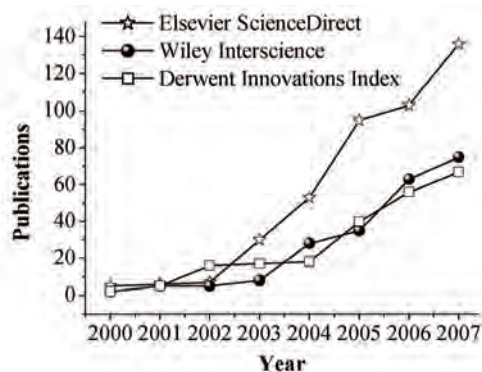


Figure 1. The increase of literature electrospinning from several databases (Search term is “electrospinning” within “source title”).

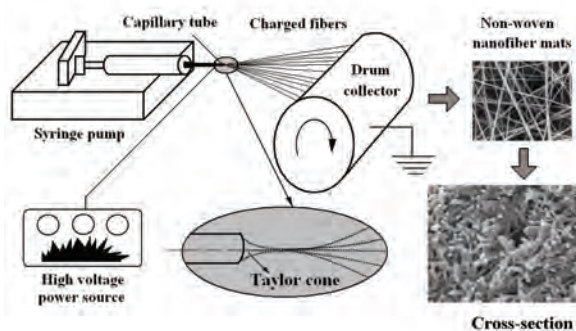


Figure 2. The process of electrospinning.

electric potential, flow rate and concentration, distance between the capillary and collection screen, ambient parameters (temperature, humidity and air velocity in the chamber) and finally motion of the target screen. By appropriately varying one or more of the above parameters, nanofibers can be successfully electrospun from a rich variety of materials that include polymers, biopolymers, DNA, protein, composites, and ceramics and even relatively small macromolecules such as phospholipids. [2-4]

A number of processing techniques such as drawing, template synthesis, phase separation and self-assembly have been used to prepare polymer nanofibers in recent years. However these methods have disadvantages such as: material limitation, they are time-consuming and they require complicated processing systems. As far as electrospinning is concerned it is not only a simple one-step top-down process for fabricating nanofibers, but also the co-processing of polymer mixtures, chemical cross-linking can be carried out that provide a variety of pathways for controlling the chemical composition of the nanofibers. These provide a wide range of properties such as strength, weight, elasticity, porosity and charged surface areas. Moreover electrospinning also provides the capacity to lace together a variety of nanoparticles or nanofillers types that can be encapsulated into a nanofi-

ber matrix. Functional micro/nano particles may be dispersed in polymer solutions, which are then electrospun to form composites in the form of continuous nanofibers and nanofibrous assemblies. All these endow electrospinning with outstanding manufacturing capabilities but utilizing an easy process and capable of excellent flexibility. Additionally, electrospinning seems to be the only method *that* can be further developed for mass production of one-by-one continuous nanofibers from various polymers. [3]

Over the past several decades, polymer sciences have been the backbone of pharmaceuticals [13]. Many pharmaceutical polymer excipients are commonly used in the development of novel drug delivery systems (DDS) now. Combined usage of electrospinning with pharmaceutical polymers provides novel strategies for developing novel DDS, and through the manipulation of electrospinning process, may offer flexibility for tailoring DDS's properties.

2. CHARACTERISTICS OF ELECTROSPUN FIBERS

Polymer nanofibers have a diameter in the order of a few nanometers to over $1 \mu\text{m}$ (more typically 50~500 nm) and possess unique characteristics, such as: extraordinary high surface area per unit mass (for instance, nanofibers with ~100 nm diameter have a specific surface of $\sim 1000\text{m}^2/\text{g}$), coupled with remarkably high porosity, excellent structural mechanical properties, high axial strength combined with extreme flexibility, low basis weight, and cost effectiveness *are* among others.

Another interesting aspect of using nanofibers is that it is feasible to modify not only their morphology and their (internal bulk) content but also the surface structure to carry various functionalities. Nanofibers can be easily post-synthetically functionalized (for example by chemical or physical vapour deposition). Furthermore, it is even feasible to control secondary structures of nanofibers in order to prepare nanofibers with core/sheath structures, nanofibers with hollow interiors and nanofibers with porous structures. [10]

Economically, the electrospinning nano-manufacturing process is relatively low cost compared to that of most bottom-up nanofiber-fabricating methods. The resulting nanofibers are often uniform, continuous and do not require expensive purification protocols. The nanofibers are relatively easy to be scaled up for productivity due to the top-down process and the designing of multiple jets for synchronous electrospinning. [14] Additionally, the nanofibers have one dimension *at* the microscopic scale but another dimension macroscopically. This unique characteristic endows nanofiber mats with both the merits possessed by functional materials on the nano-meter scale, and these have advantages *over* conventional solid membrane such as easy processing, ease

of packaging and shipping.

These outstanding properties make polymer nanofibers as good candidates for many applications. For example nanofibers mats are now being considered for composite materials reinforcement, sensors, filtration, catalysis, protective clothing, biomedical applications (including wound dressing and scaffolds for tissue engineering, implants, membranes and drug delivery systems), space applications such as solar sails, and micro- and nanooptoelectronics. Thus the properties of nanofibers make them useful for systems for developing nanofibers-based DDS.

3. CURRENT STATE OF ELECTROSPUN NANOFIBER-BASED DDS

Research about electrospun nanofibers as drug delivery systems is in the early stage of exploration. [3] Many current researches focus on the preparation and characterization of polymer nanofibers. To date, it is generally believed that nearly one hundred different polymers, mostly dissolved in solvents yet some heated into melts, have been successfully spun into ultrafine fibers. How to transit nanofibers into DDS is creating much attention. It is clear from **Figure 3** that the open publications related to electrospun nanofiber-based DDS are increasing more sharply than those related with nanofibers.

The first report about electrospinning fibers as DDS was noted by Kenawy *et al.* [5] Electrospun fiber mats were explored as drug delivery vehicles using tetracycline hydrochloride as a model drug. The mats were made either from poly (lactic acid) (PLA), poly (ethylene-co-vinyl acetate) (PEVA), or from a 50:50 blend of the two from chloroform solutions. Release profiles showed promising results when they were compared to a commercially available DDS--Actisite® (Alza Corporation, Palo Alto, CA), as well as to the corresponding cast films. An early patent registered by Ignatious and Baldoni described electrospun polymer nanofibers for pharmaceutical compositions, which can be designed to provide rapid, immediate, delayed, or modified dissolution, such as sustained and/or pulsatile release characteristics. [6]

Later studies on the preparation of nanofibers from polymers with different drug-loaded capabilities and the corresponding DDS were reported, such as transdermal, fast dissolving and implantable DDS (**Figure 4**). Most of the early work focused on the sustained release profiles and all types of active pharmaceutical ingredients were used as model drugs, such as small molecular drug, herbs, proteins, poorly water-soluble and water-soluble drugs, DNA, genes and vaccines. The polymers include biodegradable hydrophilic polymers, hydrophobic polymers and amphiphilic polymers. [3,15,16]

Zhang *et al.* reported that degradable heparin-loaded poly (ϵ -caprolactone) fiber mats were successfully fab-

ricated by electrospinning. The highly sulphated heparin hetropolymer remained homogenous in the spinning solution and was evenly distributed throughout the fabricated polymers. A sustained release of heparin could be achieved from the fibers over 14 days with the release diffusionally controlled over this period. The released heparin retained biological properties and functionality. [17] Chew *et al.* investigated the feasibility of encapsulating human β -nerve growth factor (NGF) that was stabilized in the carrier protein, bovine serum albumin (BSA) in a copolymer of ϵ -caprolactone and ethyl ethylene phosphate. Partially aligned protein encapsulated fibers were obtained and the protein was found to be randomly dispersed throughout the electrospun fibrous mesh in an aggregated form. The sustained release of NGF by diffusion was obtained for at least 3 months. PC12 neurite outgrowth assay confirmed that the bioactivity of electrospun NGF was retained throughout the period of sustained release. [18] Luu *et al.* utilized electrospinning to fabricate synthetic polymer/DNA composite for therapeutic application in gene delivery designed for tissue engineering. The composite was non-woven, nano-fibered, membranous structures composed predominantly of poly(lactide-co-glycolide) (PLGA) random

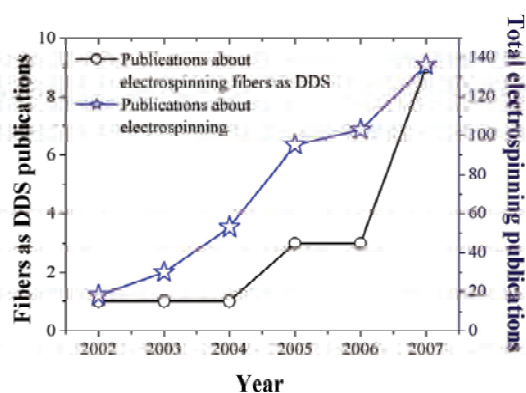


Figure 3. The increase of literature about e-spinning nanofibers as DDS (Search term is “electrospinning” in “title and “drug delivery” in “abstract”).

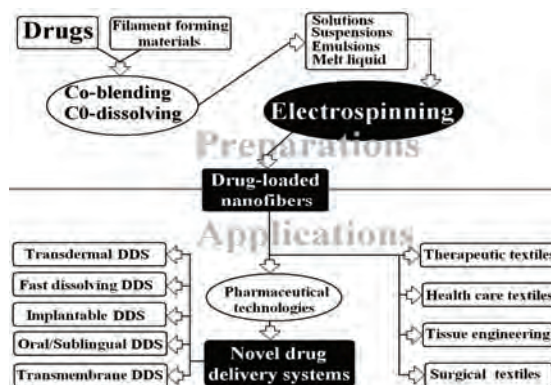


Figure 4. Applications and preparations of electrospun drug-loaded nanofibers.

copolymer and a poly(D,L-lactide)–poly(ethylene glycol) (PLA–PEG) block copolymer. Release of plasmid DNA from the composite was sustained over a 20-day study period, with maximum release occurring at ~2 h. Cumulative release profiles indicated amounts released were approximately 68–80% of the initially loaded DNA. Results indicated that DNA released directly from these electrospun fibers was indeed intact, capable of cellular transfection, and successfully expressed the encoded protein β -galactosidase. [19]

Electrospun nanofibers are often used to load insoluble drugs for enhancing their dissolution properties due to their high surface area per unit mass. Tungprapa *et al.* prepared ultra-fine fiber mats of cellulose acetate (CA) for four different types of model drugs, i.e., naproxen (NAP), indomethacin (IND), ibuprofen (IBU), and sulindac (SUL), from 16% w/v CA solutions in 2:1 v/v acetone/N,N-dimethylacetamide (DMAc) by electrospinning. The amount of the drugs in the solutions was fixed at 20 wt% based on the weight of CA powder. No drug aggregates were observed on the surfaces of the fibers. The maximum release of the drugs from loaded fiber mats were ranked as follows: NAP>IBU>IND>SUL and this did not correspond to their solubility properties. [7] Taepaiboon *et al.* reported that the molecular weight of the model drugs played a major role on both the rate and the total amount of drugs released from the prepared drug-loaded electrospun PVA nanofibers. The rate and the total amount of the drugs released decreasing with increasing molecular weight of the encapsulated drugs. [8]

Taepaiboon *et al.* also reported that mats of PVA nanofibers were successfully prepared by the electrospinning process and were developed as carriers of drugs for a transdermal drug delivery system. Besides the water insoluble drugs naproxen (NAP), and indomethacin (IND), freely water soluble sodium salicylate, was also spun into the PVA fibers. [8] Xu *et al.* proposed a novel process, i.e., ‘emulsion electrospinning’ to prepare core-sheath fibers to incorporate a water soluble drug into a hydrophobic or an amphiphilic polymer fiber. [20] Maretschek *et al.* [21] recently reported the electrospinning of emulsions composed of an organic poly (L-lactide) solution and an aqueous protein solution, which yielded protein containing nanofiber nonwovens having a mean fiber diameter of approximately 350 nm. This provided the opportunity to tailor the release profile of macromolecular active ingredients. All the above reports demonstrated that electrospun drug-loaded nanofibers were able to provide sustained release profiles for different types of active pharmaceutical ingredients.

Studies previously reported the influence of a high electrical potential on the chemical integrity of the drugs, the comparatively controlled release characteristics of

nanofibers and the release-controlled mechanisms. Tungprapa *et al.* [7] and Taepaiboon *et al.* [8] confirmed that the electrospinning process did not affect the chemical integrity of the drugs by ^1H -nuclear magnetic resonance. Taepaiboon *et al.* [8] proved that the drug-loaded electrospun PVA mats exhibited better release characteristics of four model drugs than drug-loaded as-cast films and Tungprapa *et al.* [7] showed that the release of drugs from the CA drug-loaded films was due mainly to the gradual dissolution of aggregates on the film surfaces, whilst the diffusion of the drugs incorporated within the films occurred to a lesser extent. On the contrary, since no presence of the drug aggregates was found on the surface of the drug-loaded CA fibers, the release of the drugs from the drug-loaded fiber mats was mainly by the diffusion of the drugs from the fibers, as the fiber mats could swell appreciably in the testing medium. Moreover the fibrous morphology of the drug-loaded fiber mats after the drug release assay at 24h was still intact. Verreck *et al.* confirmed that the application of electrostatic spinning to pharmaceutical applications resulted in dosage forms with better useful and controllable dissolution properties than the simple physical mixture, solvent cast or melt extruded samples. [22]

Although many types of DDS have been prepared from electrospun drug-loaded nanofibers, no related clinical experiments have been reported and only few in vivo drug delivery researches have been undertaken, which were mainly associated with the cancer research. Ranganath *et al.* reported the paclitaxel-loaded biodegradable implants in the form of microfiber discs and sheets developed using electrospinning were used to treat malignant glioma in vitro and in vivo. The fibrous matrices not only provided greater surface area to volume ratio for effective drug release rates but also provided needed implantability into the tumor resected cavity of a post-surgical glioma. [23]

The advantages of employing electrospinning technology to prepare DDS are not as yet fully exploited. Nanotechnology is now having an impact in biotechnology, pharmaceutical and medical diagnostics sciences. Nanodrugs are at the forefront of bioengineering for diseases and represent the next generation of medical therapies that will impact worldwide markets and especially the healthcare industry [24]. Furthermore electrospinning as noted before has gained more attention due in part to a surging interest in nanotechnology, as ultrafine fibers or fibrous structures of various polymers with small diameters. [25] On the other hand, electrospinning should exert more influence on new DDS development through providing novel strategies for conceiving and fabricating them.

4. NOVEL STRATEGIES PROVIDED BY ELECTROSPINNING FOR NEW DDS

From the current literature, several advantages of using electrospun polymer nanofibers as DDS are recognized, and these merit further consideration in developing new types of DDS.

Firstly, due to the high surface area to volume ratio, polymer nanofibers provide a useful pathway for delivery of water insoluble drug. With the recent advent of high throughput screening of potential therapeutic agents, the number of poorly soluble drug candidates has risen sharply and the formulation of poorly soluble compounds for oral delivery now presents one of the most frequent and greatest challenges to formulation scientists in the pharmaceutical industry. [26] Solid dispersion is considered to be the most suitable choice to improve dissolution rates and hence the bioavailability of the poorly water soluble drug. [27] However, the practical applicability of solid dispersion systems has remained limited due to difficulties in conventional methods of preparation, poor reproducibility of physicochemical properties, dosage formulation and lack of feasibility for scaling-up manufacturing processes. [28] Electrospun nanofibers may provide novel approaches as to how the dissolution rate of even very poorly soluble compounds might be improved to minimize the limitations of oral availability.

Xie *et al.* developed electrospun PLGA-based nanofibers as implants for the sustained delivery of anticancer drug to treat C6 glioma cells *in vitro*. Differential scanning calorimetry (DSC) results suggest that the drug was in the solid solution state in the polymeric micro- and nanofibers. *In vitro* release profiles suggest that paclitaxel sustained release was achieved for more than 60 days. Cytotoxicity test results suggest that the IC₅₀ value of paclitaxel-loaded PLGA nanofibers is comparable to the commercial paclitaxel formulation-Taxol®. [29]

Verreck and co-workers assessed the application of water-soluble polymer-based nanofibers prepared by electrostatic spinning as a means of altering the dissolution rate of the poorly water-soluble drug, itraconazole. DSC measurements found that the melting endotherm for itraconazole was not present, suggesting the formation of an amorphous solid dispersion or solution. Dissolution studies assessed several presentations including direct addition of the non-woven fabrics to the dissolution vessels, folding weighed samples of the materials into hard gelatin capsules and placing folded material into a sinker. [22] Studies in our laboratory have been undertaken on the solubility improvement of poorly water-soluble drugs and the corresponding fast dissolving DDS. [30] Shown in **Figure 5** is a patent product of a rapid dissolving drug delivery membrane, which can absorb water and dissolve within several seconds a poorly water-soluble drug.

Second, the drug release profile can be easily finely tailored by modulation not only of the composition of the nanofiber mats but also the morphology of nanofibers, the process and the micro-structure. Core-sheath structure is a very useful structure for all kinds of applications. Several fabrication techniques have been proposed to prepare ultrafine fibers configured in a core-sheath structure, such as self-assembly, laser ablation, template synthesis, and a tube by fiber templates process. Core-sheath fibers can be prepared by 'emulsion electrospinning'. Xu *et al.* [16] reported that uniform core-sheath nanofibers were prepared by electrospinning a water-in-oil emulsion in which the aqueous phase consists of a poly(ethylene oxide) (PEO) solution in water and the oily phase is a chloroform solution of an amphiphilic poly(ethylene glycol)-poly(L-lactic acid) (PEG-PLA) diblock copolymer. The obtained fibers are composed of a PEO core and a PEG-PLA sheath with a sharp boundary in between. By adjusting the emulsion composition and the emulsification parameters, the overall fiber size and the relative diameters of the core and the sheath can be altered. The stretching and evaporation induced de-emulsification and the transformation from the emulsion to the core-sheath fibers.

Concentric electrospinning is a very promising approach to fabricate core-sheath fibers. [31] Coaxial electrospinning (**Figure 6**) is an alternative approach to encapsulate drugs or biological activities inside polymer nanofibers. In a typical process (**Figure 6**), two or more polymer liquids are forced by an electrostatic potential to eject out through different but co-axial capillary channels, resulting in a core-shell structured composite nanofiber. As long as the shell fluid is able to be processed *along* with electrospinning, the core fluid can either be or not be electrospinnable. One advantage in using such a technique is an effective protection of easily denatured biological agents and the potential to wrap all substances

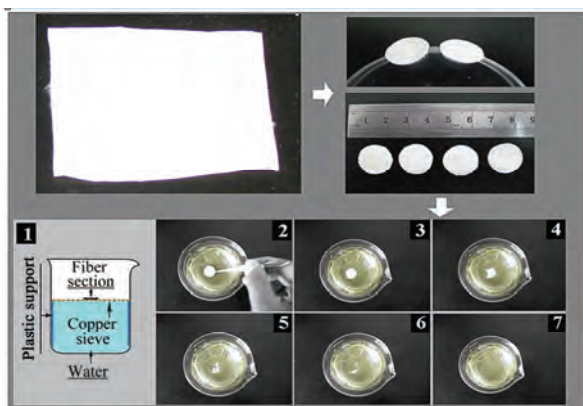


Figure 5. Fast dissolving drug delivery membrane.

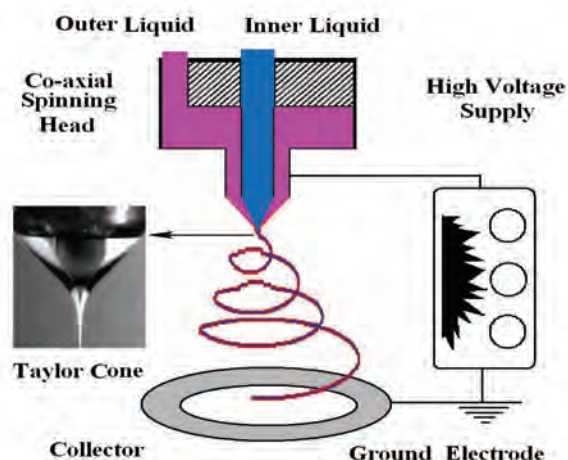


Figure 6. Co-axial electrospinning systems.

in the core regardless of drug-polymer interactions. Hence, drugs, proteins, growth factors, and even genes can be incorporated into nanofibers by dissolving them in the core solutions. [32-34]

Huang *et al.* used co-axial electrospinning to prepare core-sheath nanofibers for controlled release of multi drugs. Polycaprolactone was used as the shell and two medically pure drugs, Resveratrol and Gentamycin Sulfate, were used as the cores. The drugs were released in a controlled way without any initial burst effect. [32]

Third, there is a lot of flexibility in the use of nanofibers in designing various dosage forms to achieve maximum bioavailability of a drug moiety for different drug delivery routes. Electrospun drug-loaded nanofibers are often used as mid dosage forms. They can be further turned into different kinds of DDS for all types of drug delivery routes, such as for transdermal administration, oral administration, pulmonary administration, subcutaneous implant, or for dissolution into a liquid media for administration, such as a suspension or solution or by parenteral/intramuscular or intracavernosum injection and so on. [35]

Besides preparing DDS solely from electrospun fibers, researchers often combine the electrospinning process with other special substances to prepare DDS. Shalaby describes a partially absorbable, fiber-reinforced composite in the form of a ring, or a suture-like thread, with modified terminals for use as a controlled delivery system of bioactive agents. The composite comprised an absorbable fiber construct capable of providing time-dependent mechanical properties of a biostable elastomeric matrix containing an absorbable microparticulate ion-exchanger to modulate the release of the bioactive agents for a desired period of time at a specific biological site, such as the vaginal canal, peritoneal cavity, scrotum, prostate gland, an ear loop or subcutaneous tissue. [36]

Fourth, electrospun nanofibers often have higher drug encapsulation efficiency than other nanotechnologies.

Xie *et al.* reported that the encapsulation efficiency for paclitaxel-loaded PLGA micro- and nanofibers was more than 90%. The electrospun paclitaxel-loaded biodegradable micro- and nanofibers are promising for the treatment of brain tumour as alternative drug delivery devices. [29] Xu *et al.* showed that a water-soluble anti-cancer agent, doxorubicin hydrochloride, was totally encapsulated within the electrospun poly (ethylene glycol)-poly (l-lactic acid) (PEG-PLLA) fibers when its content in the fibers was 5 wt %. [37] Other advantages of drug-loaded nanofibers, such as small diameter of the nanofibers, can provide short diffusion passage length. Also, high surface area facilitates mass transfer and effective drug release.

As mentioned above, the drug-loaded nanofibers derived from electrospinning not only have one dimension at the microscopic scale but another dimension in the macroscopic form. This unique characteristic endows the electrospun drug-loaded nanofibers with both the merits possessed by the DDS on the nano-meter scale in altering the biopharmaceutic and pharmacokinetic properties of the drug molecule for favorable clinical outcomes, and also the advantages of conventional solid dosage forms such as easy processing, good drug stability, and ease of packaging and shipping.

5. SOME CHALLENGES AND THE POSSIBLE RESOLUTIONS

Although some reports in the literature have demonstrated that electrospinning is useful for preparing new DDS there are still some challenges associated with the preparation of electrospun nanofiber-based DDS.

Electrospinning is a simple micro-processing technique to make ultrafine or nanometer range fibers generally from high molecular weight polymer solutions or melts. The largest challenge lies firstly in understanding the electrospinning process as a fluid dynamics system. In order to control the properties, geometry, and mass production of the nanofibers, it is necessary to understand quantitatively how electrospinning transforms the fluid solution through a millimeter diameter capillary tube into solid fibers which are four to five orders smaller in diameter. Secondly, the efficiency of electrospinning is still a bottleneck. Studies on multiple nozzles need to be undertaken and these will form a platform for electrospinning industrialization. [38-40]

To date, most of the release tests have been done in vitro. What is more, several problems must be resolved for further applications such as the drug loading, the initial burst effect, the residual organic solvent, the stability of active agents, and the combined usage of new biocompatible polymers. Drug-loading is always a problem for nano DDS. Although drug loading over 50% of the total weight was reported, the drug loading in the nanofibers still needs to be increased in many cases. The

reason is that drug often influences the spinnability of the polymer solution. The viscosity range of a polymer solution which is spinnable is about 1–20 poises and the surface tension between 35 and 55 dynes/cm is suitable for fiber formation. Relatively high drug loading may also easily cause the uneven distribution of the drug in the nanofiber resulting in initial burst effects for electrospinning fibers except for co-axial fibers. [41]

The initial burst effect is a common phenomenon for nano drug delivery systems with high surface area such as nano- or microspheres, liposomes and hydrogels. The reason for this phenomenon has been investigated by a number of laboratories. For ordinary electrospinning, drug-loaded nanofibers electrospun from mixtures of drugs and polymers the drug release characteristics rely on the drug being encapsulated within the nanofibers. However due to surface effects the drug particles in the nanofibers tend to accumulate on the fiber surface. Thus, a burst release at an initial stage is inevitable unless the blend of drug and polymer carrier is fully integrated into the nanofiber at a molecular level. [32]

Zeng *et al.* studied the encapsulation of the lipophilic drug paclitaxel and the hydrophilic drug doxorubicin hydrochloride in the electrospun PLLA fiber mats and their release kinetics. Preferable encapsulation of paclitaxel was found due to its good compatibility with PLLA and solubility in chloroform/acetone solvent, whereas doxorubicin hydrochloride was observed on or near the surfaces of PLLA fibers. The release results of these drugs confirmed that the release of paclitaxel from electrospun PLLA fiber samples followed nearly zero-order kinetics due to the degradation of the fibers. However a burst release was found for doxorubicin hydrochloride due to the diffusion of the drug on or near the surfaces of the fiber sample. Therefore, the solubility and compatibility of the drugs in the drug/polymer/solvent system were the decisive factors for the preparation of the electrospun fiber formulation with constant release of the drugs. In order to encapsulate a majority of the drugs inside the polymer fibers and thus to acquire a constant and stable drug release profile, a lipophilic polymer should be chosen as the fiber material for a lipophilic drug while a hydrophilic polymer should be employed for a hydrophilic drug and the solvents used should be suitable for both drug and polymer. [41]

To smoothen or even eliminate the initial burst effects, post-treatment methods are often considered. Within this context Kenawy *et al.* reported that the burst release of ketoprofen was eliminated when the electrospun poly(vinyl alcohol) fiber mats were stabilized against disintegration in water by treatment with methanol. [5] Taepaiboon post-treated electrospun fibre mats of poly(vinyl alcohol) (PVA) containing sodium salicylate by exposing the fibre mats to the vapour from 5.6 M aqueous solution of either glutaraldehyde or glyoxal for various exposure time intervals, followed by a heat

treatment in a vacuum oven. With increasing the exposure time in the cross-linking chamber, the morphology of the electrospun fiber mats gradually changed from a porous to a dense structure. Cross-linking appreciably reduced the release of sodium salicylate from the drug-loaded fiber mats and both the rate and the total amount of the drug released decreased functions with exposure time interval in the cross-linking chamber. [42]

Certainly, the core-shell structure fiber with the drug in the core can eliminate the burst effects. Research also showed that surfactants can reduce the surface tensions and the diameter of resulted nanofibers, improve the drug uniformity and thus can smoothen the burst effect. [43]

To adapt the development of pharmaceuticals, one of the emphases is the preparation of novel polymers drug-loaded nanofibers, for example, polymer with environmental sensitive characteristics. Chunder *et al.* reported that ultrathin fibers comprising two oppositely charged weak polyelectrolytes PAA/PAH were fabricated using electrospinning. These fibers are capable of controlling drug releasing through pH changes. The releasing properties of PAA/PAH fibers was tuned by depositing different coatings onto fiber surfaces. A sustained and a temperature controlled drug releasing in PBS solutions was achieved by depositing perfluorosilane coatings and PAA/PNIPAAm multilayers onto the fiber surfaces, respectively. [44]

In theory, comprehension and clarification of the relationship between the release profiles and the electrospinning parameters help to select suitable materials, optimize electrospinning process, and thus to improve the consistence between design and manufacturing, reduce the time to market for novel DDS. Since the physical form of the active agent in a dosage form can influence the product performance, it is often necessary to quantify the different solid phases in a system for preparing a robust dosage form. In nanofibers, the possible interactions between the drugs and the excipients in the dissolution and electrospinning processes should be thoroughly investigated for further developing novel DDS.

Drug release profiles from the drug delivery systems should be precisely predicted or programmed so that any possibility of dose dumping and subject-to-subject variability can be minimized. The relationships between the drug controlled release profile and the electrospinning parameters should be elucidated. Mathematical models of drug release from nanofibers can be used to elucidate the underlying drug transport mechanism and predict the resulting drug release kinetics as a function of the nanofibers (structure, geometry and composition). In conclusion, there are still many things to do to enable the electrospun nanofiber-based DDS to go into clinical applications.

6. ACKNOWLEDGEMENT

We thank the UK-CHINA Joint Laboratory for Therapeutic Textiles and Biomedical Textile Materials, China Postdoctoral Science Foundation (NO.20080440565), and Grant 08JC1400600 from Science and Technology Commission of Shanghai Municipality for the financial support.

REFERENCES

- [1] Formhals, Process and apparatus for preparing artificial threads, *US Pat 1975504*, October-02-1934.
- [2] Doshi, J. and Reneker, D.H., (1995) Electrospinning process and applications of electrospun fibers, *Electrostatics*, **35**, 151-160.
- [3] Huang, Z.M., Zhang, Y.Z., Kotaki, M. and Ramakrishna, S. (2003) A review on polymer nanofibers by electrospinning applications in nanocomposites, *Composites Sci. Tech.*, **63**, 2223-2253.
- [4] McKee, M.G., Layman, J.M., Cashion, M.P., Timothy, E.L. (2006) Phospholipid nonwoven electrospun membranes, *Science*, **311**, 353-355.
- [5] Kenawy, E.R., Bowlin, G.L., Mansfield, K., Layman, J., Simpson, D.G., Sanders, E.H., and Wnek, G.E. (2002) Release of tetracycline hydrochloride from electrospun poly (ethylene-co-vinylacetate), poly(lactic acid), and a blend, *J. Control. Release*, **81**, 57-64.
- [6] Ignatiou, F., Baldoni, J.M. (2001) Electrospun pharmaceutical compositions, *WO Pat 0154667*.
- [7] Tungprapa, S., Jangchud, I., and Supaphol, P. (2007) Release characteristics of four model drugs from drug-loaded electrospun cellulose acetate fiber mats, *Polymer*, **48**, 5030-5041.
- [8] Taepaiboon, P., Rungsardthong, U., Supaphol, P. (2006) Drug-loaded electrospun mats of poly(vinyl alcohol) fibres and their release characteristics of four model drugs, *Nanotechnology*, **17**, 2317-2329.
- [9] Dzenis, Y. (2004) Spinning continuous fibers for nanotechnology, *Science*, **304**, 1917-1919.
- [10] Chronakis, I.S. (2005) Novel nanocomposites and nanoceramics based on polymer nanofibers using electrospinning process-A review, *J. Mat. Proc. Tec.*, **167**, 283-293.
- [11] Agarwal, S., Wendorff, J.H. and Greiner, A. (2008) Use of electrospinning technique for biomedical applications, *Polymer*, **49**, 5603-5621.
- [12] Yu, D.G., Shen, X.X., Branford-White, C., White, K., Zhu, L.M. and Bligh, S.W.A. (2009) Oral fast-dissolving drug delivery membranes prepared from electrospun PVP ultrafine fibers," *Nanotechnology*, **20**, 055104.
- [13] Pillai, O. and Panchagnula, R. (2001) Polymers in drug delivery, *Curr. Opin. Chem. Biol.*, **5**, 447-451.
- [14] Varabhas, J.S., Chase, G.G. and Reneker, D.H. (2008) Electrospun nanofibers from a porous hollow tube, *Polymer*, **49**, 4226-4229.
- [15] Shen, X.X., Yu D.G., Ranford-White, C. B. and Zhu, L.M., (2008) Preparation and characterization of ultrafine eudragit L100 fibers via electrospinning, *The 3rd International Conference on Bioinformatics and Biomedical Engineering (iCBBE'09)*, May18, Shanghai, China.
- [16] Xu, X., Chen, X., Wang, Z. and Jing, X. (2009) Ultrafine PEG-PLA fibers loaded with both paclitaxel and doxorubicin hydrochloride and their in vitro cytotoxicity, *Euro. J. Pharm. Biopharm.*, **72**, 18-25.
- [17] Zhang, Y.Z., Wang, X., Feng, Y., Li, J., Lim, C.T. and Ramakrishna, S. (2006) Coaxial electrospinning of fluorescein isothiocyanate – conjugated bovine serum albumin–encapsulated poly(ϵ -caprolactone) nanofibers for sustained release, *Biomacromolecules*, **7**, 1049-1057.
- [18] Chew, S.Y., Wen, J., Yim, E.K.F. and Leong, K.W. (2005) Sustained release of proteins from electrospun biodegradable fibers, *Biomacromolecules*, **6**, 2017-2024.
- [19] Luu, Y.K., Kim, K., Hsiao, B.S., Chu, B. and Hadjiargyrou, M. (2003) Development of a nanostructured DNA delivery scaffold via electrospinning of PLGA and PLA-PEG block copolymers, *J. Control. Release*, **89**, 341-353.
- [20] Xu, X., Zhuang, X., Chen, X., Wang, X., Yang, L. and Jing, X. (2006) Preparation of core-sheath composite nanofibers by emulsion electrospinning, *Macromol. Rapid Commun.*, **27**, 1637-1642.
- [21] Maretschek, S., Greiner, A. and Kissel, T. (2008) Electrospun biodegradable nanofiber nonwovens for controlled release of proteins, *J. Control. Release*, **127**, 180-187.
- [22] Verreck, G., Chun, I., Peeters, J., Rosenblatt, J. and Brewster, M. E. (2003) Preparation and characterization of nanofibers containing amorphous drug dispersions generated by electrostatic spinning, *Pharm Res*, **20**, 810-817.
- [23] Ranganath, S.H. and Wang, C.H., (2008) Biodegradable microfiber implants delivering paclitaxel for post-surgical chemotherapy against malignant glioma, *Biomaterials*, **29**, 2996-3003.
- [24] Devalapally, H., Chakilam, A. and Amiji, M.M. (2007) Role of nanotechnology in pharmaceutical product development, *J. Pharm. Sci.*, **96**, 2547-2565.
- [25] Rutledge, G.C. and Fridrikh, S.V. (2007) Formation of fibers by electrospinning, *Adv. Drug Del. Rev.*, **59**, 1384-1391.
- [26] Leuner, C. and Dressman, J. (2000) Improving drug solubility for oral delivery using solid dispersions, *Eur. J. Pharm. Biopharm.*, **50**, 47-60.
- [27] Chokshi, R.J., Zia, H., Sandhu, H.K., Shah, N.H. and Malick, W.A. (2007) Improving the dissolution rate of poorly water soluble drug by solid dispersion and solid solution-pros and cons, *Drug Delivery*, **14**, 33-45.
- [28] Sethia, S. and Squillante, E. (2003) Solid dispersions: Revival with greater possibilities and applications in oral drug delivery, *Crit. Rev. Thera. Drug Carrier System*, **20**, 215-247.
- [29] Xie, J. and Wang, C.H. (2006) Electrospun micro- and nanofibers for sustained delivery of paclitaxel to treat C6 glioma *in vitro*, *Pharm. Res.*, **23**, 1817-1826.
- [30] Yu, D.G., Branford-White, C., Shen, X.X., Zhang, X.F. and Zhu, L.M., (2010) Solid dispersions of ketoprofen in drug-loaded electrospun nanofiber, *Journal of Dispersion Science and Technology*, **31**, article 8.
- [31] McCann, J.T., Li, D. and Xia, Y. (2005) Electrospinning of nanofibers with core-sheath, hollow, or porous structures, *J. Mater. Chem.*, **15**, 735-738.
- [32] Huang, Z.M., He, C.L., Yang, A., Zhang, Y., Han, X.J., Yin, J. and Wu, Q. (2006) Encapsulating drugs in biodegradable ultrafine fibers through co-axial electrospinning, *J. Biom. Mat. Res.*, **77A**, 169-179.
- [33] Loscertales, I.G., Barrero, A., Guerrero, I., Cortijo, R.,

- Marquez, M. and Ganan-Calvo, A.M. (2002) Micro/nano encapsulation via electrified coaxial liquid jets, *Science*, **295**, 1695-1698.
- [34] Li, D. and Xia, Y. (2004) Direct fabrication of composite and ceramic hollow nanofibers by electrospinning, *Nano Letter*, **4**, 933-938.
- [35] Ignatious, F. and Baldoni, J.M. (2003) Electrospun pharmaceutical compositions, *US Pat 2003017208*.
- [36] Shalaby, S.W. (2007) Partially absorbable fiber-reinforced composites for controlled drug delivery, *EP-1786356*.
- [37] Xu, X.L., Yang, L.X., Xu, X.Y., Wang, X., Chen, X.S., Liang, Q.Z., Zeng, J. and Jing, X.B. (2005) Ultrafine medicated fibers electrospun from W/O emulsions, *J. Control. Release*, **108**, 33-42.
- [38] Kim, G.H., Cho, Y.S., Kim, W.D. (2006) Stability analysis for multi-jets electrospinning process modified with a cylindrical electrode, *Euro. Polym. J.*, **42(9)**, 2031-2038.
- [39] Yoon, H., Kim, G.H., Kim, W.D. (2008) Electrohydrodynamic process supplemented by multiple-nozzle and auxiliary electrodes for fabricating PCL nanofibers, *Polymer*, **32(4)**, 334-339.
- [40] Heikkila, P. and Harlin, A. Parameter study of electrospinning of polyamide-6, *Euro. Polym. J.*, **44(10)**, 3067-3079.
- [41] Zeng, J., Yang, L., Liang, Q., Zhang, X., Guan, H., Xu, X., Chen, X. and Jing, X. (2005) Influence of the drug compatibility with polymer solution on the release kinetics of electrospun fiber formulation, *J. Control. Release*, **105**, 43-51.
- [42] Taepai boon, P., Rungsardthong, U., Supaphol, P. (2007) Effect of cross-linking on properties and release characteristics of sodium salicylate-loaded electrospun poly (vinyl alcohol) fibre mats, *Nanotechnology*, **18**, 175102 (11pp).
- [43] Zeng, J., Xu, X.Y., Chen, X.S., Liang, Q.Z., Bian, X.C. and Yang, L.X. (2003) Biodegradable electrospun fibers for drug delivery, *J. Control. Release*, **92**, 227-231.
- [44] Chunder, A., Sarkar, S., Yu, Y. and Zhai, L. (2007) Fabrication of ultrathin polyelectrolyte fibers and their controlled release properties, *Colloids and Surfaces B: Bio-interfaces*, **58**, 172-179.

An ion-based chromogenic method of detecting for inorganic phosphate in serum and milk

Cai-Xia Yin^{1*}, Jing Su¹, Fang-Jun Huo^{2*}, Pin Yang¹

¹Institute of Molecular Science, Key Laboratory of Chemical Biology and Molecular Engineering of Ministry of Education, Shanxi University, Taiyuan, China; yincx@sxu.edu.cn

²Research Institute of Applied Chemistry, Shanxi University, Taiyuan, China; huofj@sxu.edu.cn

Received 10 July 2009; revised 21 July 2009; accepted 22 July 2009.

ABSTRACT

A rapid method for the determination of inorganic phosphate in serum and milk by an ion-based chromogenic is described. Serum samples were detected directly by our system, and milk was also detected after degreased through centrifugation. By this procedure the samples are not diluted. Mean serum inorganic phosphate concentration found in healthy individual is 1.14mmol/L. Values found in serum is in good agreement with those previously reported. Mean inorganic phosphate concentration from foremilk and commercial milk are 2.5mmol/L and 12.5mmol/L respectively.

Keywords: UV-Vis Spectra; Pyrocatechol Violet; Ytterbium Chloride; Phosphate; Serum; Milk

1. INTRODUCTION

Phosphate is involved in important biomineralization processes such as bone formation and also processes that are clearly pathological such as the genesis of renal stones. Consequently, its determination in biological fluids is important [1]. In a clinical setting, inorganic phosphate levels in serum are determined as part of a routine blood analysis. The typical inorganic phosphate concentration in human serum range is 0.81-2.26mmol/L [2]. Individuals with abnormally high phosphate levels are diagnosed with hyperphosphatemia, which manifests in acute or chronic renal failure, hypoparathyroidism and excessive Vitamin D intake. And we know that higher serum phosphate levels would be associated with increased mortality risk among people with CKD [3-5]. Those with low inorganic phosphate levels suffer from hypophosphatemia which can be associated with rickets, hyperthyroidism, or Fanoci Syndrome [6-8]. In addition, there is generally a reciprocal relationship between serum calcium and inorganic phosphorus levels. High in-

organic phosphorus in serum restrains the intake of calcium.

Regarding the newborn baby, foremilk or milk is the most main headspring they grow on. But exactly this time is the quickest time when young child grows, being in the bone blooming period and the cerebrum and the intelligence still being imperfect stage. So the right amount nutrition could guarantee the normal growth, and prevent malnutrition, rickets, anemia and so on. Especially if absorbing calcium phosphorus imbalance, can cause the low calcium blood sickness, the rickets [9]. Moreover iron in the milk is easy to form insolubly iron compound when affected by high phosphate and calcium, cannot be absorbed by the human body, which may cause the young child to occur lacking the iron anemia. In normal foremilk the calcium phosphorus proportion is 2: 1, is easy to be absorbed, to prevent and control the rickets. But the milk is 1: 2, is not easy to be absorbed. Therefore, determination the calcium phosphorus content from foremilk and milk is very important.

Most of the procedure for the colorimetric determination of inorganic phosphate are based on the formation of molybdophosphoric acid with further reduction to heteropolymetric molybdenum blue [10-12] on direct measurements of molybdo- and vanadomolybdophosphoric acid [13,14], or on complex formation between molybdophosphoric acid and basic dyes [15]. These chemical methods have serious shortcomings, however: Molybdate reduction is affected by slight changes in pH, the rate of complex formation is markedly influenced by protein concentration, and the acidity required leads to hydrolysis of organic phosphate, which results in over estimates of P_i concentration [16].

In our work, we developed a rapid method for the determination of phosphate in serum and milk by an ion-based chromogenic. Serum samples were detected directly by our system, and milk was also detected after degreased through centrifugation. By this procedure all samples are not diluted. Owing to our system's prominent advantages, it can serve as a hopeful substitute for

the molybdenum reagent.

2. MATERIAL AND METHODS

2.1. Reagents and Chemicals

The chemicals used were of analytical-reagent grade. PV (Pyrocatechol violet) was purchased from Shanghai and sodium monhydrogenphosphate was purchased from Beijing. Ytterbium oxide was a product of Rare Earth Graduate School of China. HEPES was purchased from Sigma. All solutions were made up with deionized water. HEPES buffer solutions were obtained by adding NaOH 0.1M solution into 10 mM aqueous HEPES using a Beckman Φ 50 pH meter. Ytterbium chloride was prepared from ytterbium oxide and 37% hydrochloric acid. Ytterbium ion solution was prepared by dissolving ytterbium chloride in water. Serum samples were collected from health volunteers and stored at -17°C until analyzed. Cow serum was purchased from commercial pured product. Human milk and commercial milk were degreased through a Centrifugal filter.

2.2. Instruments and Apparatus

pH determinations were performed using a Beckman Φ 50 pH meter. UV-v(V)is spectra were recorded on a HP8453 spectrophotometer. PO-120 quartz cuvettes (10mm) were purchased from Shanghai city of China. Finnpiptette Digitalis were purchased from Shanghai of China. BFX5-320 Low Speed Automatic Balance Centrifuge was purchased from Baiyang Centrifuge factory. Olympus 2700 Complete Automatic Clinical Biochemistry Analysis Apparatus was purchased from Japan.

2.3. Measurement Procedure

Using the PV-HEPES- Yb^{3+} ensemble, we detected inorganic phosphorus in serum and milk samples. The procedures were as follows. In 10mM, pH 7.0 HEPES buffer containing $50\mu\text{M}$ PV and $100\mu\text{M}$ Yb^{3+} (a blue solution), the serum sample from one healthy volunteer was gradually titrated into the solution. At the same time the changes in the absorption peaks of solution in the UV-Vis spectrum were recorded. When no more changes in the absorption peaks of the system took place, titration came to a halt. Then we could calculate the inorganic phosphorus concentration in serum. Likewise, the inorganic phosphorus concentrations of human milk degreased or commercial milk were obtained by above detecting method.

3. RESULTS AND DISCUSSION

3.1. UV-Vis Spectra

Figure 1a shows the UV-v(V)is spectra obtained when

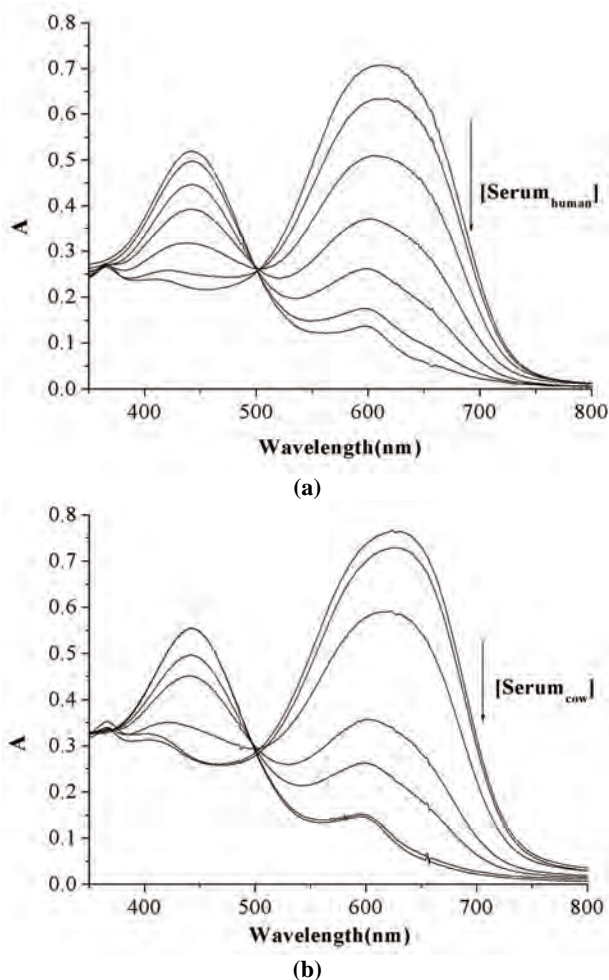


Figure 1. (a) The serum from human was added into PV-HEPES- Yb^{3+} with $V_{\text{serum}}=0-215\ \mu\text{L}$; (b) the serum from cow was added into PV-HEPES- Yb^{3+} with $V_{\text{serum}}=0-90\ \mu\text{L}$.

titrating the serum from a health human into the 10 mM, pH 7.0 HEPES buffer solution containing $100\ \mu\text{M}$ YbCl_3 and $50\ \mu\text{M}$ PV. With the addition of serum, the absorption peak at 623 nm decreased, while the peak at 444 nm increased. When the total volume of added serum reached $210\ \mu\text{L}$, titration ended. The concentration of inorganic phosphorus was $0.95\ \text{mmol/L}$. Similarly, **Figure 1b** shows UV-v(V)is spectra of serum from cow titrated. The concentration of inorganic phosphorus from cow was $2.20\ \text{mmol/L}$. **Figure 2a** shows UV-v(V)is spectra changes when titrating milk from healthy woman into our system. The inorganic phosphorus concentration of milk from lactation mother was $2.31\ \text{mmol/L}$. **Figure 2b** shows UV-v(V)is spectra changes of milk from commerce process titrated. The inorganic phosphorus concentration of milk from commerce was $11.54\ \text{mmol/L}$.

3.2. Selectivity over Other Constituents

In published paper, we addressed the selectivity of the system. We knew that the ensemble exhibited excellent

selectivity towards phosphate anions over other common anions, including Cl^- , SO_4^{2-} , CH_3COO^- , HCO_3^- and ClO_4^- [17]. Serum contains many other organic and inorganic compounds, such as creatinine, bilirubin, sugar, albumen, inorganic salts and transition ion besides the aforementioned ordinary anions. Do these compositions show some responsibility for the changes in the UV-vis spectra and color? We took the HEPES buffer as a blank, and then added 200 μL serum into it. The result shows that there is no UV-vis absorbance in the range of from 350 to 1,000 nm, suggesting that there are no other absorbance peaks coming from other compounds of the serum in the range of detection in the UV-vis spectra (Figure 3a). Thus, we may conclude that the changes in the absorbance peak in this range resulted completely from the measurement processes and there was no cumulation or disturbance. To prove that the universal existence of anions in serum incurs no dis-

turbance to exclude the possibility of interference from iron or other cations in the measurement, the following experiments were carried out. Firstly, as soon as the excessive 2 mM YbCl_3 was added into the 2 mM HPO_4^{2-} solution ($V_{\text{YbCl}_3}/V_{\text{HPO}_4^{2-}}=1.02:1$), precipitation occurred, a clear solution was gained through centrifugation and decantation processes; the solution (from 0 to 500 μL) was then added into 2 mL 10 mM HEPES buffer containing 50 μM PV and 100 μM Yb^{3+} , and no changes in absorption peak intensity and color were observed, i.e., no phosphate was detected in the solution, thus suggesting that the Yb^{3+} could completely remove HPO_4^{2-} from solution by forming sediment. Similarly, we added the excessive YbCl_3 into the collected serum samples whose content of HPO_4^{2-} was presumably quantitated with our methods. After the mixture had been treated in accordance with the aforementioned procedures, a great deal of the disposed serum sample (0–500 μL) was added into

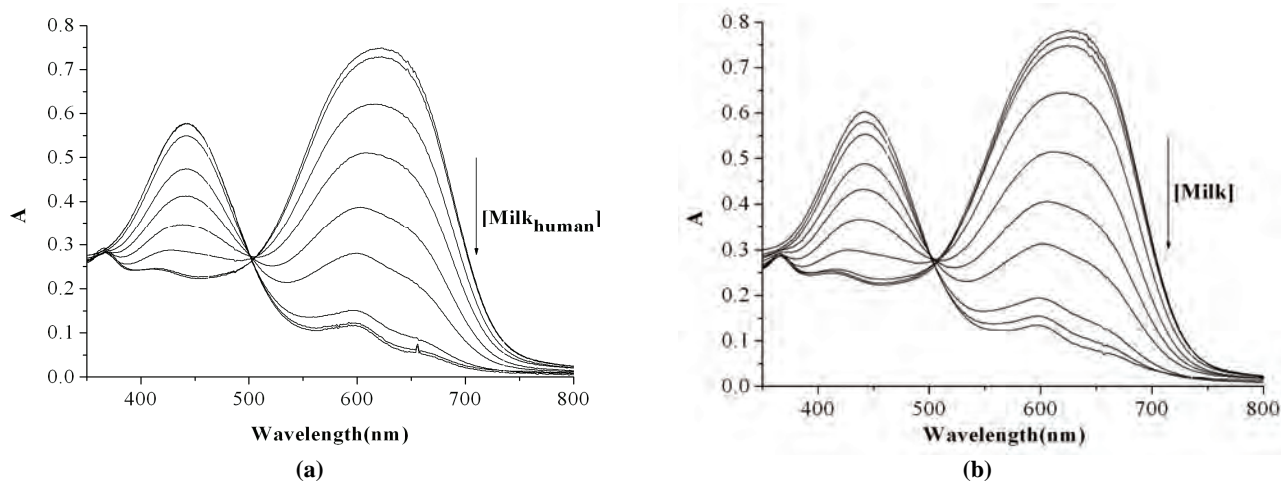


Figure 2. (a) The milk from woman was added into PV- HEPES- Yb^{3+} with $V_{\text{milk}}=0-65 \mu\text{l}$; (b) the serum from cow was added into PV-HEPES- Yb^{3+} with $V_{\text{milk}}=0-13 \mu\text{l}$.

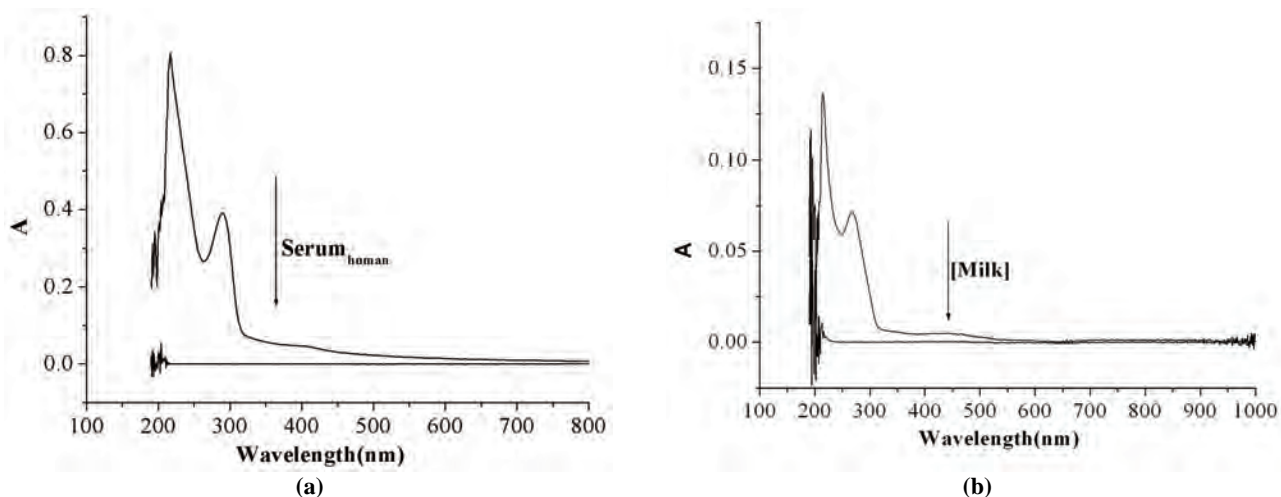


Figure 3. (a) UV/Vis spectra: Plot of absorbance (at $\lambda=200-1000 \text{ nm}$) when adding 20 μl urine into HEPES buffer (pH 7.0); (b) when adding 50 μl milk into HEPES buffer (pH 7.0).

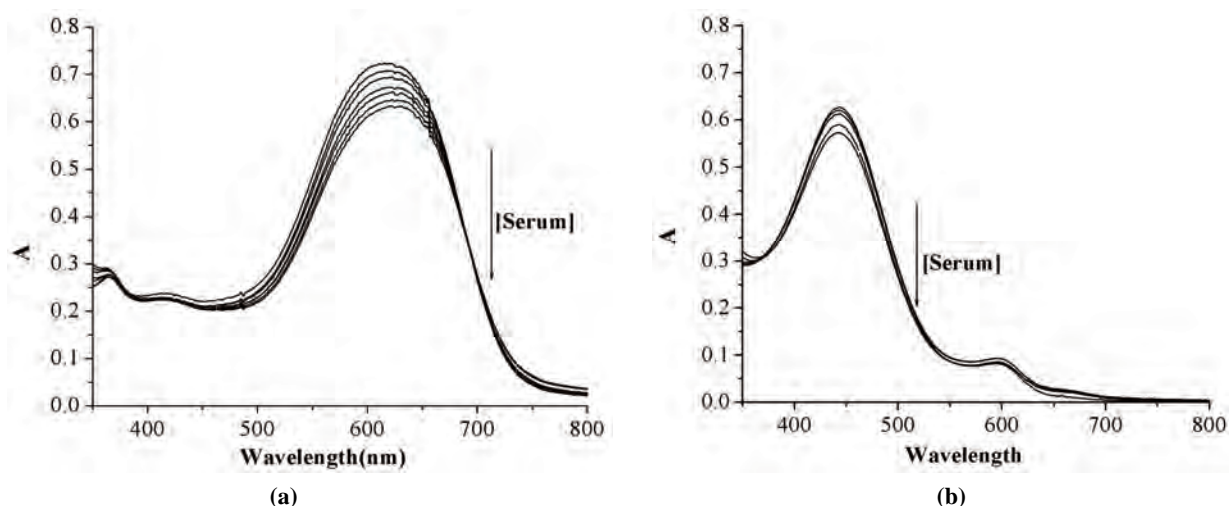


Figure 4. (a) the disposed serum sample (0-500 μ l) was added into PV-HEPES- Yb^{3+} . (b) UV/Vis spectra ($\lambda=350\sim 800\text{nm}$): no pretreatment serum sample (500 μ l) was added into HEPES-PV (50 μ M).

the 2 mL 10 mM HEPES buffer containing 50 μ M PV and 100 μ M Yb^{3+} , and no changes were observed in absorption peak intensity and system color (Figure 4a). The experiments excluded the possibility of interference from other anions with the measurement. In addition, we added an adequate amount of unpretreated serum sample into 2 mL 10 mM HEPES buffer only containing 50 μ M PV, and no change in either the UV-vis spectra or the system color was observed (Figure 4b). The system was still yellow. The experiments excluded the possibility of interference from iron or other cations with the measurement.

Now, we see about the selectivity of the detection system for milk. We took the HEPES buffer as a blank, and then added 50 μ L milk into it. The result shows that there is no UV-vis absorbance in the range of from 350 to 1,000 nm, suggesting that there are no other absorbance peaks coming from other compounds of the milk in the range of detection in the UV-vis spectra (Figure 3b). Similar process was done for proving no disturbance from other composition of milk. All results ensure that our system is special to phosphate of milk.

3.3. Linearity and Detection Limits

Most instrumental methods available for the determination of phosphate in clinical samples have a common drawback; that is, their linear calibration range is too narrow. In our experiment, we plotted the curve with absorbance values at 623 nm against concentrations /0–2.5 mM/ of serum added to the PV-HEPES- Yb^{3+} system. We found our measurement obeyed the Beer-Lambert absorption law very well within the serum concentration range of 0–2.5 mM. Linear regression with least-squares fitting yielded a correlation coefficient of

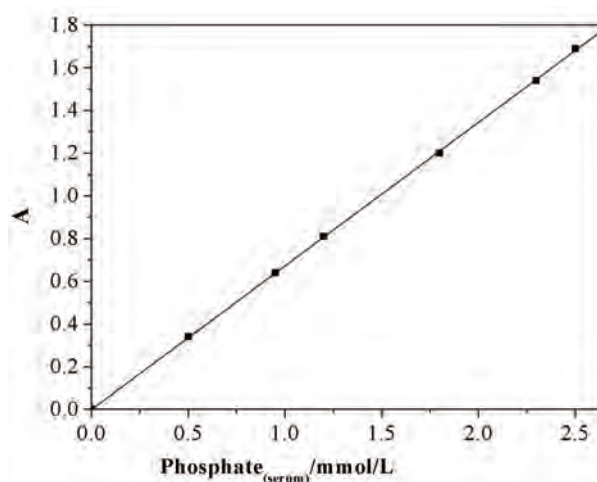


Figure 5. The working curve for serum measurement was plotted with the absorbance value against various concentrations of serum (0–2.5 mM).

0.99995 (Figure 5). The lower detection limit of our method is around 10^{-4} M. And before, we have gotten our measurement obeyed the Beer-Lambert absorption law very well within the urine concentration range of 0–70 mM [18]. Phosphorus concentrations of milk from woman or commerce are not higher than 70 mM, so this linear calibration range is enough for milk.

3.4. Validation

In order to validate the accuracy of the method, we detected serum samples by the standard procedure (molybdenum blue assay for phosphate) and obtained equivalent results with our measurement. Figure 6 and Table 1 give the results (spectra) for serum obtained with the two kinds of detection methods. Finally, the recovery experiments were performed: The results are

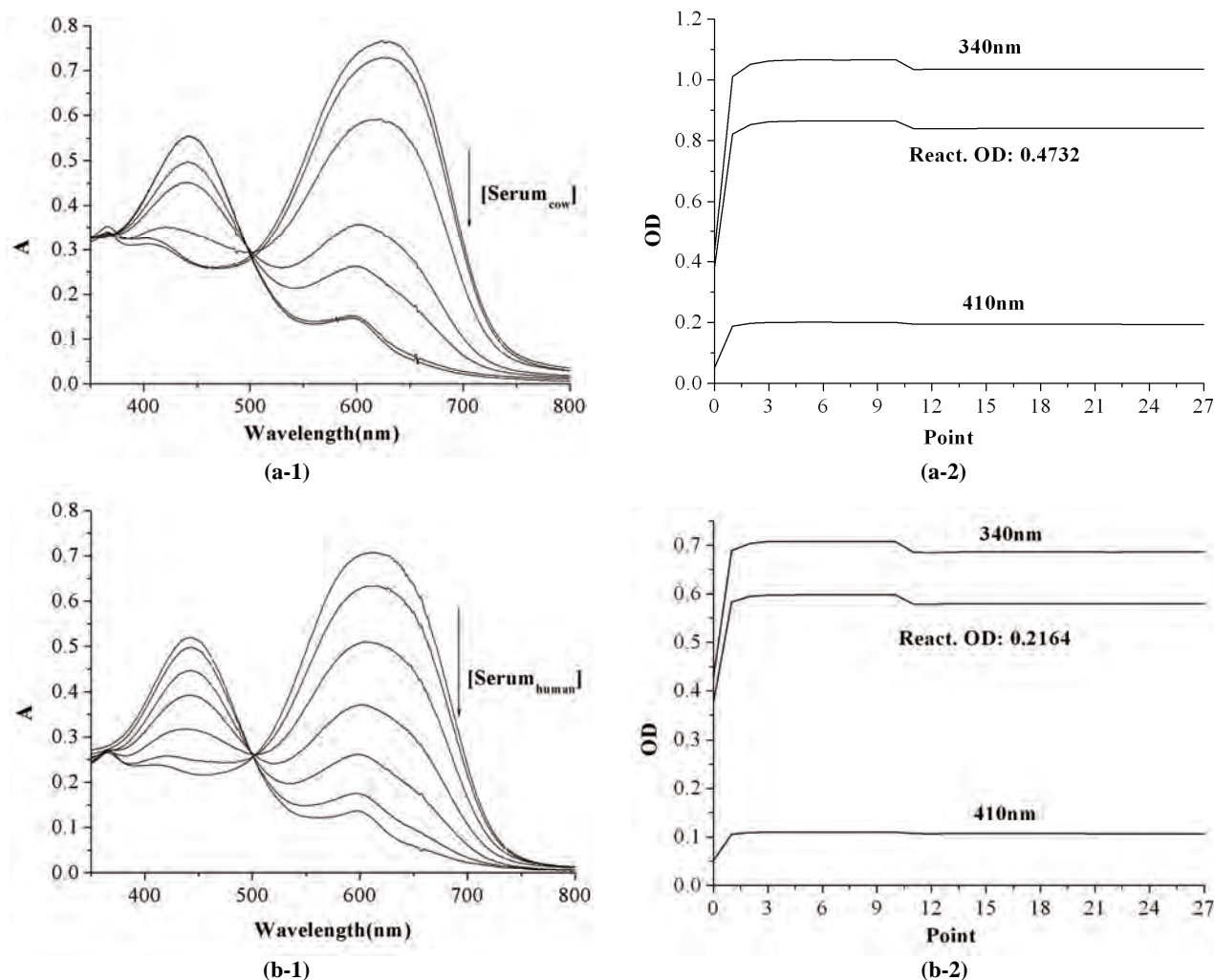


Figure 6. (a)Left: Uv-Vis spectra of cow serum sample Inorganic Phosphorus concentration from our method(2.20 mmol/L); Right: the results from Molybdenum blue assay for phosphate respectively(2.22 mmol/L); (b) Left: Uv-Vis spectra of serum sample Inorganic Phosphorus concentration from our method (0.95 mmol/L); Right: the results from Molybdenum blue assay for phosphate(0.93 mmol/L).

compiled in **Table 2**. The results indicated the accuracy of the method, as expressed by the calculated recovery values, was satisfactory.

3.5. Analysis of Results

From our data, we can see inorganic phosphorus content of milk is higher than foremilk about five times. This indicates the excessive inorganic phosphorus is disadvantageous to young child's growth. And with the people level of living enhancement, the commercial milk becomes the people basic nutriment. But in the processing commercial milk many important ingredients content are insufficient, for instance, the calcium, phosphorus ratio of is 2: 1 in milk containing the few calcium, many phosphorus, is easy to form the insoluble calcium phosphate, affects the intestinaltract absorbing calcium and

phosphorus. If provide turnips containing many calcium, few phosphorus for the child who eats the milk, can correct calcium and phosphorus proportion, namely can enhance the calcium absorbing capacity. Therefore, the reasonable increase and the adjustment can only prevent to be out of nutrition balance for one people drink milk.

3.6. Assay Advantage

Ion-based chromogenic method has proved to be a useful tool for clinical analysis because of its simplicity, repeatability, low reagent consumption and so on. We know that ion chromatography, the use of deproteinizing agents presents several disadvantages: perchloric acid and trichloroacetic acid need to be removed from the sample by time-consuming procedures otherwise they

Table 1. Results of our method against the method (molybdenum blue assay for phosphate).

Numbers of serum sample	Phosphate (mmolL ⁻¹) from Molybdenum blue assay	Phosphate (mmolL ⁻¹) from our method
1(Serum _{human})	0.96	0.97
2(Serum _{human})	0.93	0.95
2(Serum _{cow})	2.20	2.22

Table 2. Recovery of phosphate in serum and milk.

Sample	Added (phosphate) mmolL ⁻¹	Found (phosphate) mmolL ⁻¹	Recovery (%)
1(Serum)	—	1.48	
	0.6	2.02	95.9
2(Serum)	—	1.11	
	0.6	1.73	102
3(Serum)	—	0.95	
	0.6	1.53	97.3
4(Milk _{human})	—	2.34	
	1.0	3.42	104
5(Milk _{cow})	—	12.5	
	5	17.3	98.4

interfere with the elution profile; organic solvents such as acetonitrile lead to damage to the column and sulphosalicylic acid is often contaminated with sulphate, lead to sample dilution. And our method decreases the cost of analyses with respect to batch methods involving enzymes in solution. All these advantages make the method reported here be a valid alternative for the determination of phosphate in serum.

4. CONCLUSIONS

To sum up, we developed a sensitive, rapid and direct method for detecting serum and milk phosphate spectrophotometrically. Our method is suitable for performing direct determinations of phosphate in serum without any pretreatment and any interference. Now more and more people are suffering from lithiasis as a result of better living standards. Timely inspection of serum phosphate is one of the clinical means of diagnosis. Since long-time, people only pay attention to the inorganic phosphorus determination in the urine and the blood serum, to determine the inorganic phosphorus in the foremilk mother's milk and milk method very little was mentioned. In this paper, we use our invention system to quantitatively determine inorganic phosphorus concentration from milk degraded through centrifugation, the results are accurate, suit to clinical and the commerce use.

5. ACKNOWLEDGEMENTS

We acknowledge to the financial support of this work by the National Natural Science Foundation of China (No. 20801032), Shanxi Provincial Natural Science Foundation (No. 2009021006-2) and the Shanxi Province Foundation for Returness (2008).

REFERENCES

- [1] Grases, F. and March, J. G. (1990) Determination of phosphate based on inhibition of crystalline growth of calcite. *Analytica Chimica Acta.*, **229**, 249-254.
- [2] Ender, D. B. and Rude, R. K., (1999) Mineral and bone metabolism, In Tietz Textbook of Clinical Chemistry (C. A. Burtis, E. R. Ashwood, Eds.), W. B. Saunders, company: P. A. Philadelphia, 1406-1408, 1439-1440.
- [3] Kestenbaum, B., Sampson, J. N., Rudser, K. D., *et al.* (2005) Characterization of phosphate transport in rat vascular smooth muscle cells. *J Am Soc Nephrol.*, **16**, 520-528.
- [4] Levi, M. and Knochel, J. P. (1990) The management of disorders of phosphate metabolism. In *Therapy of Renal Diseases and Related Disorders* (S. G. Massry, W. N. Suki.), Boston, Martinus Nijhoff.
- [5] Levi, M., Cronin, R. E., and Knochel, J. P. (1992) Disorders of phosphate and magnesium metabolism. In *Disorders of Bone and Mineral Metabolism* (F. L. Coe, M. J Favus.), New York: Raven Press.
- [6] Biochrom Ltd Certificate No: 890333 Determination of phosphate in clinical samples.
- [7] Popovtzer, M., Knochel, J. P., and Kumar, R. (1997) Disorders of calcium, phosphorus, vitamin D, and parathyroid hormone activity. In *Renal Electrolyte Disorders*, edn 5 (R. W. Schrier.) Philadelphia: Lippincott-Raven.
- [8] Hruska, K. and Gupta, A. (1998) Disorders of phosphate homeostasis. In *Metabolic Bone Disease*, edn 3 (L. V. Avioli, S. M. Krane.) New York: Academic Press.
- [9] Greer, F. R., Steichen, J. J., and Tsang, R. C., (1982) Calcium and phosphate supplements in breast milk-related. *Rickets. Am J Dis Child.*, **136**, 581-583.
- [10] Fiske, C. H. and Subbarow, Y. J. (1925) The colorimetric determination of phosphorus. *Biol. Chem.*, **66**, 375-400.
- [11] Lowry, O. H. and Lopez, J. A. (1946) The determination of inorganic phosphate in the presence of labile phosphate ester. *J. Biol. Chem.*, **182**, 421.
- [12] Bartles, P. C. and Roijers, A. F. M. (1975) A kinetic study on the influence of parameters in the determination of inorganic phosphate by the molybdenum blue reaction. *Clin. Chim. Acta.*, **61**, 153-4.
- [13] Daly, J. A. and Ertingshausen, G. (1972) Direct method for determining inorganic phosphorus in serum. with the Centrifichem. *Clin. Chem.*, **18**, 263-265.
- [14] Urban, A. E. (1972) Simplified. serum phosphorus. analyses. by continuous-flow. ultraviolet. Spectrophotometry. *J. Clin. Chem.*, **18**, 601-4.
- [15] Fogg, A. G., Soleymanloo, S., and Burns, D. T. (1977) The spectrophotometric determination of inorganic phosphate in biological system with crystal violet. *Anal. Chim. Acta.*, **88**, 197-200.

- [16] Endres, B. D. and Rude, R. K. (1994) Mineral and bone metabolism. Tietz textbook of clinical chemistry (C. A. Burtis, E. R. Ashwood, eds.), Philadelphia: W. B. Saunders, Co., 1887-973.
- [17] Yin, C. X., Huo F. J., and Yang, P. (2005) An ion-based chromogenic detecting method for phosphate-containing derivatives in physiological condition. *Sensors and Actuators B Chemical.*, **109**, 291–299.
- [18] Yin, C. X., Huo, F. J., Yang, P. (2006) UV-Vis spectroscopic study directly detecting inorganic phosphorus in urine and our reagent kit. *Anal Bioanal Chem.*, **384**, 774-779.

Serum homocysteine concentrations of Chinese intellectuals and the influential factors concerned

Yue Hou*, Yan Hong, Wei-Qiang Chen, Dong-Lan Wang, Yi-Yong Cheng

*Institution of Hygiene and Environmental Medicine, Tianjin, China; Corresponding author: hoy77@sohu.com

Received 23 July 2009; revised 6 August 2009; accepted 7 August 2009.

ABSTRACT

Objective: To observe the concentration of serum homocysteine in intellectuals and the related influential factors. **Methods:** The concentrations serum homocysteine and saliva cortisol were measured in 138 intellectuals from three cities, Tianjin, Guangzhou and Chengdu in China. All the subjects had senior titles of technical post, aged 40-69 years. **Results:** The mean value of serum homocysteine concentration in intellectuals was $20.6 \pm 0.8 \mu\text{mol/L}$, higher than the reference value. With the increase of cortisol levels the homocysteine concentrations rise ($P < 0.05$). The mean value of homocysteine concentration was highest in 40-49 years old group. Men had higher homocysteine level than women in this investigation. According to the mean value of homocysteine concentration among different cities, Tianjin was highest, Chengdu medium, Guangzhou lowest. **Conclusion:** The serum homocysteine concentration of intellectuals is higher than the reference value. The stress level, gender and resident cities might contribute to the differences in serum homocysteine concentration in Chinese intellectuals.

Keywords: Homocysteine; Psychological Stress; Intellectual

1. INTRODUCTION

Stress induces several physiological and behavioral alterations that increase cardiovascular morbidity and mortality [1-3]. It is well known that total plasma homocysteine (tHcy) is now established as a clinical risk factor for coronary artery disease, as well as other arterial and venous occlusive disease in adult populations [4]. Nonetheless, only a few studies have evaluated the relationship between stress and tHcy level. In order to examine whether any acute effect on total plasma Homo-

cysteine (Hcy) concentrations in rats would occur four distinct acute stressors in rats, i.e., swimming, restrain, novelty and cold exposure were used. Plasma corticosterone and adrenocorticotrophic hormone concentrations were also measured to demonstrate the ability of the chosen manipulations to activate the hypothalamic-pituitary-adrenal (HPA) axis. Three of the four stressors activated the HPA axis and only restrain increased tHcy concentrations [5]. Stoney *et al.*'s study was to test if acute psychological stress could induce elevations in plasma Hcy concentrations. Thirty-four healthy women participated in this study. The results indicated significant elevations in plasma Hcy during acute psychological stress, with a return to baseline concentrations during recovery [6]. The complexity of the physiological responses to stress, the peculiarities of stress responses and the intricate regulatory systems involved in Hcy metabolism must be taken into account in order to clarify the increasing effect of restrain (mainly a psychological stressor) on total plasma Hcy in rats and to evaluate its meaning in human pathology.

Stress is one of the biggest problems faced by intellectuals today. The increasingly demanding nature of their jobs has also increased pressure levels dramatically. Research shows that intellectuals are now facing greater day-to-day problems with occupational stress than most other employees. Psychological stressors and depressive and anxiety disorders also are associated with psychosomatic disease such as heart disease, hypertension and diabetes, which have become the main factors impairing the intellectuals' health [7-10]. The intellectuals were selected from different resident cities in China as subjects and their serum Hcy levels and some influential factors were observed.

2. MATERIALS AND METHODS

2.1. Subjects

One hundred and thirty-eight volunteers between the ages of 40 and 69 years (mean age = 54.2 years) participated in the study after providing written informed consent. The 138 intellectuals come from three cities, Tianjin,

Table 1. The distribution of subjects by area, age and sex.

City	40-49(y)		50-59(y)		60-69(y)		Total
	Male	Female	Male	Female	Male	Female	
Tianjin	8	8	8	8	8	8	48
Guangzhou	5	5	5	5	5	5	30
Chengdu	10	10	10	10	10	10	60
Total	46		46		46		138

Guangzhou and Chengdu, and all the subjects had senior titles of technical post in university or science research institute or design institute. The distribution of participants is presented in **Table 1**.

2.2. Blood and Salivary Collection

The fasting blood samples were collected into chilled tubes, and immediately immersed in ice. The serums were separated by centrifugation within 30-min and stored at -20°C until analyses. The volunteers collected the saliva samples in the morning. Firstly they gargled three times, after 15 minutes they chew on citric acid slips for a few seconds to stimulate salivation (not use gum or any other food-type product) and collected the salivary with straw. The samples stored at -20°C within three hours and centrifuged before analysis [11,12].

2.3. Laboratory Analysis

Total Hcy was measured in serum by the Total-Homocysteine Enzymatic Assay method [13]. The principle of the assay is as follows. In reaction I, rHcyase specifically converts Hcy to α -ketobutyrate, ammonia, and H₂S. In reaction II, the H₂S combines with DBPDA to form 3,7-bis (dibutyl amino) phenothiazine-5-ium chlorides, which is highly fluorescent. For the reduction reaction, flat-bottomed 96-well cell culture cluster plates with low-evaporation lids were used (cat. no. 0720089; Corning). Twenty microliters of serum samples and 170 μ L of assay buffer [40mmol/L sodium phosphate buffer (pH 8.4), containing 2 mL/L Triton X-100 and 0.25 mmol/L DTT] were added to the wells. Two wells were used for each sample. Reduction reaction was carried out at 37°C for 30 min. It is necessary to break the disulfide linkages in plasma proteins and to reduce the low molecular weight disulfides Hcy and homocysteine-cysteine mixed disulfide in this reaction. For each sample, we added 30 μ L of rHcyase (0.05 g/L), the equivalent to 0.1 U, in 40mmol/L potassium phosphate buffer containing 20 μ mol/L pyridoxal phosphate. One unit of enzyme is defined as the amount that catalyzes 1 μ mol of H₂S per minute from Hcy. We added 30 μ L of enzyme buffer to the other well to serve as background. The enzymatic reaction was carried out at room temperature for 5 min. The lid was put on the dish to prevent possible loss of H₂S. The enzymatic reaction was stopped by the addition

of 30 μ L of chromophore reagent (20 mmol/L DBPDA in 3 mol/L H₂SO₄). The chromogenic reaction was carried out at room temperature for 10 min. The resulting fluorescence was measured at an excitation wavelength of 665 nm and an emission wavelength of 690 nm in Hcy special fluorescence spectral-photometer (JD Biotech Co., Ltd.).

Cortisol level was measured with a RIA kit, a product of Isotope Institute, Chinese Atomic Energy Science Academy [14].

2.4. Statistical Analysis

Continuous variables were summarized as the mean \pm SE. One-way ANOVA were used to compare group means. Statistical significance was defined as $P < 0.05$. Subjects with missing data were dropped from the analysis.

3. RESULTS

129 saliva samples were collected. The Hcy concentrations and the cortisol levels of all subjects were compared (see **Figure 1**). A significant relation between Hcy concentrations and the cortisol levels was observed ($r=0.21$, $P<0.05$). With the increase of cortisol levels the Hcy concentrations rise.

The average level of salivary cortisol was 10.3 μ g/L. The subjects was divided into two groups, low cortisol group (LCor, $<10.3\mu$ g/L) and high cortisol group (HCor, $\geq 10.3\mu$ g/L). As expected the HCor had significantly higher serum concentrations of Hcy than the LCor (see **Table 2**).

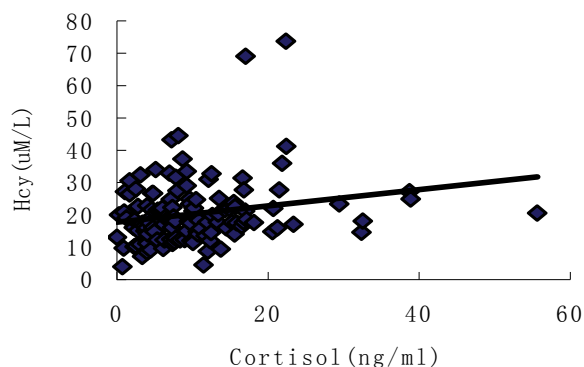
**Figure 1.** The correlation plots of serum Hcy and cortisol concentrations.

Table 2. Saliva cortisol and serum homocysteine concentrations in LCor and HCor groups ($\bar{x} \pm s_{\bar{x}}$).

Group	n	Cortisol ($\mu\text{g/L}$)	Hcy ($\mu\text{mol/L}$)
LCor	77	5.5 \pm 0.3	18.4 \pm 0.8
HCor	52	18.1 \pm 1.3	22.0 \pm 1.7
Total	129	10.3 \pm 0.7	20.3 \pm 0.9

$P < 0.05$

Table 3. Comparison of serum homocysteine concentration by age ($\bar{x} \pm s_{\bar{x}}$).

Age (y)	n	Hcy ($\mu\text{mol/L}$)
40-49	46	23.2 \pm 1.6 ^a
50-59	46	19.0 \pm 1.4 ^b
60-69	46	19.5 \pm 1.2
Total	138	20.6 \pm 0.8

Values with different superscripts are significantly different ($P < 0.05$)

Table 4. Differences of serum homocysteine concentrations between male and female ($\bar{x} \pm s_{\bar{x}}$).

Sex	n	Hcy ($\mu\text{mol/L}$)
Male	69	24.0 \pm 1.5
Female	69	16.9 \pm 0.6

$P < 0.05$

Table 5. Serum homocysteine concentrations of subjects in three cities ($\bar{x} \pm s_{\bar{x}}$).

City	n	Hcy ($\mu\text{mol/L}$)
Tianjin	48	22.4 \pm 1.5 ^a
Guangzhou	30	17.1 \pm 2.3 ^b
Chengdu	60	20.5 \pm 1.0

Values with different superscripts are significantly different ($P < 0.05$)

The mean value of serum Hcy concentration in intellectuals was 20.6 \pm 0.8 $\mu\text{mol/L}$. The mean value of Hcy concentration was highest in 40-49 years old and lowest in 50-59 years old. There was significant difference between 40-49 years group and 50-59 years group (see **Table 3**).

Among the subjects the average Hcy level of men was significant higher than women (see **Table 4**).

The average Hcy levels among the three cities were compared. The average Hcy level of the volunteers in Tianjin was highest, medium in Chengdu, lowest in Guangzhou. But only significant difference was observed between Tianjin and Guangzhou (see **Table 5**).

4. DISCUSSION

Hcy is a sulfur-containing amino acid generated through the demethylation of methionine. The resulting Hcy is either remethylated to methionine through methionine synthase (MS), a process that utilizes folate and vitamin B12 as cofactors, or catabolized by transsulfuration into cystathionine through cystathionine- β -synthetase (CBS)

if excess Hcy is present, using vitamin B6 as cofactor [15]. It is also controlled by individual genetic differences in how vitamins are utilized as cofactors in the reactions controlling Hcy metabolism. In excess quantities, Hcy is thought to be thrombophilic and to damage the vascular endothelium. Total plasma homocysteine (tHcy) is now established as a independent risk factor for coronary artery disease, as well as other arterial and venous occlusive disease in adult populations [4,16-18].

The third National Health Examination Survey showed the first data on Hcy concentration in a nationally representative sample of Americans. The Survey measured serum total Hcy concentrations for a nationally representative samples of 3766 males and 4819 females aged ≥ 12 y. The normal total plasma Hcy concentrations of Americans was in the range of 5 $\mu\text{mol/L}$ to 15 $\mu\text{mol/L}$ and affected by age, sex and race [19]. Yan *et al.* reported that Chinese average plasma Hcy level reference was (9.67 \pm 3.0) $\mu\text{mol/L}$, 95% confidence interval was 3.79 $\mu\text{mol/L}$ to 15.55 $\mu\text{mol/L}$. Zhang *et al.* investigated 1226 middle- and old-age people and the average plasma Hcy level was 9.1 $\mu\text{mol/L}$ [20]. The present study reflected that the average serum Hcy level of the intellectuals aged 40-69 in Tianjin, Guangzhou and Chengdu was higher than the level other study showed.

It is now generally accepted that psychological stress is a multi-dimensional and multi-level phenomenon that is influenced by personal, situational or structural factors. Studies of occupational stress indicate that workload and communications are significant causes. Anticipation, worry, helplessness and executive roles have all emerged from laboratory studies as psychological factors inducing stress. Several studies concur in finding that poor working conditions, especially relationships with colleagues, overload, and poor school ethos are the major causes of intellectual stress. There is considerable evidence, mainly from self-reports, that intellectuals feel ill as a consequence of excessive stress. However, available absence and retirals statistics are not sufficiently specific to support this connection [8]. Generally cortisol level was recognized to be an index judging the degree of stress [11,12]. Our study showed that the serum Hcy concentration of high saliva cortisol concentration group was significant higher than low saliva cortisol concentration group. The result indicated that psychological stress could be one of the reasons causing the increase of serum Hcy level and the stress degree may connect with the level of serum Hcy. Stoney *et al.*'s study was to test the hypothesis that acute psychological stress induces elevations in plasma Hcy concentrations. Thirty-four healthy women participated in the study. The psychological stressors included standard mental arithmetic and speech stressors and heart rate and blood samples were also monitored. Results indicated significant elevations in plasma Hcy during acute psychological stress, with a

return to baseline concentrations during recovery. The pattern of findings for blood pressure and heart rate was similar, suggesting that the rise in Hcy concentrations may have been sympathetically mediated [6]. But the related mechanism remains unclear.

It is known that many physiological variables influencing Hcy concentrations. Circulating tHcy increases with age in both genders—an effect that is partly due to decreasing renal function, partly due to increasing prevalence of subclinical and clinically demonstrable vitamin deficiency, or to other independent metabolic factors. In particular, aging may be associated with decrease CBS activity [21]. However our study showed that there is no trend of increase of Hcy concentrations with the increase of age. On the contrary in the three age group 40-49 years old group had highest level of serum Hcy. That the intellectuals in 40-49 years group carried more work, burden and stress may be the reason of their high Hcy concentration.

This investigation demonstrated that men had higher Hcy level than women and there are much epidemiological evidence identifying the similar result [22-27]. In a multicentre case-control study in Europe vascular disease of the coronary, cerebral, of peripheral vessels and 800 control subjects (570 men, 230 women) were enrolled. The tHcy comparison between the sexes was carried out among control subjects only. The results showed that fasting tHcy levels were lower in women than in men [21]. The gender difference in fasting tHcy may be caused by hormonal differences between men and women. The hypothesized tHcy-lowering effect of oestrogens is derived from the observation that tHcy concentrations are lower in pregnant than in non-pregnant women [28,29]. Strong evidence for the effects of hormones on plasma tHcy levels is derived from a study in which male to female transsexuals showed a decreased geometric mean tHcy, and female to male transsexuals an increase [30]. Dierkes *et al.*'s study comprised 336 men and women, aged 40 to 65 years, obtained from an ongoing recruitment procedure. Plasma tHcy, folate, vitamin B12, vitamin B6, fat-free mass, creatinine, testosterone and estradiol, protein, and hematocrit were detected. From the gender-related variables, tHcy correlated significantly with fat-free mass and testosterone and inversely with estradiol. The difference between genders with regard to tHcy was mainly explained by differences in fat-free mass, but also by estradiol concentration [23].

This study demonstrated that the average serum Hcy concentration of intellectuals in Tianjin was significant higher than that in Guangzhou. Tianjin and Guangzhou are located in north and south of china respectively and there are many differences in diet habit, prandial structure and economic condition between these two cities. Hao *et al.*'s study investigated 2545 subjects' plasma folate concentrations, sampled from the representative

rural and urban areas in the south and north of China aged 35 to 64 years. Plasma concentrations of folate in southern population were significant higher (16.9 nmol/L) than those in the north (8.3 nmol/L), and the prevalence of folate deficiency in the south (5.8%) was significantly lower than that in the north (37.1%) [31]. Folate level is one of the main nutrition factors that affects the level of Hcy in body, so the Hcy concentration difference between Tianjin and Guangzhou may due to the difference of folate condition in this two cities.

In conclusion, the serum homocysteine concentration of intellectuals is higher than that of normal people. The stress level, gender and resident cities might contribute to the differences in serum homocysteine concentration in Chinese intellectuals. The epidemiological study showed that Hcy is not only pro-atherogenic and pro-thrombotic, it is biologically plausible that high Hcy levels may cause brain injury and neuropsychiatric disorders. Cross-section and some longitudinal studies support increased prevalence of stroke and vascular dementia in hyper-homocysteinemic individuals. The evidence of increased neurodegeneration caused by hyper-homocysteine is accumulating [17,32-34]. Thus to study and control the serum Hcy level of intellectuals are very important to handle and improve the health condition of intellectuals. To verify the exact relation between psychological stress and the difference of Hcy level, much more study and intervention experiment should be conducted in the future.

REFERENCES

- [1] Folkow, B. (2001) Mental stress and its importance for cardiovascular disorders; physiological aspects, "from-mice-to-man". *Scand Cardiovascular Journal*, **35**(3), 163-72.
- [2] Zwerenz, R., Knickenberg, R.J., Schattenburg, L., and Beutel, M.E. (2004) Work-related stress and resources of psychosomatic patients compared to the general population. *Rehabilitation (Stuttg)*, **43**(1), 10-6.
- [3] Von Kanel, R., Mills, P.J., Fainman, C., and Dimsdale, J.E. (2001) Effects of psychological stress and psychiatric disorders on blood coagulation and fibrinolysis: A biobehavioral pathway to coronary artery disease. *Psychosomatic Medicine*, **63**(4), 531-44.
- [4] Loralie, J. L. and David, E. C. C. (1999) Homocysteine. critical reviews in clinical laboratory sciences, **36**(4), 365-406.
- [5] Oliveira, A.C., Suchecki, D., Cohen, S., and Almeida, V. D. (2004) Acute stressor-selective effect on total plasma homocysteine concentration in rats. *Pharmacology, Biochemistry and Behavior*, **77**(2), 269-273.
- [6] Stoney, C.M. (1999) Plasma homocysteine levels increase in women during psychological stress. *Life Sciences*, **64**(25), 2359-2365.
- [7] Cooper, C.L. (1993) The role of stress in the health and disease process. *British Journal of Hospital Medicine*,

- 50(9)**, 562.
- [8] Valerie, W. (2002) Feeling the Strain an overview of the literature on teachers' stress. SCRE Research Report 109, 1-33.
- [9] Cooper, C.L. and Kelly, M. (1993) Occupational stress in head teachers: A national UK study. *British Journal of Educational Psychology*, **63(Pt 1)**, 130-143.
- [10] Edwards, J.R., Cooper, C.L., Pearl, S.G., de Paredes, E.S., O'Leary, T., and Wilhelm, M.C. (1990) The relationship between psychosocial factors and breast cancer: some unexpected results. *Behavior Medicine*, **16(1)**, 5-14.
- [11] Tunn, S., Mollmann, H., Barth, J., Derendorf, H., Krieg, M. (1992) Simultaneous measurement of cortisol in serum and saliva after different forms of cortisol administration. *Clinical Chemistry*, **38(8 Pt 1)**, 1491-1494.
- [12] Bonnin, R., Villabona, C., Rivera, A., Guillen, E., Sagarra, E., Soler, J., and Navarro, M.A. (1993) Is salivary cortisol a better index than free cortisol in serum or urine for diagnosis of Cushing syndrome? *Clinical Chemistry*, **39(6)**, 1353-4.
- [13] Tan, Y., Tang, L., Sun, X., Zhang, N., Han, Q., Xu, M., An, Z., Andrew, W., Perry, and Robert, M. H. (2000) Total-homocysteine enzymatic assay. *Clinical Chemistry*, **46(10)**, 1686-1688.
- [14] Morineau, G., Boudi, A., Barka, A., Gourmelen, M., Degeilh, F., Hardy, N., al-Halnak, A., Soliman, H., Gosling, J.P., Julien, R., Brerault, J.L., Boudou, P., Aubert, P., Villette, J.M., Pruna, A., Galons, H., and Fiet, J. (1997) Radioimmunoassay of cortisone in serum, urine, and saliva to assess the status of the cortisol-cortisone shuttle. *Clinical Chemistry*, **43(10)**, 1397-407.
- [15] Finkelstein, J.D. and Martin, J.J. (1986) Methionine metabolism in mammals: adaptation to methionine excess. *Journal of Biological Chemistry*, **261(4)**, 1582-1587.
- [16] Rees, M.M. and Rodgers, G.M. (1993) Homocysteine: association of a metabolic disorder with vascular disease and thrombosis. *Thromb Research*, **71(5)**, 337-359.
- [17] Blundell, G., Rose, F.A., and Tudball, N. (1994) Homocysteine induced endothelial cell toxicity and its protection. *Biochemical Society Transactions*, **22(3)**, 341S.
- [18] McCully, K.S. (1993) Chemical pathology of homocysteine. I. Atherogenesis. *Annual of Clinical Laboratory Sciences*, **23(6)**, 477-493.
- [19] Jacques, P.F., Rosenberg, I.H., Roger, G., Selhub, J., Bowman, B.A., Gunter, E. W., Jacquelin, D., and Johnson, C. (1999) Serum total homocysteine concentrations in adolescent and adult Americans: results from The Third National Health and Nutrition Examination Survey. *American Journal of Clinical Nutrition*, **69(3)**, 482-489.
- [20] Zhang, F.R., Hao, L., Wang, J.Y., Lu, Y.Y., Zhu, M.M., Jiang, X.Y., and Yu, N. (2003) The investigation of plasma homocysteine levels in middle- and old-aged people. *Jiangsu Health Care*, **5(4)**, 31-32.
- [21] Sachdev, P. (2004) Homocysteine and neuropsychiatric disorders. *Revista Brasileira De Psiquiatria*, **26(1)**, 49-55.
- [22] Verhoef, P., Meleady, R., Daly, L.E., Graham, I.M., Robinson, K., and Boers, G.H. (1999) Homocysteine, vitamin status and risk of vascular disease—effects of gender and menopausal status. *European Heart Journal*, **20(17)**, 1234-1244.
- [23] Dierkes, J., Jeckel, A., Ambrosch, A., Westphal, S., Luley, C., and Boeing, H. (2001) Factors explaining the difference of total homocysteine between men and women in European Investigation into Cancer and Nutrition Potsdam study. *Metabolism*, **50(6)**, 640-645.
- [24] Jacobsen, D.W., Gatautis, V.J., Green, R., Robinson, K., Savon, S.R., Secic, M., Ji, J., Otto, J.M., and Taylor, L.M. Jr. (1994) Rapid HPLC determination of total homocysteine and other thiols in serum and plasma: sex differences and correlation with cobalamin and folate concentrations in healthy subjects. *Clinical Chemistry*, **40(6)**, 873-881.
- [25] Brattstrom, L., Lindgren, A., Israelsson, B., Andersson, A., and Hultberg, B. (1994) Homocysteine and cysteine: determinants of plasma levels in middle-aged and elderly subjects. *Journal of International Medicine*, **236(6)**, 633-641.
- [26] Lussier-Cacan, S., Xhignesse, M., Piolot, A., Selhub, J., Davignon, J., and Genest, J. Jr. (1996) Plasma total homocysteine in healthy subjects: sex specific relation with biological traits. *American Journal of Clinical Nutrition*, **64(4)**, 587-593.
- [27] Andersson, A., Brattstrom, L., Israelsson, B., Isaksson, A., Hamfelt, A., and Hultberg, B. (1992) Plasma homocysteine before and after methionine loading with regard to age, gender, and menopausal status. *European Journal Clinical Investigation*, **22(2)**, 79-87.
- [28] Kang, S.S., Wong, P.W.K., Zhou, J., and Cook, H.Y. (1986) Total homocysteine in plasma and amniotic fluid of pregnant women. *Metabolism*, **35(10)**, 889-891.
- [29] Andersson, A., Hultberg, B., Brattstrom, L., and Isaksson, A., (1992) Decreased serum homocysteine in pregnancy. *European Journal of Clinical Chemistry and Clinical Biochemistry*, **30(6)**, 377-379.
- [30] Giltay, E.J., Hoogeveen, E.K., Elbers, J.M.H., Gooren, L.J.G., Asscheman, H., and Stehouwer, C.D.A. (1998) Effects of sex steroids on plasma total homocysteine levels: a study in transsexual males and females. *Journal of Clinical Endocrinology and Metabolism*, **83(2)**, 550-553.
- [31] Hao, L., Tian, Y., Zhang, F., Zhong, X.Y., Zhang, B.L., Tan, M., Tang, Y., and Li, Z. (2002) Variation of plasma folate levels in adults between some areas and different seasons in China. *Chinese Journal of Prevention Medicine*, **36(5)**, 308-310.
- [32] Seshadri, S., Beiser, A., Selhub, J., Jacques, P.F., Rosenberg, I.H., D'Agostino, R.B., Wilson, P.W., and Wolf, P.A. (2002) Plasma homocysteine as a risk factor for dementia and Alzheimer's disease. *The New England Journal of Medicine*, **346(7)**, 476-483.
- [33] Mattson, M.P., Kruman, I.I., and Duan, W. (2002) Folic acid and homocysteine in age-related disease. *Ageing Research Reviews*, **1(1)**, 95-111.
- [34] Kuhn, W., Roebroek R., Blom, H., van Oppenraaij, D., Przuntek, H., Kretschmer, A., Buttner, T., Voitalla, D., and Muller, T. (1998). Elevated plasma levels of homocysteine in Parkinson's disease. *European Neurology*, **40(1)**, 225-227.

A comparison study of two breathing exercise techniques in tetraplegics

Stanley John Winser¹, Jacob George², Priya Stanley¹, George Tharion²

¹Masterskill University of Health Science (MUCH), Cheras, Malaysia; stanjwpt@gmail.com, stanjw_pt@yahoo.com, stanley@masterskill.edu.my

²Christian Medical College, Vellore, India.

Received 15 July 2009; revised 23 July 2009; accepted 25 July 2009.

ABSTRACT

Objective: To compare the effectiveness of abdominal weights and incentive spirometry for improving the strength of diaphragm in tetraplegics.

Setting: Department of Physical Medicine and Rehabilitation, Christian Medical College, Vellore, Tamil Nadu, India.

Study Design: Two group comparison study

Methods: Seventeen patients who fulfilled the inclusion criteria were assigned into an ABW or INS treatment groups using judgment sampling after obtaining an informed consent. Evaluation of the chest, respiratory status, vital signs and strength of diaphragm were done during initial assessment. ABW group underwent diaphragmatic strengthening using Abdominal weights (ABW) and INT group with Incentive Spirometer (INS) for 15 minutes daily, 6 days a week, for a period of 6 weeks. The pre and post training values of peak amplitude in electro myogram (EMG) of the diaphragm, intercostals and sternocleidomastoid muscles were measured.

Statistical analysis: The analysis was done using SPSS 11. The pre and post-training values of peak EMG amplitudes of the diaphragm, intercostals and sternocleidomastoid were compared within the groups using Wilcoxon's sign test and between the two groups using Mann-Whitney's test.

Results: The peak EMG of diaphragm of ABW group raised from 1.1289 to 1.3036 milli-volts with a significance of $p < 0.001$, whereas it fell from 1.7001 to 1.0441 milli-volts among INS group subjects with a significance of $p < 0.001$. Comparison between the 2 groups showed statistically significant improvement in diaphragmatic strength among the ABW group.

Conclusion: The results of this study suggests that, in the pulmonary rehabilitation of

motor complete tetraplegic subjects abdominal weighted training of the diaphragm has better results in improving the strength of the muscle. **Sponsorship:** Fluid research grant of Christian Medical College, Vellore.

Keywords: Spinal Cord Injury; Tetraplegia; Diaphragmatic Exercise; Surface EMG; Abdominal Weights; Incentive Spirometer

1. INTRODUCTION

Spinal cord injury (SCI) at cervical level results in tetraplegia with or without paralysis of diaphragm. Among complete tetraplegics with intercostals and diaphragmatic paralysis there is severe respiratory insufficiency especially in the acute stage of illness [1]. Respiratory insufficiency leads to high mortality rate in these patients [2]. Following cervical cord injury there is paralysis of respiratory muscles [3] which leads to accumulation of secretions. Failure of cough mechanism causes recurrent infections which further compromises lung functions and add to morbidity and mortality.

Studies on pulmonary function tests of individuals with complete tetraplegia have shown that there is a major loss of expiratory reserve volume due to paralysis of expiratory muscles causing reduction of maximal expiratory pressure. The work of breathing is increased and the diaphragm is prone to fatigue particularly in patients with high cervical cord lesion [4]. Physiotherapy management strategies aspire at improving efficiency of diaphragm and training the available accessory muscles to compensate for paralyzed respiratory muscles. Progressive resisted exercises have been used in strengthening respiratory muscles for high tetraplegic patients [5]. There are various methods describe in literature to improve the efficiency of diaphragm [6], which includes Resisted Inspiratory Muscle Training (RIMT) [7,8,9], Weighted diaphragmatic exercise [10], Abdominal binders [11], Trendlenbergs position and Incentive spirometry.

There is paucity of literature which compares the effectiveness of abdominal weighted training and incentive spirometry in improving the strength of diaphragm. This study designed at evaluating the effectiveness of two pulmonary rehabilitation programmes (weighted diaphragmatic exercise against incentive spirometry) which are commonly practiced for training the diaphragm among patients with spinal cord injury.

2. MATERIALS AND METHODS

This study was approved by the Institutional review board and ethics Committee of Christian Medical College. The background of the study was explained to the subjects in his/her language and the patients who were willing to participate were inducted into the study following an informed written consent. The sample size was calculated to be 6 in each group with ABW group as subjects trained with abdominal weights and INS group as subjects trained with incentive spirometry. The subjects with neurological level between C5 and C8 ASIA [12] grade A & B, 1 month post injury, muscle strength of diaphragm more than fair plus, medically stable patients and without any current lung infections or comorbidity were included in the study. Subjects with associated Traumatic Brain Injury (TBI), past history of Chronic Obstructive Pulmonary Disease, Tuberculosis and chronic smokers were excluded.

2.1. Sample Size & Method

The sample size was calculated with 5% alpha level and 80% power, with having a SD of 0.73 and 0.32; the sample size was found to be 6 in each group. We had adopted judgment sampling method. The subjects who underwent weighted diaphragmatic training had to lie supine. Since some subjects had pressure ulcer over the sacral region, supine lying was contraindicated, which made us to assign them into the INS group.

2.2. Evaluation of Strength [13]

The strength of diaphragm was graded using the grades as follows. "Poor power": is being graded if the subject is not able to expand his/her epigastric region fully on deep inspiration. "Fair power": if the subject is able to expand his/her epigastric region fully on deep inspiration. "Good power": the therapist's hands are placed over the epigastric region with fingers spread, and the subject is asked to inhale, while maximum manual resistance is applied. If the subject is able to complete a full epigastric raise against resistance then he/she can be graded as Good. The subjects who are able to take resistance but not able to hold can be graded as "Fair plus". Subjects with diaphragmatic power of fair plus and above were considered for progressive resisted exercises. Prior to the commencement of training, the EMG activity of the

diaphragm, intercostals and sternocleidomastoid muscles were evaluated.

2.3. Outcome Measure (EMG Analysis)

The EMG activity was measured using 3 pairs of Silver chloride bipolar surface electrode. The active electrodes were placed over T7 & T8 intercostal space, T4 & T5 intercostal space and mid portion of sternocleidomastoid to get the electrical activity of diaphragm, intercostals and sternocleidomastoid muscles respectively [14], readings of all three groups of muscles were taken simultaneously (see **Figure 1**). Electrodes were secured to the skin using adhesive plaster after skin preparation. While taking the readings the subjects were instructed to take 3 consecutive deep inspirations followed by expiration, reading were recorded for 10 seconds and the peak amplitudes in the EMG recordings noted. The investigator who performed this test was blinded to either group. Three trials were done and the best response of peak amplitude was noted.

2.4. Intervention

The subjects were allotted into both groups using the above mentioned sampling method. Subjects of both the groups concurrently underwent other rehabilitative programs such as passive range of motion exercise, activities of daily living, standing using tilt or standing table, strengthening or re-education for the available muscles. In the ABW group, diaphragm was strengthened using abdominal weights for 15 minutes per day for six days weekly for a period of 6 weeks. The subjects of INS group underwent training using incentive spirometer for the same period as ABW group.

2.5. Evaluation of Weight [15]

To train the ABW group, the appropriate weights to



Figure 1. Showing placement of surface electrodes for the assessment of EMG activity of Intercostals, Diaphragm and Sternocleidomastoid muscles.

strengthen the diaphragm were evaluated using the following method. The subject was positioned in supine lying, then a minimal weight was placed over the epigastric region (weights starts with half a kilogram) and then the subject was allowed to breath (the weight should come up fully with each inspiration). If the subject showed any signs of fatigue or started using his/her accessory muscles, the weights were taken off immediately. Adequate rest was given, then the procedure was repeated using a lesser weight, and if the patient is able to take up the weight comfortably for 15 minutes, a short break was given and the procedure was repeated by increasing the weight by half a kilogram, thus the appropriate weight for training the diaphragm was determined by trial and error method. Using the evaluated weight the diaphragm was strengthened during the study period.

2.6. Placement of Weight

The evaluated weight was placed over the epigastric region with an isosceles triangular board. The board is placed in such a way that one of the corners touches the xiphisternum and the other two corners touching the anterior borders of the ribcage (see **Figure 2**). During the training period of the ABW group, subjects were instructed to perform normal breathing with the weights on for 15 minutes and progression in weights was done for every 1 week.

2.7. Incentive Spirometry Training

The INS group subjects were trained using an Incentive spirometer, it is a flow oriented breathing exerciser. The devise is provided with 3 balls and they provide the patients an indirect indicator of the inspired volume. Three color-coded balls (3 shades of green) in each chamber provide a visual incentive for the patient. Air flows into single channel, when it passes through the chamber, it raises each of the three balls depending on the flow inhaled per second. Flow rates of the spirometer includes 600mL/sec, 900mL/sec and 1200mL/sec. By using different colors of ball it becomes easy to identify the flow rate. Subjects of this group were instructed to keep the balls of the spirometer suspended for maximum time possible, this was repeated for 15 minutes daily for a period of 6 weeks. Progression was made by increasing the suspending time of the spirometer ball.

At the end of 6 weeks training, the EMG activities of diaphragm, intercostals and the sternocleidomastoid muscles were re-examined and compared for results.

3. STATISTICAL ANALYSIS

The analysis was done using SPSS 11. Baseline values were tabulated as shown in **Table 1**. The pre and post-training values of peak EMG amplitudes of the dia-



Figure 2. Diaphragmatic strengthening using abdominal weights.

Table 1. Baseline characteristics of analysed data.

Characteristics		Group (A)	Group (B)
Mean age		36+/-12.32	27.16+/-8.91
Sex	Male	7	6
	Female	-	-
Cause of lesion	Traumatic	6	5
	Non traumatic	1	1
Time since injury (days)		68+/-32.72	74.32+/-38.71
ASIA classification	A	5	3
	B	2	3
Presence of sacral ulcers		-	5

phragm, intercostals and sternocleidomastoid were compared within the groups using Wilcoxon's sign test and between the two groups using Mann-Whitney's test.

4. RESULTS

Seventeen subjects were recruited into the study with 9 patients in group A and 8 in group B. Thirteen subjects had completed the study and were available for the post training assessment and analysis. Two subjects from each group dropped out from the study. Among 4 subjects dropped out, two were not willing to undergo post training assessment, one subject got discharged against medical advice and another subject was shifted to critical care unit. The mean age of subjects was 35 years (range 19 to 53 years).

Among 17 subjects, 13 had traumatic SCI and remaining 4 patients had infective pathology of the cord. Mean duration since injury was 71.61 days (range 32 to 142). There was a significant increase in the diaphragmatic activity of subjects in the ABW group, shown in **Table 2**, whereas there was a significant reduction in the EMG activity among the INS group, shown in **Table 3**. Comparison between the 2 groups using Mann-Whit

Table 2. Change in EMG (milli volts) within ABW group.

Group A	Pre- test		Post – test		P	Z
	Mean	SD	Mean	SD		
T4	0.8478	0.8463	1.2915	1.5638	<0.001	-23.490
T5	0.7253	0.7974	1.2366	1.4240	<0.001	-31.986
T7	1.1289	0.7862	1.3036	1.2129	<0.001	-6.273
T8	0.8188	0.6440	0.8977	0.9190	<0.001	-0.475
SCM	1.5027	1.8742	1.2527	1.5241	<0.001	-8.424

Table 3. Change in EMG (milli volts) within INS group.

Group B	Pre- test		Post – test		P	Z
	Mean	SD	Mean	SD		
T4	0.9554	0.8923	0.7368	0.7668	<0.001	-17.659
T5	1.1756	1.0081	0.9361	0.8993	<0.001	-14.078
T7	1.7001	1.4144	0.9631	0.8993	<0.001	-31.584
T8	1.8194	1.8367	0.9823	0.9823	<0.001	-25.335
SCM	2.3985	2.4365	2.0446	1.8431	<0.001	-9.838

Table 4. Comparing change in EMG (milli volts) between the 2 groups.

Muscle	Group (A)		P	Group (B)		P	Z	
	Pre	Post		Pre	Post		Pre	post
T4	0.8472	1.2915	0.00	0.9554	0.7368	<0.001	-14.019	-19.676
T5	0.7253	1.2366	0.00	1.1756	0.9631	<0.001	-40.670	-0.105
T7	1.1289	1.3036	0.00	1.7001	1.0441	<0.001	-23.396	-8.030
T8	0.8188	0.8977	0.00	1.8194	0.9823	<0.001	-32.875	-13.278
SCM	1.5027	1.2524	0.00	2.3985	2.0446	<0.001	-20.671	-27.735

ney's test showed a statistical significance ($p < 0.001$) in the improvement of diaphragmatic activity in ABW group, shown in **Table 4**. The mean EMG of diaphragm of ABW group raised from 1.1289 to 1.3036 milli-volts with a significance of $p < 0.001$, whereas it fell from 1.7001 to 1.0441 milli-volts among INS group subjects with a significance of $p < 0.001$. When comparing the EMG activities of both the groups a statistically significant improvement in diaphragmatic strength was observed among the ABW group.

5. DISCUSSION

The objective of the study was to determine which of the two techniques, (abdominal weights or incentive spirometry) improves the strength of diaphragm among complete tetraplegic patients. Results of this study have shown that patients trained with weighted diaphragmatic exercise had better improvement in the post training assessment of EMG values. Pulmonary rehabilitation exercise protocols prescribed for the spinal cord injured patients with reduced pulmonary function is very effective to provide a positive outcome. Pulmonary exercises are simple and effective without any need to procure sophisticated instruments. Studies done on the progressive resistive exercises for the respiratory muscles have proved that this method of diaphragm training may be useful in weaning high level quadriplegic patients from the ventilator.

Studies on pulmonary function tests of individuals with complete tetraplegia showed that there is a major loss of expiratory reserve volume because of paralysis of

expiratory muscles, as a result of which their maximal expiratory pressure was reduced. The vital capacity approximates their inspiratory capacity. The work of breathing is increased and the diaphragm is prone to fatigue particularly in patients with high cervical cord lesion [16].

Carolyn Kisner and Lynn Allen Colby in their discussion on various techniques used to strengthen diaphragm suggested; incentive spirometry is a form of low level resistance training that emphasizes sustained maximal inspiration. The training sessions of the above mentioned studies were typically limited to 15 to 30 minutes each, with two to three sessions a day, 5 to 7 days a week for a total period of 6 to 8 weeks.

Previous studies have compared the effectiveness of resistive inspiratory muscle training (RIMT) and abdominal weights in improving the strength of diaphragm among tetraplegic patients and have proved that both the techniques are equally effective [17]. Hwa Lin and Chy Ching Chuang observed that Abdominal weighted maximal ventilatory (AWMV) breathing evoked greater EMG activity, inspiratory flow and inspiratory volume than did (Inspiratory resistance maximal ventilatory (IRMV) breathing. The increase of diaphragmatic EMG was not statistically significant in AWMV breathing. Weighted diaphragmatic strengthening is a less commonly employed strengthening program. Studies had shown that the use of weighted diaphragmatic exercise was of great therapeutic use, and have compared the effects of abdominal weights against resistive inspiration as mentioned before. On the other hand in recent days incentive spirometry is the most commonly administered

treatment regimen in improving the strength and efficiency of diaphragm among tetraplegics. In our study we have observed, the most efficient and cost effective modality in the pulmonary management of tetraplegic patients is abdominal weighted exercise.

We hypothesized a reduction in the EMG activity of the sternocleidomastoid muscle following training due to an improvement in the efficiency of diaphragm which is the primary respiratory muscle. We found an increase in the activity of sternocleidomastoid muscle among ABW group subjects along with the increase in activity of the other groups of muscles (intercostals and diaphragm). There was a reduction in activity of sternocleidomastoid muscle among the INS group subjects. However we could not explain the reason for this phenomenon. The results of this study are not concurrent with the previous literature; instead has proved that resistive diaphragmatic breathing exercise has better therapeutic effects in improving the strength of diaphragm among complete tetraplegic patients.

There were few limitations in our study which includes the sampling technique and spasticity of the subjects. There are possibilities that disturbances from the abnormally activated trunk muscles could have reduced the accuracy of EMG activity of the diaphragm and other respiratory muscles. The sampling method had to be judgement sampling rather than single blinded simple random sampling which could have been ideal for this study.

6. CONCLUSIONS

The peak EMG amplitude showed a significant rise amongst subjects who were trained using abdominal weights. This is an apparent indication of improved performance of the target muscle with regards to strength. Cost effectiveness and ease of administration of this technique ensures its frequent usage by clinical practitioners. Thus we conclude stating Abdominal weights can be used as an effective adjunct to pulmonary rehabilitation in improving the strength of diaphragm, thereby reducing the risks associated with pulmonary complications.

7. ACKNOWLEDGEMENT

We gratefully acknowledge Mr. Ganesh, Movement Analyst who assisted us in collecting EMG recordings for all our patients and Mr. Vijayakumar for his guidance. We also acknowledge the Fluid research committee for funding our project.

REFERENCES

- [1] DeVivo, M.J., Black, K.J., and Stover, S.L. (1993) Causes during first twelve years after spinal cord injury. *Arch Phys Med Rehabil*, **74**, 248-54.
- [2] Liaw, M.-Y., Lin, M.-C., and Cheng, P.-T. (2000) Resistive inspiratory muscle training: its effectiveness in patients with acute complete cervical cord injury. *Arch. Phys. Med Rehabil*, **81**, 747-751.
- [3] Garshiek, K.A. and Gross, E.R. (2003) Spirometry testing standards in spinal cord injury. *Chest*, **123**, 725-730.
- [4] Ledsome, J.R. and Sharp, J.M. (1981) Pulmonary functions in acute cervical cord injury. *Am Rev Respir Dis*, **124**, 41-44.
- [5] Lerman, R.M. and Weiss, M.S. (1987) Progressive resistive exercise in weaning high quadriplegic from the ventilator. *Paraplegia*, **25**(2), 130-5.
- [6] Kisner, C. and Colby, L.A.. In: Therapeutic Exercises. Foundation and techniques, 3rd edn, 665-672.
- [7] Gross, D., Ladd, H.W., Riley, E.J. (1980) The effect of training on strength and endurance of the Diaphragm in quadriplegics. *The American journal of Medicine*, **68** (1), 27-35.
- [8] Wang, T.G., Wang, Y.H. (2002) Resistive inspiratory muscle training in sleep disordered breathing of traumatic tetraplegia. *Arch Phy Med Rehabil*, **83**(4), 491-496.
- [9] Rutchik, A., Weissman, A.R. (1998) Resistive inspiratory muscle training in subjects with chronic spinal cord injury. *Arch Phy Med Rehabil*, **79** (3), 293-297.
- [10] Lane, C.S. (1982) Inspiratory muscle weight training and its effect on the vital capacity of patients with quadriplegia. Boston (MA) Northern University.
- [11] Bodin, P., Fagevik Olsen, M., Bake, B. (2005) Effects of abdominal binding on breathing pattern during breathing exercises in persons with tetraplegia. *Spinal Cord*, **43**, 117-122.
- [12] American spinal injury association; standard for neurological and functional classification of SCI. (1992) Revised 1992 Chicago ASIA.
- [13] Wetzel, J. L., Lunsford, B. R. In: Scot Irwin, Teclin (ed): Cardio Pulmonary Physical therapy, 3rd edn, 584-586.
- [14] Lin, H. and C.-C. Chung. (1999) Abdominal weight and Inspiratory resistance: Their immediate effects on inspiratory muscle functions during maximal voluntary breathing in chronic tetraplegic patients. *Arch. Phys. Med. Rehabil*, **80**(7), 741-745.
- [15] Wetzel, J.L. and Lunsford, B.R. In: Scot Irwin, Teclin (ed): Cardio Pulmonary Physical therapy, 3rd edn, 588-589.
- [16] Bodin, P., Kreuter, M., Bake, B., and Fagevik Olse, M. (2003) Breathing patterns during breathing exercises in persons with tetraplegia. *Spinal Cord*, **41**, 290-295.
- [17] J. Derrickson, N. Ciesla, and N. Simpson. (1992) A comparison of two breathing exercise programs for patients with Quadriplegia. *Physical Therapy*, **72**(11), 763-769.

Evaluation of the inclusive payment system based on the diagnosis procedure combination with respect to cataract operations in Japan

-----A comparison of lengths of hospital stay and medical payments among hospitals

Kazumitsu Nawata^{1*}, Masako Ii², Hinako Toyama³, Tai Takahashi⁴

¹Graduate School of Engineering, University of Tokyo, 7-3-1 Hongo, Bunkyo-kun, Tokyo, Japan; nawata@tmi.t.u-tokyo.ac.jp

²School of International and Public Policy, Hitotsubashi University 2-1-2 Hitotsubashi, Chiyoda-ku, Tokyo, Japan

³Department of Health Service Management, International University of Health and Welfare 2600-1 Kitakanemaru, Ohtawara, Tochigi, Japan

⁴Department of Medicine and Welfare, International University of Health and Welfare 2600-1 Kitakanemaru, Ohtawara, Tochigi, Japan

Received 26 June 2009; revised 23 July 2009; accepted 25 July 2009.

ABSTRACT

Following the recommendations of a report submitted by the Central Social Insurance Medical Council concerning the 2002 revision of the Medical Service Fee Schedule, a new inclusive payment system, which is based on the Diagnosis Procedure Combination (DPC) system, was introduced in 82 special functioning hospitals in Japan, effective beginning in April 2003. Since April 2004, the system has been gradually extended to general hospitals that satisfy certain prerequisites. In this paper, the new inclusive payment system is analyzed. Data pertaining to 1,225 patients, who were hospitalized for cataract diseases and underwent lens operations from July 2004 to September 2005, are used. The lengths of hospital stay and medical payments among hospitals are compared. Even after eliminating the influence of patient characteristics, there are large differences among hospitals in average lengths of hospital stay and DPC-based inclusive payments. The highest average inclusive payment is 3.5 times as high as the lowest payment. On the other hand, there are relatively small differences in non-inclusive payments based on the conventional fee-for-service system—the largest deviation from the average of all hospitals is approximately 10%. Thus, although payments based on the DPC account for only one-third of the total medical payments for this disease, the major differences in medical payments among hospitals are caused by differences in their

DPC-based inclusive payments. The results of the study strongly suggest that revisions of the payment system in Japan are necessary for the efficient use of medical resources in the future.

Keywords: DPC; Inclusive Payment System; Cataract; Lens Operation; Length of Hospital Stay

1. INTRODUCTION

Lengthy hospitalization is one of the characteristics of the Japanese health care system. The average length of stay of a patient in 2005 was 10.2 days in Germany, 13.4 days in France, 7 days in the U.K., and 6.5 days in the U.S; however, in Japan it was nearly 20 days [1]. With the rapid increase in medical care expenses, decreasing the average length of stay in hospitals by reducing the number of instances of long-term hospitalization has become an important political issue in Japan.

Following the recommendations of a report submitted by the Central Social Insurance Medical Council concerning the 2002 revision of the Medical Service Fee Schedule, a new case-mix payment system [2] was introduced in 82 special functioning hospitals (i.e., university hospitals, the National Cancer Center, and the National Cardiovascular Center) in Japan, effective beginning in April 2003. Since April 2004, the system has been gradually extended to general hospitals that satisfy certain prerequisites. It was the largest and most important revision of the payment system since the Second World War. Under the new payment system, the medical payments are comprised of inclusive payments based on the Diagnosis Procedure Combination (DPC) system and

non-inclusive payments based on the conventional fee-for-service system. In this paper, the new payment system is referred as the DPC-based inclusive payment system, since this is the more commonly used description [3].

The DPC system is unique to Japan. It allows the classification of diseases, operations, treatments, and patient conditions using a 14-digit code. The first 6 digits classify principal diseases on the basis of the International Classification of Diseases-10 (ICD-10)¹. The remaining digits pertain to information on operations, treatments, and patient conditions such as the presence of a secondary disease. Initially, the DPC system classified patients into 1,860 categories². Currently, the number of categories is 1,572. Inclusive payments based on the DPC system cover fees for the following six categories only: basic hospital stays, medical checkups, image diagnosis, medication, injections, treatments under 1,000 points³, and medicines used during rehabilitation treatments and related activities. Fees for all other categories, such as fees for operations, are paid on the basis of the conventional fee-for-service system.

Unlike the Diagnosis-Related Group/Prospective Payment System (DRG/PPS) used in the U.S and other countries [4,5,6,7,8,9,10] the Japanese DPC-based payment system is a per diem prospective payment system. More specifically, three periods are established according to which per diem payment is applied, Period I, Period II, or Specific Hospitalization Period, which is determined for each DPC code. Period I is set as the 25th percentile of the length of hospital stay of the hospitals. Period II is set as the average length of hospital stay, that is, the 50th percentile (although this value is actually the median, it is called the “average length of hospital stay” in the DPC-based inclusive payment system). Finally, the Specific Hospitalization Period is given by the following equation: (average length of hospital stay) + 2 × (standard deviation).

The basic per diem payment is determined according to the length of hospital stay. For stays below Period I, the per diem payment to hospitals is 15% more than the average per diem payment of the patients whose stays were within the average length of hospital stay. For hospital stays between Periods I and II, the per diem payment is determined such that (per diem payment in the Period I – average per diem payments) × (number of days in Period I) equals (the average per diem payments – per diem payment between Periods I and II) × (number of days between Periods I and II). For stays between Period II and the Specific Hospitalization Period, the per diem payment is reduced by an additional 15%. Finally, for stays above the Specific Hospitalization Period, the per diem payment is determined through the conventional fee-for-service system. Note that the periods and

per diem inclusive payments are affected by the conditions of a patient, such as the presence of a secondary disease. Furthermore, for each hospital, the actual payment amount is determined by multiplying the basic payment by the individual hospital coefficient, which is the sum of a basic coefficient and an adjustment coefficient. The adjustment coefficient is determined such that the hospital's revenue does not become less than that of the previous year. This is an incentive for hospitals to adhere to the new payment system. Since the system was introduced only recently, thorough evaluations of the system have yet to be performed. Empirical studies based on data pertaining to the length of hospital stay and medical payment amounts for a wide range of hospitals are necessary for an accurate evaluation of the system. Moreover, for a thorough analysis, a simple comparison among hospitals in terms of the average length of stay is not sufficient, and differences in the types of diseases for which the patients are hospitalized should also be considered. For each disease, individual patient characteristics and treatment types must also be taken into account.

One of the major purposes of the DPC-based payment system is to reduce the long-term hospitalization cost by standardizing the medical payments so that the payments become the same amount for identical treatments, regardless of the hospital that provides them. This means that if the system works properly, the differences in the inclusive payment amounts become smaller than those of the non-inclusive payment amounts among different hospitals. In this study, this hypothesis is evaluated for cataract operations (DPC category code: 020110). Lengths of hospital stay and medical payments among hospitals are compared. The number of cataract patients in Japan has been increasing rapidly with the ageing of the population. According to a survey conducted by the Ministry of Health, Labour and Welfare, the number of cataract operations in June 2006 was 61,383 [11]. Thus, it is estimated that nearly 800,000 cataract operations are performed annually and nearly 2.5 billion yen are spent for cataract operations. The overall difficulty level of surgical and treatment procedures for cataracts is not high, owing to their standardization, and the outcomes are generally predictable. Moreover, most cataract operations are scheduled in advance, and the possibility of postoperative infections or complications is very low. Fedorowicz, Lawrence and Guttie [12] found no significant difference in outcome or risk of postoperative complications between day care and inpatient cataract surgeries. Thus cataract cases are considered to be the most suitable candidate for evaluating the various aspects of the DPC-based payment system. To accomplish this, data pertaining to 1,225 patients, who were hospitalized for cataracts or related diseases and underwent a lens operation on one eye, are used.

Table 1. Average medical payments by hospital (in points).

Hospital	Total Payment		Inclusive Payment		Non-inclusive Payment		Number of Patients
	Mean	S.D.*	Mean	S.D.	Mean	S.D.	
Hp1	25,058	3,996	10,482	2,596	14,576	2,431	60
Hp2	25,602	3,981	9,669	2,711	15,933	1,963	177
Hp3	28,492	3,309	12,808	2,789	15,684	1,313	94
Hp4	29,020	3,817	11,694	2,455	17,326	2,419	41
Hp5	25,799	1,206	11,529	1,173	14,270	109	8
Hp6	25,397	3,249	11,504	3,201	13,893	395	9
Hp7	22,617	699	7,702	88	14,914	680	111
Hp8	22,782	1,131	7,638	0	15,144	1,131	28
Hp9	21,171	5,753	4,837	1,510	16,334	4,591	78
Hp10	26,581	2,674	9,829	2,348	16,751	987	88
Hp11	24,163	7,483	8,768	6,025	15,395	1,983	25
Hp12	19,191	2,400	3,813	2,181	15,377	541	226
Hp13	29,892	2,285	15,467	1,847	14,425	783	41
Hp14	20,439	2,670	5,625	2,557	14,814	463	24
Hp15	29,073	3,408	13,311	2,833	15,762	1,497	67
Hp16	25,065	1,834	9,488	1,600	15,577	815	148
All	24,320	4,664	8,716	3,983	15,604	1,851	1,225

*: Standard Deviation.

2. DATA

2.1. Surveyed Hospitals

In this paper, data collected from 16 general hospitals (denoted as Hp1–Hp16) in Japan are used. The data were originally collected by the DPC Hospital Conference in Japan from July 2004 to September 2005 and include the following details for each patient: DPC code, dates of hospitalization and discharge from the hospital, date of birth, sex, placement after hospitalization, principal disease classification (ICD-10 code for the principal disease for which the patient was hospitalized), purpose of hospitalization, presence of secondary disease and the attending treatment if any, and medical payment amounts (including DPC-based, fee-for-service, and total payments). Since the same data officially submitted to the Ministry of Health, Labour and Welfare are used, the reliability of data is considered to be very high.

In our study, the data pertaining to patients classified under the DPC category code 020110 (ICD-10 code: H25.0-H26.9) are analyzed. These patients were hospitalized for cataract diseases and underwent lens operations. Furthermore, unlike in other countries, hospitals in Japan perform two-eye operations (where both eyes of the patient are operated on in a single period of hospitalization) in addition to one-eye operations (where only one eye of the patient is operated on in a single period of hospitalization). It is evident that the two-eye operation will require a patient to remain hospitalized for a longer period of time than that required following a one-eye operation. Therefore, we utilize data strictly pertaining to those patients who underwent cataract operations and insertion of prosthetic lens on one eye only (DPC codes: 0201103x01x000, 0201103x01x010, and 0201103x01x1x0)⁴. The number of patients included in our data set is 1,225.

talization) in addition to one-eye operations (where only one eye of the patient is operated on in a single period of hospitalization). It is evident that the two-eye operation will require a patient to remain hospitalized for a longer period of time than that required following a one-eye operation. Therefore, we utilize data strictly pertaining to those patients who underwent cataract operations and insertion of prosthetic lens on one eye only (DPC codes: 0201103x01x000, 0201103x01x010, and 0201103x01x1x0)⁴. The number of patients included in our data set is 1,225.

2.2. Medical Payments

The average total payment per patient is 24,320 points (i.e., 243,200 yen). Of the total points, inclusive payments based on the DPC system (hereafter referred to simply as “inclusive payments”) account for 8,716 points and non-inclusive payments based on the conventional fee-for-service system (hereafter referred to simply as “non-inclusive payments”) account for the remainder, that is, 15,604 points (note that pre-adjustment values are used for the inclusive payments). Thus, the share of inclusive payments is 35.8%, or approximately one-third of the total payment.

Table 1 shows the medical payment amount per patient for Hp1–Hp16. Although in general the share of

inclusive payments is approximately one-third of the total payment amount, its dispersion is rather large. For all patients, the standard deviation for non-inclusive payments is 1,851 points. On the other hand, the standard deviation for inclusive payments is 3,983 points, which is significantly higher than that in the case of non-inclusive payments. The coefficient of variation (= standard deviation/mean) of inclusive and non-inclusive payments is 45.7% and 11.7%, respectively. As is evident, the former is four times larger than the latter. Furthermore, the maximum and minimum average payments are, respectively, equivalent to 3,813 (Hp12) and 15,467 (Hp13) points for the inclusive payments and 13,893 (Hp6) and 16,751 (Hp10) points for the non-inclusive payments. Thus, the range is 11,254 points for the inclusive payments and 2,852 points for the non-inclusive payments. These facts suggest that variations in the inclusive payment amounts are the main cause of the differences in the medical payment amount per patient.

2.3. Medical Payments and Lengths of Hospital Stay

As expected, there exists a strong linear relationship between length of hospital stay (in number of days) and the inclusive payment amount. The correlation coefficient is particularly high at 0.9932 for the patients who were hospitalized for 10 days or less. This implies that for this period, almost all inclusive payment amounts are determined by the length of hospital stay (note that if the length of hospital stay is more than 10 days, the payment amounts in some cases are determined through the fee-for-service system). From the above, it is clear that a strong relationship exists between the length of hospital stay and the total amount of payment (with a correlation coefficient of 0.9101) and that the total payment amount increases as the length of hospital stay becomes longer. This, however, does not hold true for non-inclusive payments, which increase little as the length of hospital stay becomes longer (with a correlation coefficient of 0.1742).

The per diem inclusive payment is affected by various factors such as hospitalization period, the presence of a secondary disease, and the individual hospital coefficient. As a result, even if two patients undergo identical operations and treatments at two different hospitals, their payment amounts will differ. Since the length of hospital stay is an important factor in the inclusive payment amount determined for a patient, we analyze the length of hospital stay rather than the inclusive payment amount.

Table 2 shows the distribution of the average lengths of stay by hospital. Large differences can be seen among the hospitals. Hp12 has the shortest length of hospital stay, with an average of only 1.50 days, while the length

Table 2. Lengths of stay by hospital (in days).

Hospital	Mean	S/D.*	Skewness	Kurtosis**
Hp1	4.47	1.47	3.57	14.29
Hp2	4.09	1.40	1.20	3.78
Hp3	5.64	1.38	-0.47	4.68
Hp4	5.07	1.46	3.19	13.42
Hp5	5.00	0.53	0.00	3.50
Hp6	4.89	1.62	0.68	0.28
Hp7	3.00	0.00	-	-
Hp8	3.00	0.00	-	-
Hp9	1.88	0.58	0.01	-0.04
Hp10	4.20	1.42	3.41	18.21
Hp11	4.16	3.87	2.02	4.81
Hp12	1.50	0.85	1.16	-0.60
Hp13	7.22	1.13	1.62	3.55
Hp14	2.21	1.02	-0.19	-1.65
Hp15	5.99	1.64	1.20	4.21
Hp16	3.85	0.79	1.84	12.88
All	3.68	1.96	1.06	3.21

*: Standard Deviation.

** : The kurtosis value is set as 0 for the normal distribution.

of hospital stay was the longest in Hp 13, with an average of 7.22 days, which is 5.72 days longer than that of Hp12. Two hospitals, Hp7 and Hp8, have a standard deviation of zero, that is, all the patients at these hospitals were hospitalized for exactly three days during the survey period. This reflects the fact that the length of hospital stay at these hospitals is determined by the hospital's clinical paths. Finally, the skewness and kurtosis values are large for some of the hospitals. In other words, the distributions for these hospitals are different from the normal distribution: the large skewness and kurtosis values for certain hospitals imply that some patients remained in the hospital for a long period of time.

3. MODELS

3.1. Length of Hospital Stay

The length of hospital stay is a discrete-type variable taking positive integers (1,2,3,...). Moreover, the skewness and kurtosis values for some of the hospitals are large. Therefore, the use of ordinary methods such as the least-squares method would not be suitable for analyzing the length of hospital stay (the results of the least-squares estimation are available from the authors upon request). Therefore, the length of hospital stay is analyzed by applying the model of Nawata *et al.* [13] to hospital profits.

First, let us consider the procedure that hospitals use

to decide when to discharge patients, which determines the length of hospital stay. For cataract operations, the length of hospital stay is typically short. Therefore, we assume that the hospital can decide when to discharge the patient. However, the hospital must also consider its reputation, which can be affected by the length of hospital stay. A hospital's reputation has asset value because it can affect the hospital's revenue; for example, a highly reputed hospital would be the first choice for people when they become ill.

Suppose that the revenue and cost of the hospital are given by

$$b_i = b(t, x_{1i}, u_{1i}) \text{ and } c_i = c(t, x_{2i}, u_{2i}), \quad (1)$$

where x_{1i} and x_{2i} are vectors of explanatory variables affecting the hospital's revenue and cost, respectively. The revenue includes not only direct monetary payments but also improvements in its asset value owing to high-quality medical services, and the cost also includes an opportunity cost arising from the loss of revenue that the hospital suffers because of the unavailability of beds for new patients.

Next, let

$$g(t, x_i, u_{1i}, u_{2i}) = \frac{\partial c_i}{\partial t} - \frac{\partial b_i}{\partial t} \quad (2)$$

where x_i is a vector of the explanatory variables contained in x_{1i} , and x_{2i} . Moreover, $g(t)$ is assumed to be an increasing function of t . This is because if $g(t)$ is not an increasing function of t , it implies that the patient never leaves the hospital. While this may be applicable for patients with fatal diseases such as heart disease, brain disease, and cancer, cataract patients rarely have prolonged hospital stays. Therefore, for the cases included in our data set, we can reasonably assume that all the patients left the hospital at some point. We assume that

$$z_i(t) \equiv g(t, x_i, v_i) = \alpha_1 t^{\alpha_2} - (x_i' \beta + v_i) \quad (3)$$

where $\alpha_1, \alpha_2 \geq 0$ and $v_i = h(u_{1i}, u_{2i})$.

Since the model is the same if we put $z_i(t) = \alpha_1^* \{(t^{\alpha_2} - 1) / \alpha_2\} - (x_i' \beta^* + v_i)$, it is considered as the Box-Cox transformation [14] of t , which is widely used in various fields. Here, v_i is an error term that follows the standard normal distribution. We have made the term $(x_i' \beta + v_i)$ negative so that the length of hospital stay increases as the value of $x_i' \beta$ becomes larger. Further, to remove the influence of a small number of patients who remained in the hospital over a long period of time, we limit the maximum number of days that patients could stay at the hospital to T . For patients staying more than T days, we just use the information such that they stay in the hospital more than T days.

The length of hospital stay is a discrete variable taking

positive integers. Therefore, the condition for the i -th patient to leave the hospital on the t_i -th day is given by

$$\begin{aligned} z_i(t_i) &\geq 0, \text{ if } t_i = 1 \\ z_i(t_i - 1) &< 0, z_i(t_i) \geq 0, \text{ if } t_i > 1 \end{aligned} \quad (4)$$

Note that if the error term follows a normal distribution, the probability of a patient leaving the hospital becomes positive for any positive t . To maintain consistency in the model, we treat $z_i(t_i) \geq 0$ if $t_i = 1$. Thus, the probability of the i -th patient leaving the hospital on the t_i -th day ($t_i \leq T$) is given by

$$P_i = \begin{cases} P[\alpha_1(t_i)^{\alpha_2} - x_i' \beta \geq v_i], & t_i = 1 \\ P[\alpha_1(t_i - 1)^{\alpha_2} - x_i' \beta < v_i \leq \alpha_1 t_i^{\alpha_2} - x_i' \beta], & 1 < t_i \leq T \end{cases} \quad (5)$$

Let Φ be a distribution function of the standard normal distribution. Then,

$$P_i = \begin{cases} \Phi(\alpha_1 t_i^{\alpha_2} - x_i' \beta), & t_i = 1 \\ \Phi(\alpha_1 t_i^{\alpha_2} - x_i' \beta) - \Phi[\alpha_1(t_i - 1)^{\alpha_2} - x_i' \beta], & 1 < t_i \leq T \end{cases} \quad (6)$$

The probability of the i -th patient staying in the hospital for a period longer than $T_0 + T$ is given by

$$P[\alpha_1 T^{\alpha_2} - (x_i' \beta + v_i) < 0] = 1 - \Phi(\alpha_1 T^{\alpha_2} - x_i' \beta) \quad (7)$$

From Eq.5-7, we obtain the following likelihood function:

$$\begin{aligned} L(\alpha_1, \alpha_2, \beta) &= \prod_{t_i=1} [\Phi(\alpha_1 t_i^{\alpha_2} - x_i' \beta)] \\ &\times \prod_{1 < t_i \leq T} [\Phi(\alpha_1 t_i^{\alpha_2} - x_i' \beta) - \Phi\{\alpha_1(t_i - 1)^{\alpha_2} - x_i' \beta\}] \quad (8) \\ &\times \prod_{t_i > T} [1 - \Phi(\alpha_1 T^{\alpha_2} - x_i' \beta)] \end{aligned}$$

We obtain the maximum likelihood estimator (MLE), $\hat{\alpha}_1, \hat{\alpha}_2$, and $\hat{\beta}$ by maximizing the likelihood function. A program that was specifically developed for this study is employed to estimate the model.

3.2. Non-Inclusive Payments

Let y_i be the non-inclusive payment. Since y_i can be treated as a continuous variable, it is analyzed using the regression model given by

$$y_i = x_i' \gamma + \varepsilon_i \quad (9)$$

As in the previous model, x_i is a vector of explanatory variables affecting the effectiveness of treatment and ε_i is the error term with mean 0 and variance σ_ε^2 , respectively.

4. ESTIMATION RESULTS

4.1. Length of Hospital Stay

In this paper, we employ variables that represent 1) the characteristics of patients, 2) the principal disease classification based on ICD-10, and 3) influence of hospitals as explanatory variables. The variables that represented the characteristics of the patient are sex, age, usage of an ambulance, hospital's own outpatient or not, place of hospital stay post-hospitalization, and information about the secondary disease and treatment. The Female dummy (= 1 if the patient was female and 0 if the patient was male) is used to indicate the sex of the patient. The numbers of male and female patients are 518 and 707, respectively. Since the length of hospital stay tends to increase with patient age and the number of young patients under 30 is small, the Below 30 dummy (= 1 if the patient was below 30 years and 0 if otherwise), the Age 30 dummy (= 1 if the patient was between 30 and 40 years of age and 0 if otherwise), and the Age 40 dummy (= 1 if the patient was over 40 years old and 0 if otherwise) are used. The numbers of patents by age in the Age 40 group is further subdivided into 546 in their seventies, 289 in their eighties, and 253 in their sixties. The total number of patients in the Below 30 and Age 30 groups is 13. For the other patient characteristics, the Ambulance dummy (= 1 if the patient used an ambulance and 0 if otherwise), the Own Outpatient dummy (= 1 if the patient is an outpatient of the hospital where they underwent surgery and 0 if otherwise), and the Home dummy (= 1 if the patient returned home post-hospitalization and 0 if otherwise) are used. Since the outpatient care is exempt from the prospective payment, hospitals may choose to shift necessary medical checkups, medication, injections, and treatments to outpatient settings, as happened in the U.S. when prospective payment was introduced into the Medicare program system [15]. This may affect the length of hospital stay. The Own Outpatient dummy evaluates this effect.

For secondary diseases and treatments, we use the Secondary Disease dummy (= 1 if the patient had a secondary disease and 0 if otherwise) and the Secondary Treatment dummy (= 1 if the patient underwent secondary treatment and 0 if otherwise). Although all hospitalizations were planned in advance, five patients used ambulances. A total of 985 patients went directly to the hospital where they were treated, while 240 were referred there by other hospitals. Post-hospitalization, 1,088 patients returned home, whereas 137 went to another hospital or facility. Of the total, 766 patients did not have any secondary diseases and treatments, 499 patients had secondary diseases but did not undergo any secondary treatments, and 10 patients had secondary diseases for which they underwent treatment.

For principal disease classifications, dummy variables based on the H25.0 (Senile incipient cataract) category are used. For classification, 173 patients had diseases classified under H25.0, 555 had diseases under H25.9 (Senile cataract, unspecified), and 382 had diseases under H26.9 (Cataract, unspecified). The number of patients with diseases under other categories is relatively small: 90, 6, and 19 patients with diseases classified under H25.1 (Senile nuclear cataract), H25.2 (Senile cataract, morgagnian type), and H25.8 (Other senile cataract), respectively. Since the average length of hospital stay is the shortest for Hp12, dummy variables based on Hp12 are used to represent the influence of hospitals.

$x_i' \beta$ of Eq.3, becomes

$$\begin{aligned} x_i' \beta = & \beta_0 + \beta_1 (\text{Female dummy}) + \beta_2 (\text{Below30 dummy}) \\ & + \beta_3 (\text{Age30 dummy}) + \beta_4 (\text{Age40 dummy}) \times (\text{Age-40}) \\ & + \beta_5 (\text{Ambulance dummy}) + \beta_6 (\text{Own Outpatient dummy}) \\ & + \beta_7 (\text{Home dummy}) + \beta_8 (\text{Secondary Disease dummy}) \quad (10) \\ & + \beta_9 (\text{Secondary Treatment dummy}) \\ & + \sum_j \beta_j (j\text{-th Principal Disease dummy}) \\ & + \sum_k \beta_k (k\text{-th Hospital dummy}) \end{aligned}$$

We select $T = 10$. Note that a total of 7 patients—less than 1% of all patients—stayed at the hospital for more than 10 days.

Table 3 presents the estimates for α and β . The estimate for α_2 is significantly smaller than 1.0, which implies that certain patients remained at the hospital for a long period of time. The estimate for the Female dummy is positive and significant at the 5% level. Moreover, the estimates for the Below 30 dummy, Age 30 dummy, and Age 40 dummy are positive and significant at the 5% level, negative and significant at the 1% level, and positive and significant at the 1% level, respectively. This implies that sex and age affect the length of hospital stay. The estimates for the Ambulance and Own Outpatient dummies are negative but not significant at the 5% level. We could not find an evidence that the length of stay depends on whether the patient is an outpatient of the hospital. The estimate for the Secondary Disease dummy is positive and significant at the 1% level and exerts a strong influence on the length of hospital stay. The estimates for the Secondary Treatment and Home dummies are negative but not significant at the 5% level. None of the estimates for the Principal Disease dummies are significant at the 5% level. In other words, differences in the principal disease that patients suffer from do not significantly affect the length of hospital stay. This may support the suitability of the DPC groups with respect to cataract patients.

All values for the Hospital dummies are positive, with a maximum value of 5.290. This implies that the length

Table 3. Estimation results for length of hospital stay.

Variable	Estimate	Standard Error	t-value
Constant	2.1310	0.6044	3.5256**
Female dummy	0.1588	0.0695	2.2843*
Below 30 dummy	1.4054	0.6979	2.0137*
Age 30 dummy	-1.3652	0.2580	-5.2920**
Age 40 dummy	0.0174	0.0037	4.7029**
× (Age – 40)			
Ambulance dummy	-0.1051	0.7809	-0.1346
Own Outpatient dummy	-0.0808	0.0914	-0.8842
Secondary Disease dummy	0.3001	0.0769	3.9009**
Secondary Treatment dummy	0.1581	0.4822	0.3279
Home dummy	-0.1173	0.1528	-0.7678
Principal Disease Dummies			
H25.1	0.0286	0.6069	0.0471
H25.2	0.4881	0.6197	0.7875
H25.8	-0.0316	0.5090	-0.0621
H25.9	-0.1577	0.4230	-0.3728
H26.9	-0.0565	0.4167	-0.1356
Hospital Dummies			
Hp1	3.2520	0.4535	7.1709**
Hp2	2.9639	0.1484	19.9733**
Hp3	4.3442	0.1727	25.1563**
Hp4	3.8194	0.2109	18.1121**
Hp5	3.7617	1.3073	2.8775**
Hp6	3.6674	0.3619	10.1326**
Hp7	2.0452	0.4871	4.1983**
Hp8	2.0845	1.2731	1.6373**
Hp9	0.9070	0.1843	4.9222**
Hp10	3.1095	0.4354	7.1414**
Hp11	2.5642	0.1213	21.1454**
Hp13	5.2897	0.4018	13.1664**
Hp14	1.0896	0.4695	2.3208*
Hp15	4.3771	0.4742	9.2311**
Hp16	2.7421	0.1645	16.6733**
α ₁	2.9848	0.4021	7.4237**
α ₂	0.5245	0.0394	13.3112**
LogL		-1743.192	

*: Significant at the 5% level. **: Significant at the 1% level.

of hospital stay is the shortest for Hp12 even if the influence of factors such as patient characteristics is eliminated. Thus, despite the exclusion of the effects of patient characteristics and treatment types, large differences remain among hospitals.

4.2. Non-Inclusive Payments

The non-inclusive payment variable z_i is estimated by the least-squares method. x_i is chosen such that $x_i'\gamma$ of **Eq.9** becomes

$$\begin{aligned}
 x_i'\gamma = & \gamma_0 + \gamma_1(\text{Female dummy}) + \gamma_2(\text{Below 30 dummy}) \\
 & + \gamma_3(\text{Age30 dummy}) + \gamma_4(\text{Age50 dummy}) \\
 & + \gamma_5(\text{Age60 dummy}) + \gamma_6(\text{Age70 dummy}) \\
 & + \gamma_7(\text{Age80 dummy}) + \gamma_8(\text{Ambulancedummy}) \\
 & + \gamma_9(\text{OwnOutpatient dummy}) + \gamma_{10}(\text{SecondaryDisease dummy}) \\
 & + \gamma_{11}(\text{SecondaryTreatment dummy}) + \gamma_{12}(\text{Home dummy}) \\
 & + \sum_j \gamma_j (j\text{-th Principal Disease dummy}) \\
 & + \sum_k \gamma_k (k\text{-th Hospital dummy})
 \end{aligned}
 \tag{11}$$

Since there is no clear trend with respect to patient age, the dummy variables based on the age 40's (the Age 80 dummy includes all patients over 80 years old) are used. However, with the exception of the variables for age, the definitions of all the variables are the same as those in the previous section.

The estimation results are presented in **Table 4**. The Female dummy is positive but not significant at the 5% level. While the estimate for the Age 30 dummy is negative and significant at the 5% level, the other estimates are not significant. The estimates for the Ambulance, Own Hospital Outpatient, and Secondary Disease dummies are positive but not significant at the 5% level. Again, we could not find an evidence that the hospitals' medical treatments depend on whether the patient is an outpatient of the hospital. The estimate for the Secondary Treatment dummy is positive and significant at the 1% level. In fact, the value of this variable is estimated at 5,999 points, which implies that there is a large increase in the non-inclusive payment amount when secondary treatment is carried out. The estimate of the Home dummy is negative but not significant at the 5% level. With respect to the principal disease classifications, the estimate for the H25.8 dummy is negative and significant at the 5% level, but none of the other estimates is significant at this level. The maximum value for the Hospital dummies is 1,535, while the minimum value is -1,708; thus, the difference between the maximum and minimum values is 3,243. This implies that although there exist significant differences among the hospitals, they are not very large as compared to the estimates for the other variables such as those for secondary treatment.

Table 4. Estimation results for non-inclusive payments.

Variable	Estimate	Standard Error	t-value
Constant	15,340	509	30.1517*
Female dummy	106	94	1.1206
Below 30 dummy	232	805	0.2876
Age 30 dummy	-1,004	508	-1.9776*
Age 50 dummy	-218	459	-0.4750
Age 60 dummy	-229	421	-0.5441
Age 70 dummy	-378	406	-0.9309
Age 80 dummy	-198	417	-0.4749
Ambulance dummy	1,785	2,611	0.6837
Own Outpatient dummy	94	99	0.9479
Secondary Disease dummy	246	128	1.9319
Secondary Treatment dummy	5,999	478	12.5625**
Home dummy	-98	119	-0.8266
Principal Disease Dummies			
H25.1	401	263	1.5252
H25.2	572	441	1.2977
H25.8	783	372	2.1037*
H25.9	172	245	0.7030
H26.9	42	219	0.1924
Hospital Dummies			
Hp1	-684	393	-1.7388
Hp2	554	169	3.2817**
Hp3	232	167	1.3927
Hp4	847	224	3.7858**
Hp5	-1,429	232	-6.1556**
Hp6	-1,708	201	-8.4847**
Hp7	-421	123	-3.4213**
Hp8	-43	340	-0.1276
Hp9	839	520	1.6113
Hp10	1,535	261	5.8827**
Hp11	-507	410	-1.2371
Hp13	-1,237	217	-5.6959**
Hp14	-433	259	-1.6730
Hp15	-28	246	-0.1138
Hp16	-29	131	-0.2222
R2		0.231551	

*: Significant at the 5% level. **: Significant at the 1% level.

5. COMPARISON OF LENGTHS OF HOSPITAL STAY AND MEDICAL PAYMENTS AMONG HOSPITALS

In this section, we compare lengths of hospital stay and non-inclusive payments, taking into consideration patient characteristics and principal disease classifications for each hospital. Let us consider a 70-year-old male patient whose DPC code is 0201103x01x000 (cataract operations and insertion of prosthetic lens, no secondary disease or treatment) and who does not use an ambulance, is an outpatient and returns home after his hospital stay, and has a principal disease classified under the ICD-10 code H25.0. **Table 5** presents the patient's estimated average length of hospital stay, inclusive payment amount, non-inclusive payment amount, and total payment amount at each of the surveyed hospitals. The average length of hospital stay is estimated as 3.99 days for all the hospitals, with a standard deviation of 1.49 days. The shortest length of hospital stay is estimated as 1.41 days in Hp12. On the other hand, the longest average length of hospital stay is estimated as 6.97 days in Hp13,

Table 5. Lengths of hospital stay and medical payments after eliminating the influence of patient characteristics by hospital*

Hospital	Length of Stay(days)	Payments (in points)		
		Inclusive	Non-inclusive	Total
Hp1	4.18	9,808	14,278	24,086
Hp2	3.93	9,332	15,516	24,848
Hp3	5.65	12,523	15,194	27,717
Hp4	4.95	11,243	15,809	27,052
Hp5	4.88	11,123	13,533	24,656
Hp6	4.78	10,949	13,254	24,203
Hp7	2.99	7,374	14,541	21,915
Hp8	2.98	7,339	14,919	22,258
Hp9	2.01	5,085	15,800	20,886
Hp10	4.07	9,587	16,497	26,084
Hp11	3.54	8,525	14,455	22,980
HP12	1.41	3,590	14,962	18,552
Hp13	6.97	14,772	13,725	28,497
Hp14	2.12	5,365	14,529	19,894
Hp15	5.74	12,673	14,934	27,607
Hp16	3.66	8,765	14,933	23,698
All				
Mean	3.99	9,253	14,805	24,058
Standard Deviation	1.49	3,013	869	2,905

*: Considering a 70-year-old male patient whose DPC code is 0201103x01x000 (cataract operations and insertion of prosthetic lens, no secondary disease or treatment) and who does not use an ambulance, is an outpatient and returns home, and has a principal disease classified under the ICD-10 code H25.0.

which is approximately 5 times that of Hp12. The average inclusive payment for all the hospitals is 9,253 points, with a standard deviation of 3,013 points. The lowest and highest inclusive payments are 3,590 points (Hp12) and 14,772 points (Hp13), respectively, thus exhibiting a range of 11,183 points.

The average non-inclusive payment for all the hospitals is 14,805 points, and the standard deviation is 869 points. The lowest and highest payments are 13,254 points (Hp6) and 16,497 points (Hp10), respectively, thus exhibiting a range of 3,243 points. The coefficient of variation among the hospitals is 5.9%, and the range among the hospitals is 21.9% of the overall average. Thus, the variation is much smaller than that among the hospitals' inclusive payment amounts.

The average total payment is 24,058 points for all the hospitals. The share of inclusive payments in the total payments is 38.5%. Although the share of inclusive payments is small, both the standard deviation and range for inclusive payments are 3.5 times larger than those for non-inclusive payments. We thus conclude that the differences in the total medical payment amounts among hospitals are largely due to the differences in the inclusive payment amounts, which are determined by the length of hospital stay.

6. EVALUATION OF THE NEW PAYMENT SYSTEM

As mentioned before, one of the major purposes of the DPC-based payment system is to reduce the long-term hospitalization cost by standardizing the medical payments. However, this study found that for cataract patients, the differences in the non-inclusive payment amounts—which are conventional fee-for-service reimbursements—are relatively small, whereas those in the inclusive payment amounts are quite large among sixteen different hospitals. This result shows that the DPC system, in fact, works in reverse of its intended purpose to standardize the medical payments. The relatively small difference in non-inclusive payment amounts among the hospitals can be explained as follows: 1) since for the patients in our data set, other operations—such as ones for glaucoma and vitreous—are performed in addition to the cataract operations, the diseases are classified into other DPC categories and thus the homogeneity of the patients is high (for example, operations for glaucoma and vitreous are classified under the DPC code 020340); and 2) the operation and treatment procedures for cataracts are standardized, and therefore, the difficulty levels for cataract operations are not high.

The correlation coefficient between non-inclusive payments per diem and total payments is -0.872 . To reduce the total medical payment for this disease, it may

be effective to shorten the length of hospital stay and spend medical resources intensively within a short period of time. However, since the current system is a per diem prospective payment system, hospitals may not have a strong incentive to reduce the length of hospital stay. For example, since the probability of postoperative infections or complications is very small in the case of cataract operations, few medical resources for medical treatment and examination are necessary after the operation. In other words, the direct cost to hospitals is a decreasing function of time. Moreover, even if the payment per diem is reduced, empty beds may be worse for hospital managers so long as the marginal revenue exceeds the marginal cost. Further, for cataract operations, the length of hospital stay is generally a few days, which is not a very long period of time. Since the patient does not change hospitals unless the benefit of reducing the length of hospital stay exceeds the cost of finding a new hospital, the hospital can usually make the final decision with respect to the patient's length of hospital stay. Indeed, the hospital may even choose to keep the patient in the hospital until a new patient is admitted to fill the bed. If so, the new payment system may not offer hospitals a sufficiently strong incentive to reduce their patients' length of hospital stay.

To make the new payment system work effectively in the case of cataract operations, it may be necessary to reduce the per diem payment by a large amount for long-term hospitalizations and encourage hospitals to spend medical resources intensively within a short period of time. Furthermore, the introduction of the DRG/PPS may merit serious reconsideration in Japan. In the DRG/PPS, a hospital is paid a fixed fee on the basis of the classification of the DRG, regardless of the length of hospital stay. Although ten hospitals in Japan had adopted the DRG/PPS on a trial basis in 1998, the medical society expressed strong disapproval with the DRG/PPS. Moreover, since the Japanese medical system has been following the fee-for-service payment system for over half a century, it would have been extremely difficult to adopt the DRG/PPS system nationwide without any modifications. Therefore, the DPC inclusive payment system was introduced. Thus, although the current system essentially employs the same method nationwide to classify diseases, it is necessary to revise the system, taking into consideration the characteristics of diseases and hospital specialties to facilitate the effective use of medical resources. Furthermore, individual hospitals must improve their medical systems by introducing clinical paths, efficiently managing hospitalization schedules [16], and adopting proper medical technologies [17] to reduce the length of hospital stay.

7. CONCLUSIONS

In this paper, the Japanese DPC-based inclusive payment

system, which was introduced in 2003, was evaluated. We utilized data pertaining to 1,225 patients who were hospitalized for cataract diseases and underwent lens operations from July 2004 to September 2005. The lengths of hospital stay and medical payments among hospitals were compared. The variables found to affect the length of hospital stay were those pertaining to the patients' sex and age and the presence of secondary diseases. We found large differences in the length of hospital stay among hospitals, even after eliminating the influence of patient characteristics and principal disease classifications. The highest average inclusive payment for the hospitals was 3.5 times as high as the lowest payment.

Next, non-inclusive payments were analyzed. The variables affecting the non-inclusive payment were the Age 30 dummy, Secondary Disease dummy, and H25.8 dummy. The differences among hospitals in terms of non-inclusive payments based on the conventional fee-for-service system were relatively small. The largest deviation from the average of all hospitals was approximately 10%. Thus, we can conclude that the major differences among hospitals with respect to medical payments are caused by differences in their DPC-based inclusive payments, which account for only one-third of the total medical payments for cataract patients. The results of the study strongly suggest that in future revisions of the payment system, the characteristics of diseases must be considered when determining the efficient use of medical resources.

In the present study, only cataract operations were analyzed. To evaluate the DPC-based inclusive payment system more precisely, it is necessary to analyze other important cases such as cancer, cardiac infarction and stroke, and compare the results of the cataract operations with the other cases. These are subjects to be analyzed in future studies.

8. ACKNOWLEDGEMENT

The data used in this study were originally collected by the DPC Hospital Conference of Japan and are used with the approval of the conference's Data Analysis Division. We are grateful to the anonymous referee for his/her helpful comments. We also thank the research participants from various hospitals for their sincere cooperation. This study is supported by the Grant-in-Aid for Scientific Research "Analyses of the Japanese Medical Information and Policy using the Large Scale Individual-Level Survey Data (Grant Number: 20243016)" of the Japan Society of Science.

REFERENCES

- [1] OECD, (2007) *Health Data 2007: A Comparative Analysis of 30 Countries*.
- [2] Okamura, S., Kobayashi, R. and Sakai, T. (2005) Case-mix payment in Japanese medicare, *Health Policy*, **74**, 282-285.
- [3] Yasunaga, H., Ide, Y. H. Imamura, T., *et al.* (2005) Impact of the Japanese diagnosis procedure combination-based system on the cardiovascular medicine-related costs, *International Heart Journal*, **46**, 855-866.
- [4] Frank, R. G. and Lave, J. R. (1986) Per Case Prospective Payment for Psychiatric Inpatients: An Assessment and Alternatives, *Journal of Health Politics, Policy and Law*, **11**, 83-96.
- [5] Newhouse, J. and Byrne, D. (1988) Did medicare's prospective payment system cause length of stay to fall? *Journal of Health Economics*, **7**, 413-416.
- [6] Rogers, W. H., Draper, D., Khan, K. L., *et al.* (1990) Quality of care before and after implementation of the DRG-based prospective payment system, *Journal of the American Medical Association*, **264**, 1989-1994.
- [7] Kahn, K. L., Rusbenstein, L. Draper, V., D., *et al.* (1990) The effects of the DRG-based prospective payment system on the quality of care for hospitalized medical patients, *Journal of the American Medical Association*, **264**, 1953-1955.
- [8] Dillard, G. E. P., J. F., and Smith, H. L. (1999) "The effect of the prospective payment system on rural health care, *Accounting Form*, **23** (4), 327-358.
- [9] Newhouse, J. (1996) Reimbursing health plans and health providers: Efficiency in production versus selection, *Journal of Economic Literature*, **34**, 1236-1263.
- [10] Preston, A. M., Chua, W., and Neu, D., (1997) The diagnosis-related group – prospective payment system and the problem of the government of rational health care to the elderly, *Accounting, Organization and Society*, **22**, 147-164.
- [11] Ministry of Health, Labour and Welfare, (2008) *Patient Survey 2006*.
- [12] Fedorowicz, Z., Lawrence, D. J., and Guttie, P. (2006) A cochrane systematic review finds no significant difference in outcome or risk of postoperative complications between day care and in-patient cataract surgery, *Saudi Medical Journal*, **27**, 1296-1301.
- [13] Nawata, K., Niita, A., Watanabe, S., and Kawabuchi, K. (2006) An analysis of the length of stay and the effectiveness of treatment for hip fractured patients in japan: evaluation of the revision of the 2002 medical service fee schedule, *Journal of Health Economics*, **25**, 722-739.
- [14] Box, G. E. P. and Cox, D. R. (1964) An analysis of transformation, *Journal of the Royal Statistical Society B*, **26**, 211-252.
- [15] Ellis, R. and McGuire, T. (1996) Hospital response to prospective payment: Moral hazard, selection, and practice-style effects *Journal of Health Economics*, **15**, 257-277.
- [16] Vissers, J. M. H., Van Der Bij, J. D., and Kusters, R. J. (2001) Toward decision support for the waiting lists: An operations management view, *Health Care Management Science*, **4**, 133-142.
- [17] Ghodeswar, B. M. and Vaidyanathan, J. (2006) Adoption of medical technology by hospitals: A review of innovation attributes and a conceptual model of the resulting service, *World Review of Science, Technology and Sustainable Development*, **3**, 362-380.

Notes

1. The ICD-10 comprises a wide range of categories—from general categories to very specific ones—and uses codes consisting of one alphabet and three-digit numbers.

2. The initial classification was done based on data obtained from about 300,000 patients hospitalized in the special functioning hospitals from July 2002 and October 2002. The revisions were done in April 2004, April 2006, and April 2008, based on the renewed data.

3. In Japan, medical care fees are measured in points. This system was first launched in 1943. Under the system, each point corresponds to 10 yen, which has been effective since 1958.

4. In the case of 0201103x01x000 (cataract operations and insertion of prosthetic lens, no secondary disease and no secondary treatment), the per diem inclusive payment during the sample period was 2,536 points for up to 3 days, 1,882 points for 4–6 days, and 1,600 points for 7–10 days. After 10 days, the payment was determined by the conventional fee-for-service system.

Ceruloplasmin levels in human sera from various diseases and their correlation with patient's age and gender

Viorica Lopez-Avila^{1*}, William H. Robinson², Kirk Lokits³

¹Agilent Technologies, Santa Clara, CA, USA; Corresponding author: viorica_lopez-avila@agilent.com

²Stanford University, Stanford, CA, USA

³University of Cincinnati, Cincinnati, OH, USA; Present address: Midwest Research Institute, 425 Volker Blvd, Kansas City, MO, USA

Received 7 July 2009; revised 5 August 2009; accepted 7 August 2009.

ABSTRACT

Ceruloplasmin (Cp), a copper metalloprotein in human serum has been a valuable diagnostic marker in Wilson's disease where Cp levels tend to be low while high levels in serum were associated with myocardial infarction, neoplastic and inflammatory conditions. There is no standardized reference method for Cp and current immunologic and bichromatic assays have a number of drawbacks. The method described here uses immunoaffinity chromatography to remove six of the most abundant proteins from a serum sample and high-pressure liquid chromatography (HPLC) with a size-exclusion column to separate Cp from other serum proteins and any free Cu prior to analysis of ⁶³Cu and ⁶⁵Cu by inductively-coupled plasma mass spectrometry (ICPMS). Identification of Cp is based on retention time match of the unknown protein in the serum sample with the Cp external standard and the presence of ⁶³Cu and ⁶⁵Cu at a ratio of 2.2 ± 0.1 . The method accuracy, as established independently by two of the authors with a reference serum certified for Cp, is 98 to 101% and the coefficient of variation is 6.4% and 5.4%, respectively. The assay was used to analyze a total of 167 human sera for Cp from patients with myocardial infarction (MI), pulmonary embolism (PE), rheumatoid arthritis (RA), systemic lupus erythematosus (SLE), other forms of arthritis, and a set of healthy patients as normal controls (NC). Our data show that Cp concentrations tend to be higher in MI, RA, and SLE patients, higher in female as compared to male patients, and we did not observe a correlation between Cp concentration and patient's age for the set of 70 patients for which we had gender and age information.

Keywords: Ceruloplasmin; HPLC-ICPMS; Immunoaffinity Chromatography

1. INTRODUCTION

Ceruloplasmin (Cp) is a blue alpha-2 glycoprotein with a molecular weight of 132,000 u [1]. It binds 90-95% of blood plasma copper (Cu), has 6-7 Cu ions per molecule [1] and exhibits ferroxidase activity [1,2], amine oxidase activity [1], superoxidase activity [1] as well as it is involved in Cu transport and homeostasis [1]. Hellman and Gitlin, however, reported that Cp plays no essential role in the transport and metabolism of Cu [2] and in a separate study [3] reported that analysis of Cu incorporation into apoceruloplasmin (apoCp) in vitro showed that failure is intrinsic to mutant proteins. Linder *et al.* [4] claim that newly absorbed dietary Cu is transported by plasma protein carriers (i.e., albumin, transcuprein, and Cp) from intestine to liver and kidney, and that Cp is involved primarily in transport of Cu from liver to other organs. Prohanska and Gybina [5] provide details on the transport process in which Cu, imported by plasma membrane protein Ctr1, binds to Cu chaperone proteins like Atox1, which then docks with ATP7B and delivers Cu to plasma Cp.

Current analytical procedures for the determination of Cp include immunoturbidimetry and nephelometry [6], in which Cp is reacted with anti-Cp antibodies to give insoluble aggregates whose absorbance is proportional to the concentration of Cp in the sample [6], radial immunodiffusion (RID) test [7], and bichromatic assay [8]. When comparing RID with immunonephelometry a significant bias was found that was in part attributed to the variation in the antisera sources used in the two methods [7]. In the case of the bichromatic method, the procedures are based on the oxidase activity of Cp on diamines such as benzidine. The bichromatic method requires special precautions (i.e., benzidine is a known

carcinogen) and purification of substrates [9], detects only Cp and not the apoCp [10], and it is not very effective since Cp does not have its own substrate [11]. The immunologic methods also have drawbacks because antisera cross-react with apoCp thus giving higher concentrations for Cp [9]. Evidence suggests that patients with Wilson's disease may have exhibited normal serum concentrations of Cp because the immunologic assay could not distinguish between the apoCp and Cp [10]. In general, a normal person has 0.2 to 0.5 mg/mL of Cp in serum [11].

Although low serum concentration of Cp has been an important diagnostic indicator of Wilson's disease [10], high Cp concentrations were reported in patients with macular degenerations as compared with controls (i.e., Cp concentration 0.691 ± 0.153 mg/mL vs 0.312 ± 0.064 mg/mL) by Newsome *et al.* [12], in patients with MI by Reunanen *et al.* [13], and in a variety of neoplastic and inflammatory conditions like carcinomas, leukemia, Hodgkin disease, primary biliary cirrhosis, systemic lupus erythematosus, and rheumatoid arthritis [14].

This paper describes the peer verification of a new method for the determination of Cp in human serum at biologically relevant concentrations > 0.01 mg/mL using a reference serum certified for Cp and a set of 167 human sera from several diseases. This method, which was published recently [15], uses HPLC to separate Cp from other proteins including transcuprein (molecular weight 270,000 u) and from inorganic ions, and ICPMS to detect Cu isotopes at mass-to-charge (m/z) ratios of 63 and 65, and to identify Cp from the HPLC retention time and the signal ratios of Cu isotopes ^{63}Cu and ^{65}Cu measured with ICPMS. To eliminate possible interference from highly abundant proteins, some of which may bind Cu to form protein-Cu complexes, the serum sample is first depleted of albumin, IgG, IgA, transferrin, haptoglobin, and anti-trypsin using immunoaffinity chromatography prior to HPLC. Quantitation of Cp in the depleted serum is performed by external standard calibration with a Cp standard.

2. EXPERIMENTAL

Materials: the standard of Cp purified from human plasma was from EMD Biosciences/Calbiochem (La Jolla, CA) in lyophilized form from 133 μL of 50 mM potassium phosphate, pH 6.8, 100 mM potassium chloride, 200 mM ϵ -amino-n-caproic acid and 5mM EDTA, with a purity of $>95\%$. The 167 serum samples were as follows: 37 patients with MI, 50 with RA, 24 with SLE, 8 with PE, 16 NC, and 32 sera (identified as "other" in this paper) were from patients with different forms of arthritis: osteoarthritis, juvenile rheumatoid arthritis, reactive arthritis, inflammatory arthritis; myositis and

dermatomyositis, fibromyalgia, anthralgia, ankylosing spondylitis, spinal stenosis, Sjogren, Reiter's syndrome, connective tissue disease, scleroderma, polymyalgia rheumatica and palindromic rheumatism gout and CREST syndrome.

ERM DA470 is a human serum certified for 15 proteins including Cp [16,17] and was purchased from RTC (Laramie, WY).

Serum preparation: all human samples were collected and utilized under Institutional Review Board approved protocols and with informed consent. To summarize, blood samples were withdrawn using sterile conditions and allowed to clot at room temperature for a minimum of 10 min. Serum was separated by centrifugation for 10 min at 4000 rpm, divided among several vials to minimize freeze-thawing, and kept at -80°C until analysis.

Immunoaffinity chromatography: high-abundant protein removal from human serum was performed on a 4.6 x 100 mm immunodepletion column (Agilent Technologies) with a capacity of 40 μL of non-diluted human serum (capacity is defined as the amount of original serum that can be loaded onto the column such that 99% of the targeted high-abundant proteins are removed for at least 200 injections on a particular column). After a 5-fold dilution of serum sample with buffer A and filtration through a 0.22 μm spin filter, 150 μL of the diluted sample was injected onto the column in 100% Buffer A at a flow rate of 0.5 mL/min for 10.0 min. After collection of the flow-through fraction (2 mL), the column was washed and the bound proteins were eluted with 100% Buffer B at a flow rate of 1.0 mL/min (volume of bound protein fraction 3 mL). The immunoaffinity column was then regenerated by equilibrating it with Buffer A for 13 min bringing the total run cycle to 30.0 min. Fraction collection of flow-through proteins was time-controlled and corresponded to the UV 280 nm absorbance of the eluting proteins. The flow-through fraction was collected and kept at 4°C using the thermostated fraction collector, was reduced to a final volume of 30 μL using spin concentrators and analyzed by HPLC-ICPMS. Bound proteins (i.e., albumin, IgG, IgA, transferrin, haptoglobin and anti-trypsin) were eluted from the immunodepletion column and selected samples were analyzed by ICPMS (data not included here). Buffer A is a phosphate buffer (pH 7.4) and buffer B is a concentrated urea buffer in water (pH 2.25).

Instrumentation: An Agilent 1100 LC system equipped with a binary pump, degasser, autosampler (300 μL loop) with thermostat, diode array detector with 6 mm flow cell, and a thermostated fraction collector was used for the immunodepletion work. Protein separation was achieved on a silica TSKGel column SW3000 (30 cm x 4.6 mm id x 4 μm particles x 250 nm pore size)

from Tosoh Bioscience (Montgomeryville, PA). All HPLC analyses were performed on an Agilent Technologies 1100 Series High Performance Liquid Chromatography system equipped with a binary pump, degasser, autosampler (100 μ L loop) and diode array detector (215 nm and 280 nm). 0.1 M Tris (pH 7) was used as mobile phase at a flow rate of 0.3 mL/min. The liquid flow from the HPLC column was converted into aerosol droplets by a Micromist nebulizer with a dual pass spray chamber. ^{63}Cu and ^{65}Cu scan was performed on an Agilent 7500ce ICPMS system with a quadrupole mass analyzer and an Octapole Reaction System (ORS) for matrix-based interference removal. High levels of Na in the sample can cause the formation of $^{40}\text{Ar}^{23}\text{Na}$ polyatomic species that overlap with ^{63}Cu . Similarly, ^{31}P based molecular species ($^{31}\text{P}^{16}\text{O}^{16}\text{O}$ and $^{31}\text{P}^{18}\text{O}^{16}\text{O}$) can overlap with the ^{63}Cu and ^{65}Cu isotopes. The ORS with He (99.999 % purity) as collision gas at 3.5 mL/min was used to eliminate these interfering species and to improve signal to noise. ICPMS conditions: outer gas (Ar) flowrate 15 L/min; carrier gas (Ar) flowrate 0.8 L/min; makeup gas (Ar) flowrate 0.15 L/min; RF power 1.55kW, sampling depth 8 mm.

3. RESULTS AND DISCUSSION

3.1. Method Performance

The performance of this method (see **Table 1**) was established independently by two of the authors (in separate laboratories) with a reference human serum ERM DA470 that is certified for Cp at 0.205 mg/mL using identical instrumentation. This serum was reconstituted with high purity water and analyzed in triplicate in Laboratory 1 and in seven replicates over a period of two months in Laboratory 2. The results are summarized in **Table 1**. The agreement between the concentration of Cp in the certified serum and the reconstituted serum analyzed by this method is excellent (method accuracy is 101% in Laboratory 1 and 98.0% in Laboratory 2). The coefficient of variation (CV) for the three replicate measurements of the freshly reconstituted serum in Laboratory 1 is 5.4 %. The CV of the seven replicates performed over a period of two months in Laboratory 2 is 6.4%.

Method performance data are included in **Table 2**. The method detection limit was established from the instrument detection limit and applies only to sample injection volumes of 5 μ L; larger injection volumes would allow a lower method detection limit but such experiments were not pursued here. The method dynamic range is given as 0.01 to 5 mg/mL since this is the range of concentrations that were tested here. Although the instrument dynamic range is 9 orders of magnitude, that would involve adjustments in ICPMS operating parameters to accommodate such a wide range. Expected

Table 1. Concentration of Cp in the ERM DA 470 reference serum.

	Certified value (mg/mL)	Conc measured in this study (mg/mL)	$^{63}\text{Cu}/^{65}\text{Cu}$
ERM DA 470 Reference Serum (Laboratory 1)	0.205 (0.011) ^a	0.208 (5.4 %) ^b	2.1 (3.6%) ^b
ERM DA 470 Reference Serum (Laboratory 2)	0.205 (0.011) ^a	0.201 (6.4%) ^c	2.2 (7.3%) ^c

^aUncertainty (mg/mL) – defined as half-width of the 95% confidence interval of the mean value (K factors were chosen according to the t-distribution depending on the number of labs) [12, 13].

^bAverage of 3 determinations; value given in parentheses is the coefficient of variation.

^cAverage of 7 determinations; value given in parentheses is the coefficient of variation.

Table 2. Cp determination by HPLC-ICPMS-method performance^a.

Method indicator	Value
Detection Limit	0.01 mg/mL
Dynamic Range	0.01 – 5.0 mg/mL (tested only until 5 mg/mL)
Reproducibility	CV for immunodepletion : 0.07% to 2.2 % CV for injection into HPLC: 5.3% (Cp standard at 1 mg/mL) Overall CV: <10%
Accuracy using ERM DA470	101 % (Laboratory 1); 98.0% (Laboratory 2)
Cp Identification	from retention time match of the unknown peak in the sample to the Cp standard and the presence of ^{63}Cu and ^{65}Cu at a ratio of 2.2 \pm 0.1

^aThis method takes approximately 95 min/sample from start to finish (15 min dilution and filtration, 30 min immunoaffinity chromatography, 20-30 min concentration, and 20 min HPLC-ICPMS analysis).

concentrations of Cp in human sera are in the 0.1-2 mg/mL range, therefore a 30 μ L volume of the original serum is sufficient to detect Cp at 0.1 mg/mL if the final volume of the depleted serum is 30 μ L. The overall CV for method reproducibility is <10 % and it is shown in **Table 2** for various steps in the analysis. The identification of Cp is based on retention time match of the unknown peak in the sample to the Cp standard and the ratio of $^{63}\text{Cu}/^{65}\text{Cu}$. The average HPLC retention time for 8 consecutive injections of the Cp standard is 8.389 min with a CV of 0.059%. The relative abundance of the ^{63}Cu is 69.17% and ^{65}Cu is 30.83%, thus the theoretical ratio for $^{63}\text{Cu}/^{65}\text{Cu}$ is 2.24; based on our experimental data we set the acceptance limits for $^{63}\text{Cu}/^{65}\text{Cu}$ to 2.2 \pm 0.1 [15].

In addition, we validated the Cp measurements by performing a total Cu analysis on a set of 23 depleted sera and compared those measurements with the Cp concentrations measured by HPLC-ICPMS (see **Figure 1**). Regression analysis gave a correlation coefficient of

0.9, which confirms literature reports that most Cu in depleted serum is bound by Cp [1]. Furthermore, we verified the number of Cu atoms bound by Cp in the ERM DA470 reference serum by determining the total Cu in the depleted sample. At a Cp concentration of 0.2

mg/mL (measured in this study for the ERM DA470 serum), 6 Cu atoms per Cp molecule would correspond to a total Cu concentration of 596 ng/mL and 7 Cu atoms per Cp molecule would correspond to 695 ng/mL. Because the total Cu measured in the depleted reference serum was in the range of 618-661 ng/mL, we concluded that Cp must contain between 6 and 7 atoms per molecule, consistent with the published data for Cp [1]. Also as part of method validation, a Cp standard, the ERM DA470 certified serum and one of the depleted MI sera were fractionated by HPLC and the corresponding fractions containing Cp were collected manually, and were then subjected to one gel electrophoresis followed by Cp band excision, in-gel digestion, and electrospray MS of the digest to confirm the presence of Cp [15].

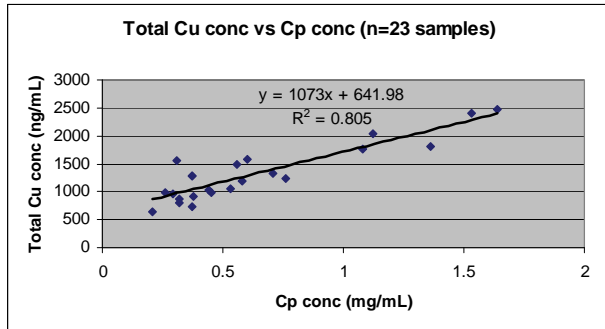


Figure 1. Total Cu vs Cp concentration for 23 serum samples (7 PE, 1 NC, 14 MI and ERM DA470).

Figure 2 shows HPLC-UV and ICPMS chromatograms for a Cp standard and a depleted serum sample; the HPLC chromatograms show the complexity of the

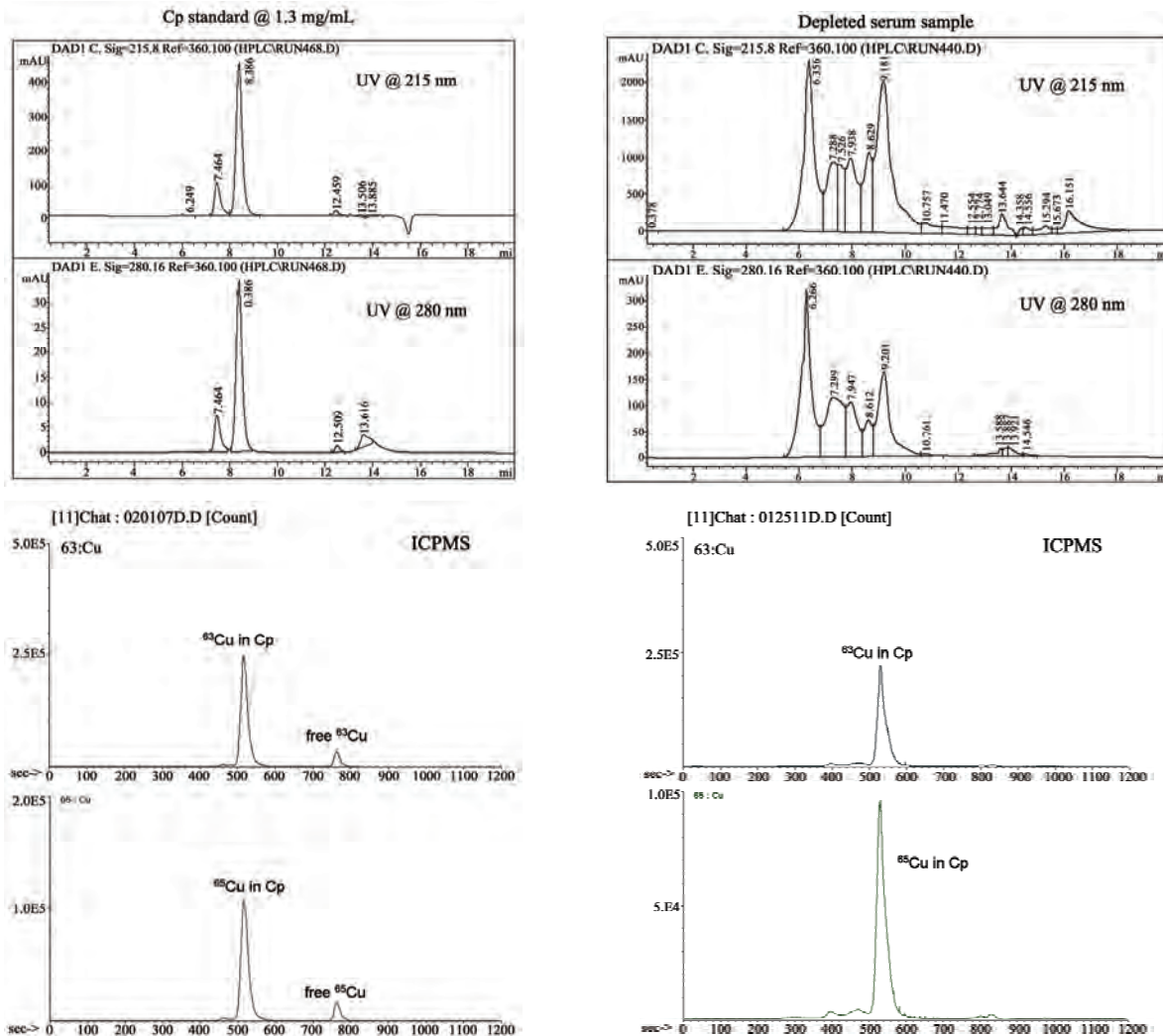


Figure 2. HPLC-ICPMS chromatograms for Cp standard and depleted serum sample.

serum sample even after its depletion of the high abundant proteins whereas the ICPMS chromatograms show only the ^{63}Cu and ^{65}Cu signals at a retention time that matches that of the Cp standard and are in a ratio corresponding to 6-7 Cu atoms per Cp molecule.

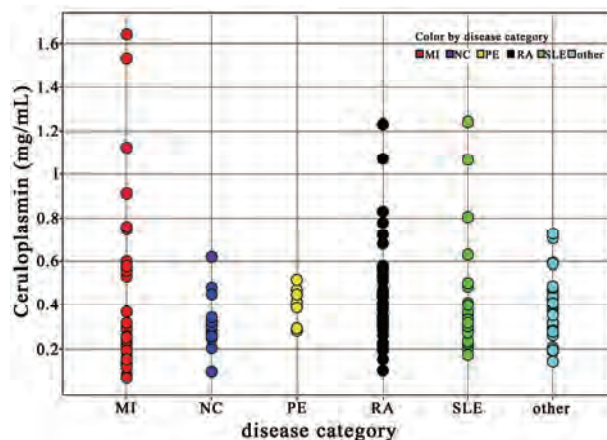
3.2. Ceruloplasmin Levels in Sera from Different Diseases

Figure 3 shows the distribution of Cp concentration across several diseases, including MI, PE, RA, SLE, other forms of arthritis (i.e., osteoarthritis, juvenile rheumatoid arthritis, reactive arthritis, inflammatory arthritis) and NC sera (167 serum samples in all). Samples derived from patients experiencing MI (37 in our study) had an average Cp concentration of 0.402 ± 0.377 mg/mL and exhibited Cp concentrations as high as 1.64 mg/mL, while a subset of 50 RA patients and 24 SLE patients had average concentrations of 0.447 ± 0.215 mg/mL and 0.426 ± 0.264 mg/mL and exhibited elevated Cp concentrations as high as 1.23 mg/mL and 1.24 mg/mL, respectively (**Figure 3**). Normal Cp concentrations are in the 0.2-0.5 mg/mL range [11] and the average Cp concentration in the set of NC sera in our study (16 patients) was 0.316 ± 0.120 mg/mL. When comparing Cp concentrations for our MI, RA, SLE, and “other” sera with our set of NC sera, only the RA and SLE data were statistically different from the NC in a t test (i.e., p values were 0.0037 and 0.0837 for RA and SLE sera, respectively). The MI data reported here show a much higher variation than our NC data, and this variation is statistically significant (F value is 9.92, F crit is 2.22, and $p < 0.001$). Reunanen *et al.* [13], using serum from 104 patients with MI or stroke and 104 matched controls, concluded that high Cp concentrations in serum were significantly associated with higher incidents of MI but not of stroke.

Hantzschel *et al.* [18] reported for RA and polymyalgia rheumatica an average Cp concentration for 23 RA patients (22 females) of 0.7 ± 0.4 mg/mL and for 16 polymyalgia rheumatica patients (all females) 0.5 ± 0.1 mg/mL. The authors suggested that clinical data, including a history of hip and shoulder muscle tenderness and lack of positive rheumatoid factor, and a normal Cp level could distinguish polymyalgia rheumatica from rheumatoid arthritis. We observed a similar trend for RA patients as compared with patients with “other” forms of arthritis. The average Cp concentrations for RA of 0.447 ± 0.215 mg/mL were significantly different from the average Cp concentrations for “other” diseases, which had an average Cp concentration of 0.376 ± 0.145 mg/mL, only when doing a one-tail test (p value was 0.041). Perhaps Cp concentrations above 0.5 mg/mL would be indicative of disease severity, however characterization of larger sample sets will be necessary to substantiate this observation.

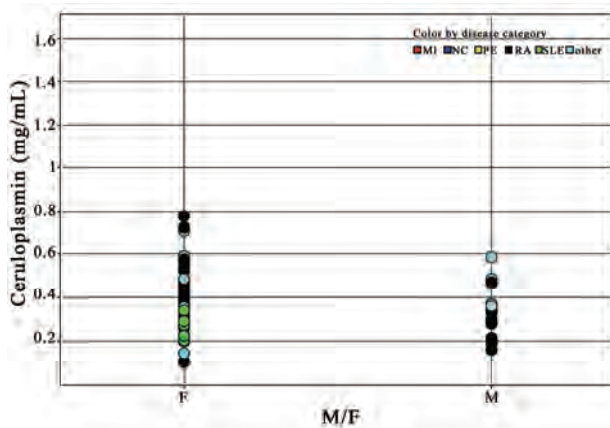
Figures 4 and 5 show Cp concentrations as a function of patient’s gender and age, respectively. Although this is a very limited sample set (70 sera from 33 RA, 5 SLE and 32 “other” arthritis patients with 49 females and 21 males) it is interesting to note that female patients exhibited slightly higher Cp concentrations (ave \pm SD of 0.392 ± 0.153 mg/mL) than male patients (0.319 ± 0.123 mg/mL) that were statistically significant at 5% significance level (48 degrees of freedom, $t_{\text{stat.}}$ 2.104, $t_{\text{crit.}}$ 2.011, probability for a two-tail test was 0.0410). However, when we averaged only the Cp concentrations for the 33 RA patients by gender (24 females and 9 males) we found a larger difference between the female patients and male patients (0.417 ± 0.158 mg/mL vs 0.278 ± 0.096 mg/mL, respectively) that was statistically significant at 5% significance level (24 degrees of freedom, $t_{\text{stat.}}$ 3.059, $t_{\text{crit.}}$ 2.064, probability for a two-tail test was 0.005). Data reported by Lyngbye and Kroll [19] for a normal population (280 patients, 149 males and 111 females) also indicate significantly higher concentrations of Cp in female patients which are known to be caused by use of oral contraceptives [20].

There does not seem to be a correlation between the Cp concentration and patient’s age across these 70 patients with RA and arthritis (**Figure 5**). The average Cp concentration for RA patients was 0.370 ± 0.149 mg/mL and 0.384 ± 0.163 mg/mL for <50 y.o. and > 50 y.o., respectively ($t_{\text{stat.}}$ of 0.247 is less than $t_{\text{crit.}}$ 2.059, p for a two-tail test was 0.807, indicating that the results were not statistically different). The average Cp concentrations for “other” arthritis patients were 0.387 ± 0.162 mg/mL and 0.356 ± 0.110 mg/mL for <50 y.o. and > 50 y.o., respectively ($t_{\text{stat.}}$ 0.645 is less than $t_{\text{crit.}}$ 2.048, p for a two-tail test was 0.524), indicating again that the



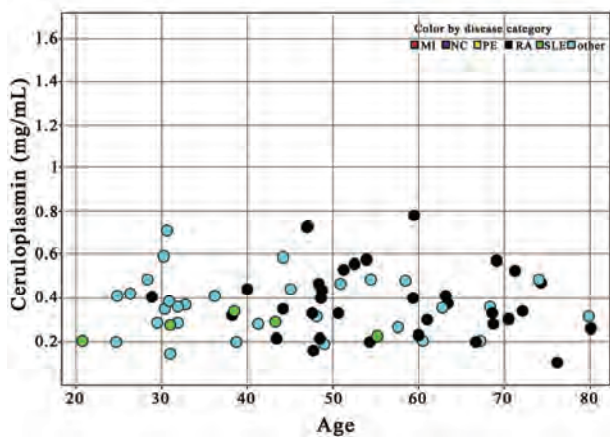
167 serum samples consist of 37 MI (myocardial infarction), 16 NC (normal controls), 8 PE (pulmonary embolism), 50 RA (rheumatoid arthritis), 24 SLE (systemic lupus erythematosus) and 32 other diseases (osteoarthritis, gout, dermatomyositis, ankylosing spondylitis, myositis, juvenile rheumatoid arthritis, etc)

Figure 3. Cp concentration for various diseases and normal controls.



70 serum samples from 33 RA patients, 5 SLE, and 32 other diseases
M – male (21 patients)
F – female (49 patients)

Figure 4. Cp concentration as a function of patient's gender.



70 serum samples from 33 RA patients, 5 SLE, and 32 other diseases

Figure 5. Cp concentration as a function of patient's age.

results were not statistically significant). Results for a normal population indicated no age variation in adults [19], however in another study Revnic [21] reported differences ($p < 0.05$) between Cp concentrations in RA patients < 50 y.o. and > 70 y.o. We have looked at Cp concentration for 22 RA patients < 50 y.o. (12 patients) and > 66.6 y.o. (10 patients) and found no significant differences at $p < 0.05$. Age related changes in human Cp concentrations were attributed to oxidative modifications, which can likely cause conformational changes around the Cu sites [22].

4. CONCLUSIONS

The method described here uses immunoaffinity chromatography and HPLC to separate Cp from the serum proteins prior to analysis by ICPMS. By removing the six most abundant proteins from serum with immunoaffinity chromatography and by using HPLC to separate Cu bound by Cp from any free Cu in the serum sample,

we demonstrated that we can measure Cp in the ERM DA470 reference serum with an accuracy of 98 to 101%. The HPLC-ICPMS method was used to analyze 167 serum samples from several diseases and a set of NC for Cp. Our data for the 167 human sera show that Cp concentrations tend to be higher in MI, RA, and SLE patients. Cp concentrations were higher in female as compared to male patients, and this trend was most prominent in patients with RA. We did not observe a correlation between Cp concentration and patient's age for the limited set of 70 patients for which we had gender and age information. Thus, measurement of Cp levels by ICPMS represents a biomarker that when combined with conventional clinical and laboratory data may provide increased diagnostic value.

5. ACKNOWLEDGEMENTS

The authors thank Toshiaki Matsuda of Agilent Tokyo Analytical Division, Tokyo, Japan, for making available an ICPMS system for performing this research, Alex Apffel of Agilent Labs, Santa Clara, CA for making available an HPLC system with fraction collection and for assistance with the immunodepletion process.

REFERENCES

- [1] Takahashi, N., Ortel, T., and Putnam, F. (1984) Single-chain structure of human ceruloplasmin: The complete amino acid sequence of the whole molecule. *Proc Nat Acad Sci USA*, **81**, 390-4.
- [2] Hellman, N.E. and Gitlin, J.D. (2002) Ceruloplasmin metabolism and function. *Annu Rev Nutr*, **22**, 439-458.
- [3] Hellman, N.E., Kono, S., Mancini, G.M., Hoozeboom, A.J., de Jong, G.J., and Gitlin, J.D. (2002) Mechanisms of copper incorporation into human ceruloplasmin. *J Biol Chem*, **48**, 46632-46638.
- [4] Linder, M.C., Wooten, L., Cerveza, P., Cotton, S., Shulze, R., and Lomeli, N. (1998) Copper transport. *Am J Clin Nutr*, **67**, 965S-971S.
- [5] Prohanska, J.R. and Gybina, A.A., (2004) Intracellular copper transport in mammals. *J Nutr*, **134**, 1003-1006.
- [6] DakoCytomation (1998) Application note guideline for determination of ceruloplasmin in serum/plasma on hitachi 911, **3**.
- [7] Buffone, G.J., Brett, E.M., Lewis, S.A., Iosefson, M., and Hicks, J.M. (1979) Limitations of immunochemical measurement of ceruloplasmin. *Clin Chem*, **25**, 749-51.
- [8] Hohbadel, D.C., McNeely, M.D., and Sunderman, F.W. (1975) Automated bichromatic analysis of serum ceruloplasmin. *Annals Clin Lab Sci*, **5**, 65-70.
- [9] Twomey, P.J., Viljoen, A., House, I.M., Reynolds, T.M., Wierzbicki, A.S., (2005) Relationship between serum copper, ceruloplasmin, and non-ceruloplasmin-bound Copper in routine clinical practice. *Clin Chem*, **51**, 1558-9.
- [10] Macintyre, G., Gutfreund, K.S., Martin, W.R., Camicioli, R., Cox, D.W. (2004) Value of an enzymatic assay for the determination of serum ceruloplasmin. *J. Lab. Clin. Med.* **144**, 294-301.

- [11] Hahn, S.-H., Jang, Y.-J., Lee, S.-Y., Shin, H.-C., Park, S.-Y., Yu, E.-S., and Han, H.-S. (2004) US patent 6,806,044 B2—Method of measuring ceruloplasmin concentration in a blood spot, kit and method of diagnosing Wilson's disease.
- [12] Newsome, D.A., Swartz, M., Leone, N.C., Hewitt, A.T., Wolford, F., and Miller, E.D. (1986) Macular degeneration and elevated serum ceruloplasmin. *Investig Ophthalmol & Visual Sci*, **27**, 1675-80.
- [13] Reunanen, A., Knekt, P., and Aaran, R.K. (1992) Serum ceruloplasmin level and the risk of myocardial infarction and stroke. *Amer J Epidemiol*, **136**, 1082-90.
- [14] Interpath Laboratory, Inc.
www.interpathlab.com/TechnicalUpdates/ceruloplasmin.htm
(Accessed November 2006)
- [15] Lopez-Avila, V., Robinson, W.H., and Sharpe, O. (2006) Determination of ceruloplasmin in human serum by SEC- ICPMS. *Anal Bioanal Chem*, **386**, 180-7.
- [16] Emons, H. (2005) Certificate of analysis ERM DA470, Institute for Reference Materials and Measurements, Geel, Belgium.
- [17] Baudner, S., Bienvenu, J., Blirup-Jensen, S., Calstrom, A., Johnson, A.M., Milford Ward, A., *et al.* (2005) Certification report – The certification of a matrix reference material for immunochemical measurement of 15 serum proteins, institute for reference materials and measurements, Geel, Belgium.
- [18] Hanzschel, H., Bird, H.A., Seidel, W., Kruger, W., Neumann, G., Schneider, G., and Wright, V. (1991) Polymyalgia rheumatica and rheumatoid arthritis of the elderly: A clinical, laboratory, and scintigraphic comparison. *Annals of the Rheumatic Diseases*, **50**, 619-22.
- [19] Lyngbye, J. and Kroll, J. (1971) Quantitative immunoelectrophoresis of protein in serum from a normal population: season-, age-, and sex-related variations. *Clin Chem*, **17**, 495-500.
- [20] Sontakke, A.N. and More, U. (2004) Changes in serum ceruloplasmin levels with commonly used methods of contraception. *Indian J Clin Biochem*, **19(1)**, 102-104.
- [21] Revnick, F. (1995) The significance of serum ceruloplasmin in diagnosis of rheumatoid arthritis, *Toxicol Lett*, **78(1)**, 70-71.
- [22] Musci, G., Bonaccorsi, di Patti, M.C., Fagiolo, U., and Calabrese, L. (1993) Age-related changes in human ceruloplasmin, *J Biol Chem*, **268(18)**, 13388-13395.

Appendix

List of Abbreviations:

Cp - ceruloplasmin

HPLC - high-pressure liquid chromatography

ICPMS - inductively-coupled plasma mass spectrometry

MI - myocardial infarction

NC - normal control

PE - pulmonary embolism

RA - rheumatoid arthritis

SLE - systemic lupus erythematosus

CREST- form of systemic sclerosis

ERM - European Reference Materials

Non-invasive foetal heartbeat rate extraction from an underdetermined single signal

Ranjan Acharyya¹, Neil L Scott¹, Paul D Teal²

¹Industrial Research Ltd, Wellington, New Zealand; r.acharyya@irl.cri.nz, n.scott@irl.cri.nz

²Victoria University of Wellington, Wellington, New Zealand; mailto:paul.teal@vuw.ac.nz

Received 17 June 2009; revised 20 July 2009; accepted 23 July 2009.

ABSTRACT

Extraction of foetal heartbeat rate from a single passive sound sensor on the mother's abdomen is demonstrated. The extraction is based on the assumption that a disjoint band of frequencies exist and foetal signal is concentrated in this band, and further that it can be represented conveniently as a set of wavelet coefficients. The algorithm has been applied to each stream of data obtained from six different channels and the detection performance is elaborated. The algorithm has also been tested on signals from non-pregnant abdomens to show successful rejection of adult heartbeat. The extraction of the desired signal is done in two stages so as to eliminate components from the maternal heartbeat.

Keywords: Underdetermined System; Foetal Heartbeat Rate; Wavelet, Blind Source Separation; Non-Invasive; Passive.

1. INTRODUCTION

Monitoring of foetal heartrate using a non-invasive technique is still a challenging problem with a variety of approaches [1,2]. Usually, foetal heartbeat is monitored using a Doppler ultrasound device which transmits ultrasonic sound waves into the uterus. Most researchers consider that the power used in these devices is perfectly safe, although there are some exceptions [6]. In many cases women prefer that ultrasound is not used on them. Detailed motivation for development and use of accurate, non-invasive techniques for monitoring the foetal heart is covered in the excellent introduction of [1]. This paper describes a method for detection of the foetal heart with a passive acoustic monitoring device (PAM). The process involves collection of signals with microphones and subsequent signal processing.

The passive monitoring of foetal heartrate may be

considered as one class of Blind source separation (BSS) problem, which has been an active research area for several decades now. It refers to the problem of estimating the original sources from a mixture. In most cases the mixing system and the number of sources are unknown. Sensors placed on the maternal abdomen provide signals which are mixtures of an unknown number of sources and the nature of the mixing is also unknown. In this section a quick review of other techniques and overview of the technique of this paper is given.

Independent Component Analysis (ICA) is a technique to obtain statistically independent components from a mixture and a solution technique for BSS problems. One way to categorise BSS problems is based on the number of sensor and source signals. Three different scenarios are, the number of sensors are greater than, equal to or less than the number of sources. The third case, which is equivalent to solving for an underdetermined system or for an overcomplete basis, resembles the problem at hand. Detail and an in-depth analysis of algorithms can be found in [3,4,5]. A well known algorithm for sparse sources is known as DUET (degenerate unmixing estimation techniques) [5], which does time-frequency masking. The applicability of the algorithm depends on a W disjoint orthogonal [5] condition of the sources and availability of at least two sensor signals.

Extraction of foetal heartrate using ICA [7] has been attempted in [8] and some interesting results were obtained. In this paper a new algorithm is developed based on certain assumptions on the foetal heartbeat signal. This paper is an extension of an earlier work [9] demonstrating estimation of the foetal heartrate by frequency masking. A crucial difference of this paper compared to [9] is that it avoids filtering of the signal in the time domain. Filtering in the time domain was done in [9] to suppress the maternal heartbeat. The issue of suppressing the maternal signal in the overlap region is addressed in this paper by performing the filtering in two steps. In addition to filtering in the frequency domain the resolution of the signals is enhanced by using a wavelet transformation. The process is discussed in detail in later sections. The method described in this paper requires only

one mixture provided the sources satisfy certain conditions.

The work reported in [10,11] using SCICA (single-channel independent component analysis) is perhaps the closest to this work in its assumption of disjoint frequency bands for the noises in the mixtures.

In Section 2, the experimental setup and the sensor structure is shown. The assumptions on the sources are explained in Section 3. In Section 4 the algorithm is discussed in detail. Results of the application of the algorithm to a mixture of signals from a pregnant maternal and a non-pregnant abdomen is elaborated in Section 5. Finally, in Section 6 the conclusion and future work are discussed.

2. EXPERIMENTAL SETUP

The sensor is similar to that described in [9] which was designed for work using multiple sensors. The sensor structure array is an array of 16 piezo film (PVDF, Polyvinylidene Fluoride) contact microphones of type CM-01B in a mat placed against the mother's abdomen. Use of the existing 16-sensor array allowed recording multiple channels simultaneously, although the algorithm proposed here uses only a single sensor signal. The signals are conditioned in a 16 channel low noise amplifier with band pass filtering (7.2 – 130Hz) and then recorded in a data logger. **Figure 1** shows the block diagram of the Passive Acoustic Monitor (PAM) and **Figure 2** the complete sensor array.

3. ASSUMPTIONS ON SOURCES

The model is that the sensor signal is a mixture of signals from multiple sources including foetal heartbeat, maternal heartbeat, other noises internal to the mother's abdomen and external noises from the environment. In addition the mixing system seems to vary with time. The most important assumption is that sound from the foetal heart is band limited and part of the band is isolated from the other sources, including maternal heartbeat. In other words, sources do not share the whole band of the foetal heart beat sound. This conclusion is motivated by the assumption that the characteristics of sound have direct relation to the size of the object generating the sound. The foetal heart is considerably different in size from the maternal heart or any other sound sources inside the maternal abdomen. However, it is expected that there may be overlap of the frequency band of the foetal heart and the maternal heart beat. The maternal heart beat is considered to be the strongest noise present with respect to the desired signal. In addition to being band limited the foetal heartbeat sound is also expected to be compact in the time domain. This implies the signal is assumed to be absent for short periods between heartbeats. Hence, application of wavelet transformation to

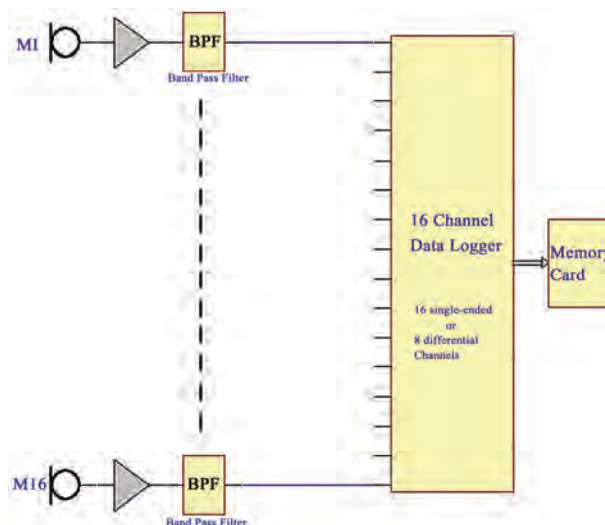


Figure 1. Block diagram of Passive Acoustic Monitor (PAM).

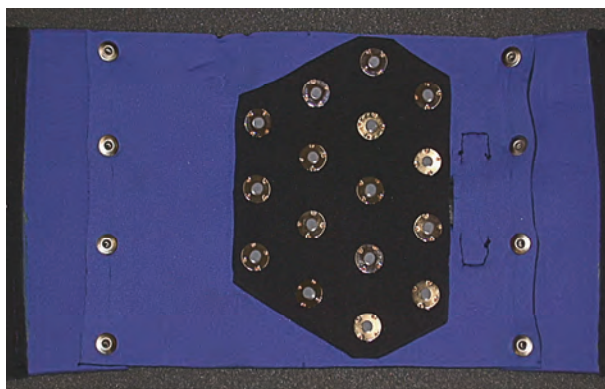


Figure 2. The 16 channel sensor array.

the signal is expected to enhance detection of the heartbeat. The effect of the wavelet transformation will be shown in the next section.

There are further assumptions on the energy content of the signal. In each data block, after initial processing the energy of the processed data in the foetal band needs to be more than a specified threshold value. This is essential to reduce the risk of accepting the adult heartbeat as the foetal one. The energy of the foetal heartbeat needs to be more than a specified threshold value at two different stages. This has a disadvantage that if the signal strength of the foetal heartbeat is very weak then the algorithm can fail to detect it at any particular time. It has been observed that the foetal heartbeat sound is location dependent and it is strong at a certain portion of the maternal abdomen; the strength of the signal is not equal at every point on the abdomen. Further the position where the signal is strongest may vary from time to time.

4. DETAILS OF THE ALGORITHM

The algorithm has been developed to exploit the beha-

viour of the signals given the assumptions mentioned above. The mixture signal obtained from an acoustic sensor is subjected to filtering in both the frequency and wavelet domains. The procedure is an extension of the process discussed in [9], where both maternal and foetal heartbeat were extracted. The algorithm developed here can be extended to extract the maternal heartbeat as well although it is not required for estimation of the foetal heart rate. First, we describe the components of the algorithm and then provide a step by step algorithm description.

The first filtering step is performed in the frequency domain. The spectrum of the mixture signal is multiplied by a profile derived from a Gaussian mixture before inverse Fourier transform. The procedure to derive the profile of the mixture of the Gaussians is as in [9]. The Gaussian mixture so obtained is then modified such that

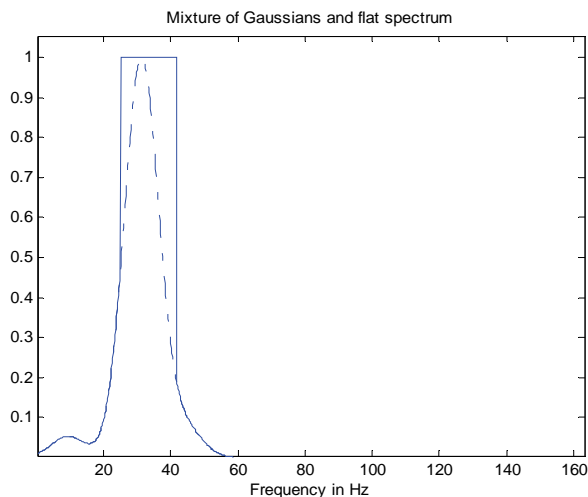


Figure 3. The solid line is mixture of Gaussian and the dashed line is the derived one.

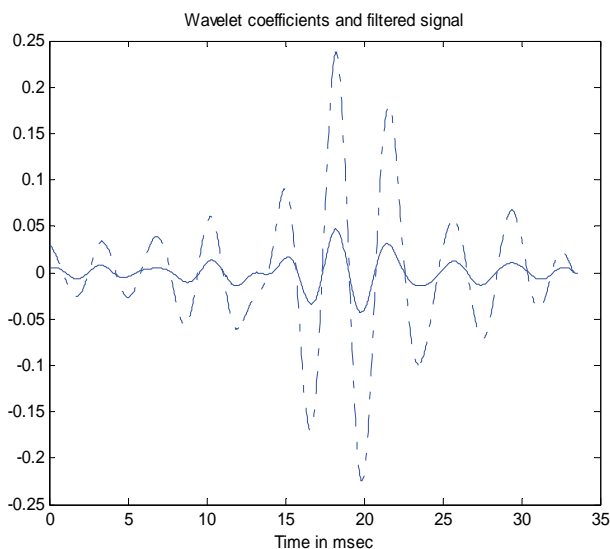


Figure 4. Comparison between filtered signal and its wavelet coefficients (dashed).

a range of values around the peak of the mixture are set to unity. This makes the frequency profile flat around the middle portion. The reason for this modification is that the peak energy frequency bin may vary from foetal heart to heart or it may fluctuate from beat to beat.

Therefore a general form of frequency profile in the first stage of filtering seems to be more appropriate. **Figure 3** shows the frequency profile derived in [9] and the profile that is utilized in this paper. The mixture signal is filtered by this derived spectrum.

After filtering, the energy of the signal is compared to the energy of the signal prior to filtering. The filtered signal must meet the energy criterion which is set by a specified threshold value, in order to proceed to the next stage of processing, which is carried out for the portions of signals which are expected to have a foetal heartbeat.

Next, a stationary wavelet transform (SWT) of type Discrete Meyer as defined in MATLAB, is applied to the signal. The number of coefficients in each level of stationary wavelet transform has the same number of samples as the original signals. The approximate coefficients of the 5th level are considered [12]. **Figure 4** shows a small block of the filtered signal and the corresponding 5th level wavelet coefficients.

As can be seen in the figure, the portion where the foetal heart beat is expected i.e. higher energy portion of the signal is inflated. Next, the locations of the foetal heartbeat in a block are estimated by determining the peaks of the energy of the wavelet coefficients. The algorithm should detect the peaks corresponding to each heartbeat. Often the change of sign of the derivative is used for detecting a peak. However, the foetal heart signal is essentially oscillatory in nature, each heartbeat event includes several oscillation peaks hence, the change of sign of the derivative would return many peaks which are not of interest. To get rid of this problem the change of sign of derivative algorithm is applied twice. An algorithm returns the first peak estimator as the points of change of sign of the derivative. The same algorithm is then applied to the absolute values of the set of first peaks to determine the overall peak estimates. **Figure 5** shows the peaks detected by the algorithm in the first and second stages. The arrows mark the final peaks detected by the algorithm. The two stage peak detector is an alternative to the other peak estimation methods that require a strict threshold value.

The peaks obtained from the second stage are close to the actual maxima, as observed by eye.

The signal around the peaks so selected is expected to be made up of foetal heartbeat signal. At this stage a few peaks may remain from maternal heartbeats. Next, the signal is multiplied by a window function around the peak values. The window function is shown in **Figure 6**. The purpose of this window function is to attenuate all other sources near the desired foetal heartbeat. Emphasis may be given to the point that the objective of this paper is to recover the foetal heartbeat *rate* rather than the

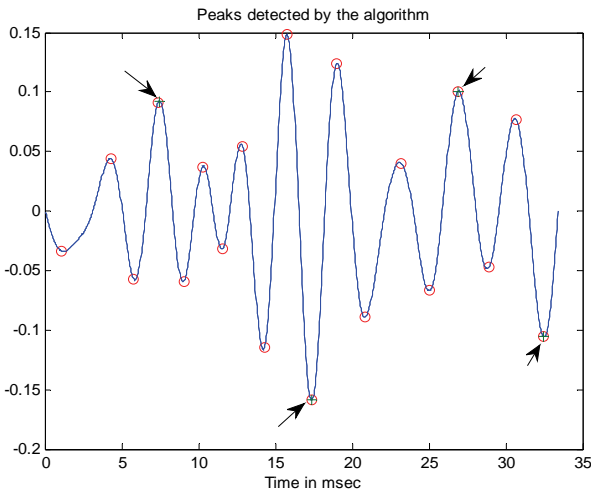


Figure 5. The 'o' are the peaks obtained first and arrow shows the accepted peaks.

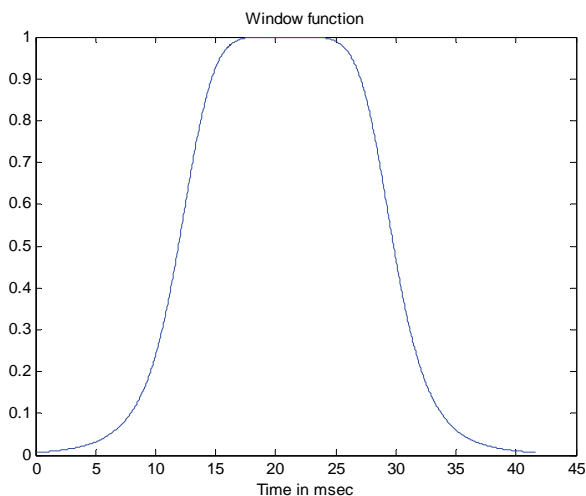


Figure 6. Window to multiply the time domain signal.

waveform. The use of the window function may change the actual waveform of the foetal heartbeat but it is expected not to affect the foetal heartbeat rate. This ends the first stage of the algorithm.

The signal obtained after applying the window function is subjected to another filtering step in the frequency domain. The spectrum of the signal is once again multiplied by a profile derived from a set of Gaussians before inverse Fourier transformation. These new set of Gaussians are obtained in the same way as before [9]. However, the band of the spectrum is shifted towards higher frequencies. For example if the frequency range of the mixture of Gaussians were 15 to 45 Hertz earlier the derived frequency range would be from 30 to 60 Hertz. The motivation for this shifting is to pass the signals which have only foetal heart beat. As mentioned before, the lower part of foetal spectrum overlaps with the maternal heartbeat spectrum. The second step is expected to minimize the energy in the overlap and hence the con-

tribution from the maternal heartbeat. To remove the maternal part this second step of filtering is performed. The maternal heartbeat is much stronger than the foetal one and hence this type filtering helped recover the foetal signal from the noise floor. Similar to the previous step, the filtered signal must meet an energy criterion which is set by a specified threshold value, in order to consider it to be a foetal heartbeat. In the final steps the signal is passed through a peak detector twice (like the previous step) so that only those parts of the signal with relatively large peaks can be considered as foetal heartbeat.

The complete steps of the algorithm are given below:

- The data is divided into equal sized blocks. Each of which is filtered by the following steps. In our case the block size is 14400 samples; 6 seconds of data at the sampling frequency 2400 samples per second.
- Multiply in the frequency domain the block of data by the mixture of Gaussians derived as in [9] with flat all pass section at mid band.
- Check the energy content of small blocks of contiguous 2000 samples and compare the ratio of total energy before and after filtering. If a block has a ratio of the energy, after and before filtering greater than the threshold value of 0.005 the block is accepted for the next step of processing. A small block of 2000 samples is chosen instead of 14400 samples so the a whole block of 6 sec data is not lost.
- Perform a stationary wavelet transform and retain the approximate coefficients (low pass filtered part) of level 5 for further processing. The Discrete Meyer wavelet is utilized.
- Find the peaks of each block by passing data through a peak detector twice. The peak detector is based on the change of sign of the derivative of the signal. The peak detector output is passed on if it exceeds the specified threshold value of 0.0067.
- Multiply the frequency content of the block of data with the spectrum derived from the mixture of Gaussians with flat all pass in the mid band.
- Window the signal with a 1000 sample window about each peak.
- Multiply the frequency content of the block of wavelet coefficients with the mixture of Gaussians and perform an inverse Fourier transform.
- Check the energy content of small blocks of wavelet coefficients of 2000 samples and compare the ratio of total energy before and after filtering. If a block has a ratio of the energy of the signal after and before filtering is greater than the threshold value of 0.1 the block is accepted for the next step of processing.
- Find the peaks of each block by passing data through a peak detector twice. Pass all peaks exceeding a specified threshold value of 0 .02.
- Count the number of peaks per minute to find the heart beat rate.

- Multiply the signal with a window of 1000 samples so that only selected portions of the energy are kept to produce an audible confidence signal.

5. RESULTS

The algorithm was applied to four different datasets. Two sets of data came from pregnant women and two from non-pregnant abdomens. The purpose was to verify that the algorithm can detect foetal heartbeat while not falsely detecting a heartbeat when none is present. Data sets were collected with equipment comprising either 6 or 16 sensor. The sensor elements are identical while the 6-sensors equipment samples at 2400 data samples per second and the 16-sensor at 300 samples per second. Data sets were regularized by decimating the 2400 data to 300. As the Gaussian mixture algorithm was designed for 2400, both data types were then up-sampled to 2400 samples per second. It has been observed that the foetal

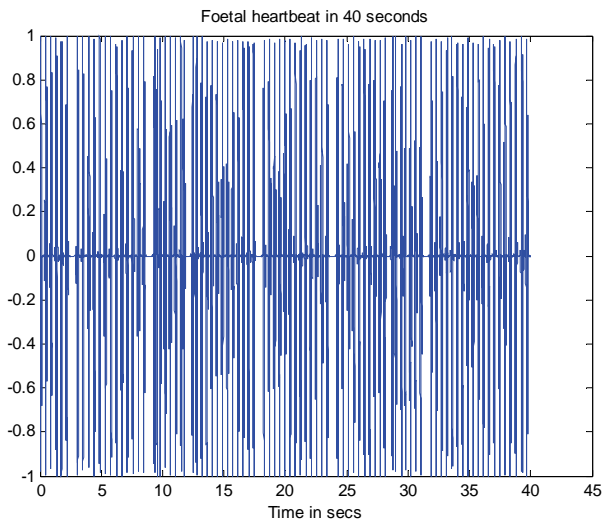


Figure 7. Foetal heartbeat for 40 seconds.

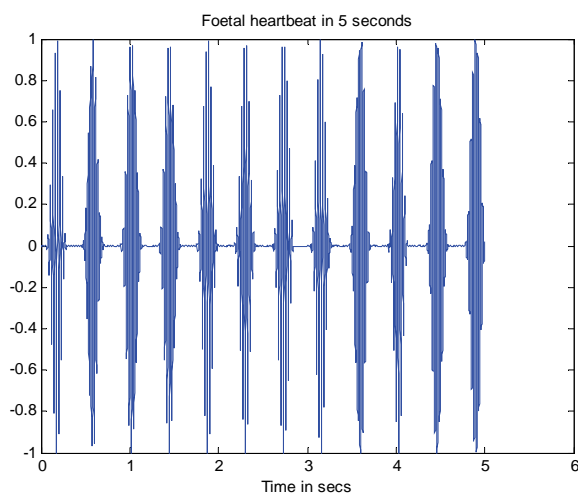


Figure 8. Foetal heartbeat for 5 seconds.

heart beat sound is prominent at one sensor at a time. This has been noticed in two different sets of data.

Figures 7 and 8 show the foetal heartbeat for a period of 40 seconds and 5 seconds respectively. In the 40 second data one can observe that the foetal heartbeat sound has been missed a few times. From the signals illustrated, a heartbeat rate of 144 beats per minute can easily be estimated. A separate Doppler sensor used at the same time reported a rate between 135 and 160 beats per minute. Similar results were obtained from the other foetal data set.

Data were collected from non-pregnant abdomens for a total of 10 minutes being 5 minutes each from two people. There were 16 channels and altogether the total number of adult heartbeats expected was 11520 assuming 72 heartbeat per minute. The number of false detections as foetal heart beat signal was 154 which is 1.3% of 11520. In addition the 154 falsely detected pulses were randomly scattered which indicated that they won't contribute significantly to the calculations of foetal heart rate.

6. CONCLUSIONS

It has been shown that foetal heartbeat rate can be extracted from a single microphone sensor non-invasively. The rejection of the adult heart rate by the algorithm is established. Future research will look into adjustment of the processing parameters adaptively. In addition the frequency profile of foetal heart beat may be adjusted adaptively.

REFERENCES

- [1] Varady, P., Wildt, L., Benyó, Z., and Hein, A. (2003) An advanced method in fetal phonocardiography, *Computer Methods and Programs in Biomedicine*, **71**, 283-296.
- [2] Kovacs, F., Torok, M., Habermajer, I. (2000) A rule-based phonocardiographic method for long-term fetal heart rate monitoring. *IEEE Trans. on Biomed. Eng.*, **47**(1).
- [3] Haykin, S. (2000) Unsupervised adaptive filtering, Vol 1: Blind source separation, Wiley.
- [4] Makino, S., Lee, T., and Sawada, H. (2007) Blind speech separation, Springer.
- [5] Yilmaz, O. and Rickard, S. (2004) Blind separation of speech mixtures via time frequency masking, *IEEE Transaction on Signal Processing*, **52**(7), 1830-1847.
- [6] Kieler, H., Cnattingius, S., Haglund, B., Palmgren, J., and Axelsson, O. (2002) Ultrasound and adverse effects, *Ultrasound in Obstetrics and Gynaecology*, **20**(1), 102-103.
- [7] Hyvarinen, A., Karhunen, J. and Oja, E. (2001) Independent component analysis, John Wiley & Sons.
- [8] Acharyya, R., Scott, N.L., Teal, P., Deuss, E., and Flierl, J. (2008) Signal separation for non-invasive monitoring of foetal heartbeat, *BioMedical Engineering and Informatics*.

- [9] Acharyya, R. and Flierl, J. (2008) Blind source separation by time frequency masking of an underdetermined system, *International Conference on Bioinformatics and Biomedical Engineering*.
- [10] Jimenez-Gonzalez, A. and James, C.J. (2008) Blind source separation to extract foetal heart sounds from noisy abdominal phonograms: A single channel method, *4th IET International Conference on Advances in Medical, Signal and Information Processing, MEDSIP'08*.
- [11] Jiménez-González, A., James, C.J. (2009) Extracting sources from noisy abdominal phonograms: A single-channel blind source separation method, *Medical and Biological Engineering and Computing*, **47(6)**, 655-64.
- [12] Strang G. and Nguyen, T. (1997) *Wavelet and filter banks*, Wellesley-Cambridge Press.

Comparison between static and dynamic warm-up exercise regimes on lower limb muscle power

Jose Shelton¹, G. V. Praveen Kumar²

¹Victoria University, Melbourne, Australia; josenoel2008@gmail.com

²School of Biotechnology, Chemical & Biomedical Engineering, VIT University, Vellore, India; gidi99_5611@yahoo.co.in

Received 26 April 2009; revised 17 May 2009; accepted 10 June 2009.

ABSTRACT

Aim: The purpose of this study was to compare static and dynamic warm-up regimes on lower limb muscle power and thereby the performance of the individual. **Methodology:** Twenty eight (28) subjects were assigned into groups consisting of 2 members. From each group, 1 subject performed the static stretching and the other subject performed dynamic stretching as warm-up. This was followed by non-counter movement jumps on a force platform and the vertical jump heights were recorded. Data were analysed using one-way ANOVA and paired t-test at 0.05 alpha. **Result:** The results showed that dynamic stretching as warm-up causes significant increase ($p=0.01$) in the vertical jump height as compared to static stretching ($p=0.03$). **Discussion:** The increase in vertical jump height could be related to the increase in force production which plays an important role during the vertical jump test. On the other hand the decrease in vertical jump height following static stretching could be attributed to a decrease in the force production in the muscles. **Conclusion:** Dynamic warm-up increases the vertical jump height, whereas static stretching decreases the jump height of the athlete.

Keywords: Static Stretching; Dynamic Stretching; Force Production; Post Activation Potentiation

1. INTRODUCTION

The primary aim of exercise physiologists, personal trainers, bio-mechanical engineers and sports scientists is to monitor and increase the performance levels of the athletes under their training. When it comes to training and prescribing exercises, there is always a debate between the types of stretching that are being used as warm up before activity. This could also be used to check the performance of the athlete owing to the particular type

of stretching.

Static stretching involves holding the muscle in the stretched position for some time. This type of stretching has been used as a traditional method of warm up as well as performance enhancement for quite some time now. But research performed by Rosenbaum and Hennig (1995) [1], shows that static stretching decreases peak force by 5% and rate of force production by 8%, thereby actually decreasing muscle strength. Static stretching of calf, hamstrings and quadriceps reduces the peak vertical velocity of a vertical jump according to studies done by Knudson *et al.*, 2000 [2]. Studies done by Kokkonen *et al.*, 1998 [3], have documented a rather harmful effect of acute static stretching, that it actually decreases the performance of those tasks where success is related to maximal force development. Further studies by McNeal and Sands, 2003 [4], with younger populations have also illustrated impairment in jumping performance in teenagers following static stretching.

Dynamic stretching consists of functional based exercises which use sport specific movements to prepare the body for movement. It consists of controlled leg and arm swings that are taken gently to the limits of range of motion. Studies done by Fredrick G. A., 2000 [5] have shown the effectiveness of dynamic stretching, as this increases core temperature, muscle temperature, elongates the muscles and stimulates the nervous system, thereby decreasing the chances of injury. Faigenbaum *et al.*, 2005 [6] studied dynamic warm-up versus static stretching in different age groups and a variety of athletes. And found that compared to static stretching, dynamic warm up increases flexibility and also improved performances among children for vertical jump. Long-jump performance also improved in the dynamic warm-up. Studies by Duncan M. J. and Woodfield L. A., 2006 [7] suggest that there may be some advantage to performing a low to moderate dynamic warm up protocol prior to activities that require high power outputs.

The purpose of this study is to find out which type of stretching exercise used as warm-up affects lower limb muscle power and therefore affects performance of an individual.

2. METHODOLOGY

2.1. Subjects

Twenty eight moderately trained subjects (16 male and 12 female) ranging in the age group of 20 to 35 years were taken for the study. They were randomly divided into groups consisting of 2 members. From each group, one subject performed the static stretching and the other subject performed the dynamic stretching as part of the warm up.

2.2. Procedure of Data Collection: Baseline Measurement

Both the groups performed an initial non-counter movement jump with both hands on the hips on a force platform and the vertical jump height was recorded.

The subjects in both the groups were made to jog 12 laps (up to 60% VO₂ max) up and down in the corridor after which the heart rate (Carotid artery) was recorded. Then they performed the first non-counter movement jump on the force platform and the vertical jump heights were recorded.

2.3. Stretching Protocol

The static stretching group subjects actively performed some static calf, hamstrings, quads, gluteal and hip flexor stretching exercises for 2 repetitions 30 seconds each, for both the legs.

While the dynamic stretching group subjects performed some dynamic stretching exercises like tip-toe walking, forward and backward leg swings, sagittal plane leg swings, walking knee pull ups, walking lunges with hip rotation and walking quads stretches for 2x10 repetitions for both legs.

2.4. Post Stretch Measurement

Then the second heart rate (Carotid artery) was recorded for both the groups. After which they performed the second non-counter movement jump on the force platform and the vertical jump heights were recorded. Then the subjects were asked to remain standing, without doing any activity for 10 minutes. Then they performed the third and final non-counter movement jump on the force platform and the vertical jump heights were recorded. Finally the vertical jump heights and heart rate readings for both the static and dynamic groups were recorded.

2.5. Data Analysis

Descriptive statistics of range, mean and standard deviation were computed on all data. One way ANOVA was calculated across the recording of both the groups. A paired t-test was computed to compare the static and dynamic stretching groups. Level of significance was set

at 0.05 alpha.

3. RESULTS

The mean and standard deviation of the jump heights of the subjects in both the static and dynamic stretching groups are shown in **Tables 1** and **2**.

The static stretching group showed a decrease of 0.61% in the final jump as compared to the dynamic

Table 1. Jump heights of the subjects in the static stretching group (N=14)

Subjects	Initial Jump	Jump I	Jump II	Jump III	HR I	HR II
n=1	0.139	0.184	0.138	0.175	104	96
n=2	0.174	0.164	0.186	0.202	128	100
n=3	0.134	0.108	0.123	0.152	180	128
n=4	0.086	0.145	0.127	0.137	172	126
n=5	0.132	0.132	0.107	0.141	168	88
n=6	0.288	0.331	0.309	0.293	152	100
n=7	0.265	0.208	0.149	0.183	138	102
n=8	0.255	0.309	0.28	0.291	144	88
n=9	0.124	0.223	0.205	0.21	150	100
n=10	0.176	0.201	0.193	0.158	92	64
n=11	0.15	0.216	0.18	0.158	140	94
n=12	0.084	0.083	0.055	0.047	132	96
n=13	0.345	0.345	0.203	0.233	144	92
n=14	0.149	0.171	0.192	0.206	150	112
AVG	0.172	0.201	0.174	0.184	142.42	99
STDEV	0.077	0.079	0.066	0.063	24.04	15.95

Table 2. Jump heights of the subjects in the dynamic stretching group (N=14).

Subjects	Initial Jump	Jump I	Jump II	Jump III	HR I	HR II
n=1	0.35	0.27	0.406	0.338	120	104
n=2	0.119	0.156	0.149	0.163	156	141
n=3	0.251	0.146	0.244	0.121	176	148
n=4	0.135	0.129	0.156	0.187	132	128
n=5	0.224	0.159	0.15	0.19	144	120
n=6	0.12	0.01	0.118	0.12	168	120
n=7	0.188	0.201	0.214	0.212	152	140
n=8	0.098	0.092	0.107	0.102	160	132
n=9	0.099	0.092	0.105	0.101	160	130
n=10	0.237	0.272	0.304	0.264	164	128
n=11	0.164	0.179	0.156	0.168	180	108
n=12	0.282	0.282	0.259	0.266	118	100
n=13	0.187	0.169	0.189	2	100	88
n=14	0.245	0.231	0.353	0.296	140	128
AVG	0.192	0.170	0.207	0.323	147.85	122.5
STDEV	0.075	0.077	0.094	0.488	23.46	17.09

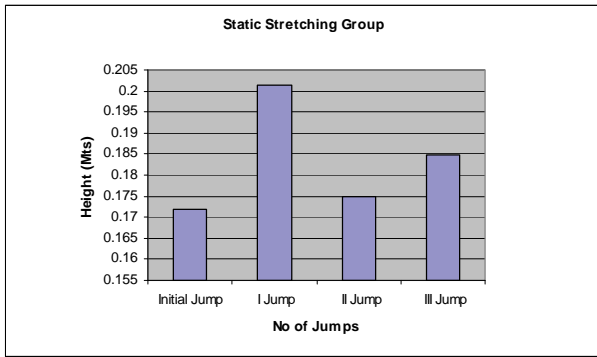


Figure 1. Graph showing the differences in vertical jump height in the static stretching group.

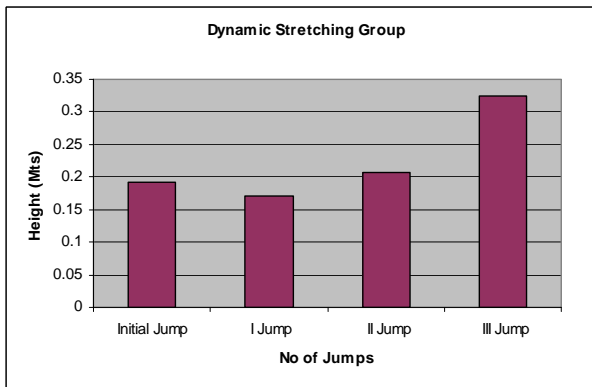


Figure 2. Graph showing the differences in vertical jump height in the dynamic stretching group.

stretching group which showed an increase of 13.06%, as shown in **Figures 1** and **2**.

4. DISCUSSION

As the result shows dynamic warm up can definitely increase the vertical jump height and therefore significantly influences fitness performance, as compared to the group that did static stretching as warm up. These findings are similar to the studies done by Duncan and Woodfield 2006 [7] and Faigenbaum *et al.*, 2005 [6] which show that dynamic stretching increases flexibility as well as muscle power.

Among the subjects who did static stretching, from **Figure 3**, we can see that there is a decrease in jump height between the first and second jumps. This shows that static stretching might actually reduce force production, which is similar to the studies done by Rosenbaum and Hennig, 1995 [1]. The main muscles involved in a vertical jump are the calf, quadriceps and hamstrings. These muscles were part of the static stretching protocol of the warm up. On the other hand, we can see an increase in the vertical jump height between second and third jumps, this change could be because of the ten minutes rest period in between the jumps. And this rest period would have given time for the muscles to recover

after the period of static stretching. This implies that static stretching actually causes a decrease in the force production in these muscles as also shown in the studies by Kokkonen *et al.*, 1998 [3] and Knudson *et al.*, 2000 [2]. Therefore the performance of the activity (vertical jump height) is also decreased as a result of static stretching which is also similar to the studies done by McNeal J. and Sands W., 2003 [4]. The reason for this decrease in performance could be attributed to an increase in the musculo-tendinous unit (MTU) compliance, leading to a decrease in the MTU ability to store elastic energy in its eccentric phase as reported by Fletcher IM, Jones B, 2004 [8]. The above evidences suggest that static stretching prior to activity is not the best solution. Static stretching does not necessarily lead to a decrease in injury but may actually decrease the force production and thereby decrease the vertical jump height for the athlete.

On the other hand we can see from **Figure 4**, there is a significant increase in the vertical jump height in the group that did dynamic stretching as part of the warm up, which is similar to studies done by Faigenbaum *et al.*, 2005 [6]. Studies by Duncan and Woodfield, 2006 [7] have suggested that performing pre-event dynamic warm up protocols may create an optimal environment for ex-

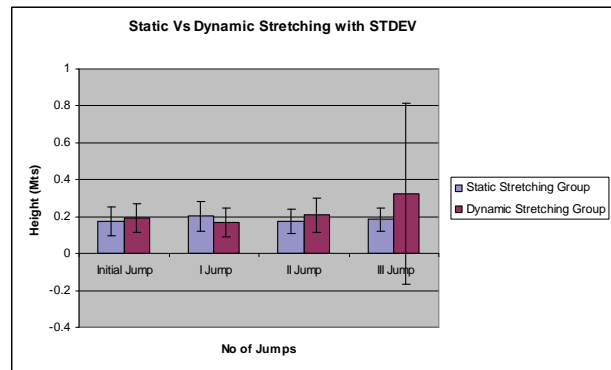


Figure 3. Graph showing the differences in vertical jump height between the static and dynamic stretching groups (Using AVERAGE +/- STDEV).

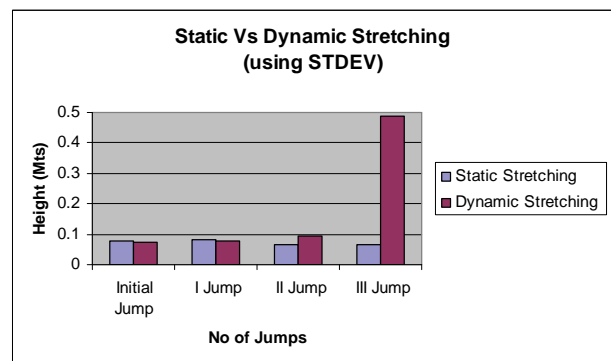


Figure 4. Graph showing the differences in vertical jump height between the static and dynamic stretching groups (Using STDEV values).

plosive force production by enhancing neuromuscular function. This occurrence has been termed the 'postactivation potentiation' (PAP) [9] and is believed to increase the rate of force development, thereby increasing speed and power production. This finding was similar to the study done by Faigenbaum *et al.*, 2005 [6]. Dynamic warm up activities used in the study may have influenced the excitability of fast twitch motor units and therefore readied these units to play a more significant role during the vertical jump test. However no tests of neuromuscular activation were performed in this study. Neuromuscular activation studies can be done in future to measure the excitability of fast twitch motor units. The results of the current study suggest that there may be some advantage to performing a low to moderate dynamic warm up protocol prior to activities that require high power outputs. And the increase in vertical jump height following dynamic warm up compared to static warm up is considerable.

Faigenbaum *et al.* 2005 [6] in his study also says that the evidence supporting the injury-reducing and performance-enhancing potential of static stretching is presently lacking. So it may be desirable to perform dynamic stretching during the warm up period and static stretching during the cool down. The purpose of warm up exercise is to warm-up the body, but static stretching seems to cause cool down of the body.

5. CONCLUSIONS

From the above study it can be concluded that the effect of dynamic stretching as warm up has the following benefits. Dynamic Stretching increase force production prior to activity, which in turn can improve the vertical jump height of the athlete.

As exercise physiologists and sports scientists our main objective is to decrease the injury levels and increase the performance levels of the athletes. And the above evidences from related literature suggest that dy-

amic stretching is the best type of stretching that can be performed during warm-up in order to increase the jump height of the athlete and to increase performance levels of the athlete. From the findings of the study in order to increase the vertical jump height of the athlete we can recommend a sports performance program that includes dynamic activities during warm up and static stretching as part of the cool down.

REFERENCES

- [1] Rosenbaum, D. and E. M. Hennig (1995) The influence of stretching and warm-up exercises on Achilles tendon reflex activity. *Journal of Sport Sciences*, **13(6)**, 481-90.
- [2] Knudson, D., Bennet, K., Corn, R., Leick, D., Smith, C., (2000) Acute effects of stretching are not evident in the kinematics of the vertical jump. *Research Quarterly for Exercise and Sport*, **71(1-Supplement)**, A-30.
- [3] Kokkonen, J., Nelson, A. G., Cornwell, A. (1998) Acute muscle stretching inhibits maximal strength performance. *Research Quarterly for Exercise and Sport*, **69**, 411-415.
- [4] McNeal, J. and Sands, W., (2003) Acute static stretching reduces lower extremity power in trained children. *Pediatric Exercise Science*, **15**, 139-145.
- [5] Frederick, G.A. (2001) Baseball part-1 dynamic flexibility. *Strength & Conditioning Journal*, **23(1)**, 21-30.
- [6] Faigenbaum, A.D., Bellucci, M.A., Bernieri, A, Bakker, B., Hoorens, K., (2005) Acute effects of different warm up protocols on fitness performance in children. *Journal of Strength & Conditioning Research*, **19(2)**, 376-381.
- [7] Duncan, M.J. and Woodfield, L.A., (2006) Acute effects of warm up protocol on flexibility and vertical jump in children. *Journal of Exercise Physiologyonline*, online, **9(3)**, 9-16.
- [8] Fletcher, I.M. and Jones, B., (2004) The effects of different warm up stretch protocols on 20metre sprint performance in trained rugby union players. *Journal of Strength and Conditioning Research*, **18(4)**, 885.
- [9] Sale, D., (2002) Postactivation potentiation: Role in human performance. *Exercise Sport Science Review*, **30(3)**, 138-143.

Pattern recognition of surface electromyography signal based on wavelet coefficient entropy

Xiao Hu, Ying Gao, Wai-Xi Liu

School of Mechanical and Electric Engineering, Guangzhou University, Guangzhou Higher Education Mega Center, Guangzhou, China; huxiaocz@163.com

Received 26 April 2009; revised 15 May 2009; accepted 21 May 2009.

ABSTRACT

This paper introduced a novel, simple and effective method to extract the general feature of two surface EMG (electromyography) signal patterns: forearm supination (FS) surface EMG signal and forearm pronation (FP) surface EMG signal. After surface EMG (SEMG) signal was decomposed to the fourth resolution level with wavelet packet transform (WPT), its whole scaling space (with frequencies in the interval (0Hz, 500Hz]) was divided into 16 frequency bands (FB). Then wavelet coefficient entropy (WCE) of every FB was calculated and correspondingly marked with WCE(n) (from the n th FB, $n=1,2,\dots,16$). Lastly, some WCE(n) were chosen to form WCE feature vector, which was used to distinguish FS surface EMG signals from FP surface EMG signals. The result showed that the WCE feature vector consisted of WCE(7) (187.25Hz, 218.75Hz) and WCE(8) (218.75Hz, 250Hz) can more effectively recognize FS and FP patterns than other WCE feature vector or the WPT feature vector which was gained by the combination of WPT and principal components analysis.

Keywords: Surface EMG Signal; Wavelet Packet Transform; Entropy; Pattern Recognition

1. INTRODUCTION

Due to its noninvasive measurement, surface EMG (SEMG) signal has been widely applied in many fields [1-3]. In this paper, the SEMG signal recorded from the skin surface over limb muscles in the process of the limb actions is called action SEMG (ASEMG) signal. Containing the electrical and functional properties of limb muscle contraction [4] and providing the information about the neuromuscular activity from which ASEM signal originates [5], ASEM signal has been widely

researched and used in rehabilitation and the controls of prosthetic devices for individuals with amputations or congenitally deficient limbs [6].

ASEMG signal is constituted by many motor unit action potentials (MUAPs) from many recruited motor units under surface electrode and noise [7]. There are three layers of tissues between motor unit and surface electrode: muscle layer, fat layer and skin layer [8]. The tissues introduce low-pass filter effect on MUAPs [9]. MUAPs from the motor units closer to surface electrode distribute in higher frequency band, and MUAPs from the motor units farther (deeper) fall in lower frequency band. The contributions of different muscles to the spectral energy distribution of ASEM signal are different, because some muscles influence on the high-frequency spectrum and other muscles influence on the low-frequency spectrum. Therefore, the spectral analysis may be an effective means for disclosing the electrical and functional properties of muscle contraction and obtaining the diagnostic information about muscles.

So far, many methods such as time-frequency distribution [5] have been used to analyze the spectral energy distribution of ASEM signal. However, due to its non-invasive measurement, there was still an obvious motivation to explore some more effective algorithms to extract the features from shorter surface EMG signal and to reduce the error identification rate.

This paper introduced a novel and simple algorithm based on wavelet transform. Firstly, SEMG signal was decomposed to the fourth resolution level with WPT, its whole scaling space (with frequencies in the interval (0Hz, 500Hz]) was divided into 16 frequency bands (FB). Secondly, WCE of every FB was calculated and correspondingly marked with WCE(n) (from the n th FB, $n=1,2,\dots,16$). Lastly, some WCE(n) were chosen to form WCE feature vector, which was used to distinguish FS surface EMG signals from FP surface EMG signals.

The following paragraphs were firstly to explain the scheme of acquiring surface EMG signal; then to introduce the method of calculating WCE feature vector and recognizing FS and FP pattern; lastly to analyze and discuss the research results.

2. SURFACE EMG SIGNAL'S ACQUISITION

All surface EMG signals were recorded by Metr-1-10UK (made by Mega Electronics Ltd) in the EMG room at Hua Shan Hospital in Shanghai, China. Because the power density function of SEMG signal outside the range from 5-10 Hz to 400-450 Hz has negligible contributions [10], the low cut-off frequency and the high cut-off frequency of Metr-1-10UK were set 5Hz and 500Hz respectively. The sampling frequency f_s was determined at 1000Hz. It was about 2cm between two measuring surface electrodes (diameter = 5mm) which were put on the skin surface over the pronator teres in the right forearm along the flexor. And the ground electrode (denoted the capital letter "G") was on the flexor carpi radialis and the palmaris longus (see **Figure 1** for their arrangement). The negative electrode (denoted by the symbol "-") was placed nearer subject's heart than the positive electrode (denoted by the symbol "+") to form a differential comparator amplifier.

During every acquiring process, every subject was instructed to do two different kinds of limb actions: forearm supination (FS) and forearm pronation (FP). The whole acquiring process was divided into three stages: preparing stage, acting stage and sustaining stage. At the preparing stage, every subject put his right forearm on the measure platform flatly and naturally (see **Figure 1 (b)**). At the acting stage, there were two cases: FP and FS. In the process of FP, the forearm was quickly transformed from the pose at **Figure 1(b)** to that at **(a)**, and in the process of FS, the forearm was quickly transformed from the pose **Figure 1(b)** to that at **(c)**. The whole process of FS or FP must be finished within 0.5 second. After finishing FS or FP, every subject kept the end condition of the limb actions for one or two seconds, the stage was the sustaining stage.

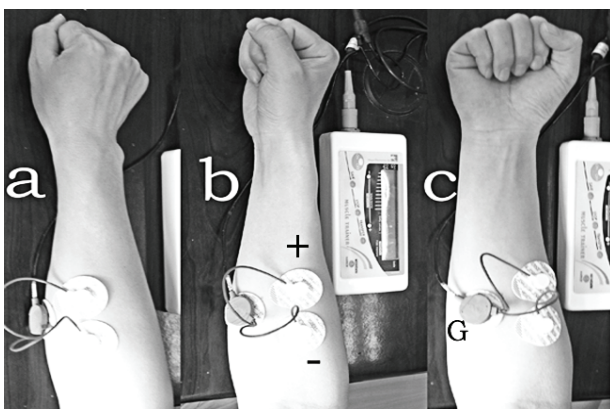


Figure 1. The forearm posture. (b): the forearm posture before forearm actions; (a) and (c) are respectively the posture after forearm pronation and forearm supination; +, -, G represent respectively the positive, negative electrodes and the ground.

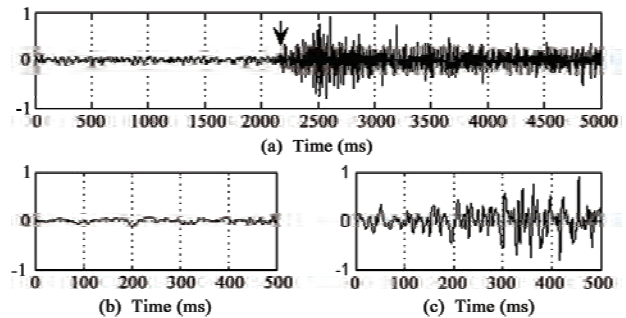


Figure 2. Raw surface EMG signal and its segments (a): Raw surface EMG signal; (b) and (c) are respectively the segments of the raw surface EMG signal on (a) at preparing stage and acting stage. The arrow on (a) points the start of the acting stage.

30 healthy subjects participated in study. Two sets of surface EMG signals (FS and FP) were respectively recorded from every subject's forearm flexor. **Figure 2** showed the wave of a set of recorded surface EMG signal. The arrow at **Figure 2** pointed to the start time of forearm action. The start time could be determined by an amplitude criterion [11]. A 50-points window slid along the surface EMG signal from left to right. At the same time, the number of the points above one threshold in the window was calculated. The first time when the number was above 10 was regarded as the starting time of forearm action.

After the start time of forearm actions and immediate to the start time, one 0.5-second surface EMG signal (500 samples) was segmented from every raw surface EMG signal, see **Figure 2(c)**. Thus, 60 segments of surface EMG signals obtained in all, there were two surface EMG signal patterns: FS and FP, 30 sets for each pattern.

3. WAVELET COEFFICIENT ENTROPY

Multiresolution analysis was first proposed in 1989 by Mallat [12]. Since then, the advanced research and development in wavelet analysis have applied in many fields such as signal processing and pattern recognition [13]. Wavelet packets were introduced by Coifman and Wickerhauser (1992) [14] as a generalized family of multiresolution orthogonal or biorthogonal basis. Unlike wavelet transform which is realized only by a low-pass filter bank, wavelet packet transform is implemented by a basic two-channel filter bank which can be iterated over either a low-pass or a high-pass branch. So the information in high frequencies can be analyzed as well as that in low frequencies in wavelet packet transform. As a result, finer frequency bands can be gained by wavelet packet transform than by wavelet transform. Therefore, WPT has been widely applied in biomedical signal analysis and many encouraging results have been obtained [15,16].

Given a finite energy signal, $s(t)$, whose scaling space

is assumed as U_0^0 , wavelet packet transform can decompose U_0^0 into small subspaces U_{-j}^n in dichotomous way.

The dichotomous way is realized by the following recursive scheme.

$$U_{-j-1}^n = U_{-j}^{2n} \oplus U_{-j}^{2n+1}, j \in Z; n \in Z_+ \tag{1}$$

where j is the resolution level and \oplus denotes orthogonal decomposition. U_{-j-1}^n , U_{-j}^{2n} and U_{-j}^{2n+1} are three close spaces corresponding to $u_n(t)$, $u_{2n}(t)$ and $u_{2n+1}(t)$. $u_n(t)$ satisfies the following equation [14]

$$\begin{cases} u_{2n}(t) = \sqrt{2} \sum_{k \in Z} h(k) u_n(2t - k) \\ u_{2n+1}(t) = \sqrt{2} \sum_{k \in Z} g(k) u_n(2t - k) \end{cases} \tag{2}$$

where the function $u_0(t)$ can be identified with the scaling function ϕ and $u_j(t)$ with the mother wavelet ψ . $h(k)$ and $g(k)$ are the coefficients of the low-pass and the high-pass filters respectively. The sequence of function $\{u_n\}$ ($n=0,1,\dots,\infty$), which is generated from a given function u_0 by (2), is called wavelet packet basis function. **Figure 3** shows the WPT tree.

When a finite energy signal, $s(t)$, is decomposed to the fourth resolution level ($j=4$) with wavelet packet transform, the whole scaling space U_0^0 with frequencies in the interval $(0, 2^{-1}f_s)$ is divided into 16 subspaces with frequencies correspondingly in the interval $((n-1)2^{-j-1}f_s, n2^{-j-1}f_s, n=1,2,\dots,16)$. The sub-signal at U_{-j}^{n-1} , the n th subspace on the j th level, can be reconstructed by

$$s_j^n(t) = \sum_k D_k^{j,n} \psi_{j,k}(t), k \in Z \tag{3}$$

where $\psi_{j,k}(t)$ is the wavelet function, $D_k^{j,n}$ was the wavelet packet coefficients at U_j^{n-1} and it is calculated by the recursive formula

$$\begin{cases} D_k^{j,2n} = \sum_{l \in Z} D_l^{j-1,n} h(l - 2k) \\ D_k^{j,2n+1} = \sum_{l \in Z} D_l^{j-1,n} g(l - 2k) \end{cases} \tag{4}$$

where, k is the k th wavelet packet coefficient at each subspace on the j th level, $k=1,2,\dots,K, K=500$ (samples) $/2^j$.

Thus, the finite energy signal, $s(t)$ can be reconstructed as

$$s(t) = \sum_{n=1}^{2^{-j}} s_j^n(t) = \sum_{n=1}^{2^{-j}} \sum_k D_k^{j,n} \psi_{j,k}(t) \tag{5}$$

After surface EMG signal $s(t)$ was decomposed into 16 FB by wavelet packet transform. The wavelet packet coefficient in the n th FB was assumed as

$$D_n = \{d_n(k), k = 1, 2, \dots, K\} \tag{6}$$

Here, k symbolizes time too. And then, these coefficient functions were assembled and normalized to a coefficient matrix.

$$D = \begin{Bmatrix} D_1 \\ D_2 \\ \dots \\ D_{2^j} \end{Bmatrix} = \begin{Bmatrix} d_1(1), d_1(2), \dots, d_1(K) \\ d_2(1), d_2(2), \dots, d_2(K) \\ \dots \\ d_{2^j}(1), d_{2^j}(2), \dots, d_{2^j}(K) \end{Bmatrix} \quad j=4 \tag{7}$$

After normalized, the values in coefficient matrix were within $[-1, 1]$. The interval $[-1, 1]$ was decomposed into M regions with identical size

$$[-1, a_1], [a_1, a_2], \dots, [a_{m-1}, a_m], \dots, [a_{M-1}, 1].$$

Supposed the number of $d_n(k)$ within $[a_{m-1}, a_m)$ was N , thus, a probability of the m th region could be calculated

$$p_n(m) = N / K. \tag{8}$$

WCE of the n th FB was

$$WCE(n) = - \sum_{m=1}^M p_n(m) \ln[p_n(m)] \tag{9}$$

Englehart K. (2003) [17] combined WPT and principal components analysis to get a WPT features. The WPT features could get much lower error identification rate than the features gained by conventional methods. So the WPT features were adopted to compare with WCE features in this paper.

The WCE features and the WPT features were respectively used to identify FP surface EMG signal and FS surface EMG signal, and the error identification rate with the increase of signal's sampling points was computed.

In order to effectively remove noise from SEMG signal, we should make the MUAPs from one muscle in charge of one kind of limb actions centralize on one

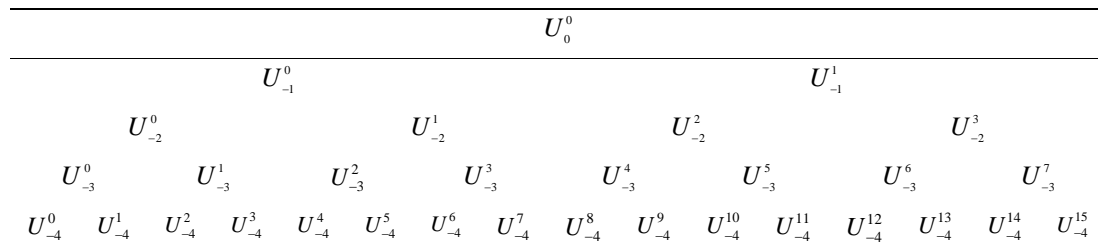


Figure 3. The tree structure of wavelet packet transform (U_{-j}^{n-1} shows the n th subspace the j th resolution level).

narrow frequency band as much as possible, rather than make them spread out over one wide frequency band. It is well known that the information carried by the coefficients of WPT depends on the joint characteristics of the analyzed signal and the selected wavelet function; the more similar are the two functions, the less spread are the significant coefficients in the time scale plane. Because Daubechies family of wavelet packets most seems to resemble MUAPs [18] and the simplest of these wavelets is db2, db2 is adopted as the mother wavelet. At the same time, Martha Flanders (2002) [18] pointed out that the length of the db2 at the forth level resolution was approximately the length of a MUAP.

4. THE ERROR DECISION RATE BASED ON BAYES DECISION

Let ω_1 and ω_2 be the two classes (FS and FP ASEMG signal patterns) to which our patterns belong. Feature vector x represents an unknown pattern. The Bayes rule is

$$P(\omega_i / x) = \frac{p(x / \omega_i)P(\omega_i)}{\sum_{i=1}^2 p(x / \omega_i)P(\omega_i)} \quad (10)$$

$p(\omega_i/x)$ is the i th conditional probability. $p(\omega_i/x)$ is the class-conditional probability density function, see the two curves at **Figure 3**. $p(\omega_i)$ is priori probability. In this paper, $p(\omega_1)=p(\omega_2)=1/2$.

The Bayes classification rule can be stated as

If $p(\omega_1/x) > p(\omega_2/x)$, x is classified to ω_1

If $p(\omega_1/x) < p(\omega_2/x)$, x is classified to ω_2

If the straight line at x_0 is the threshold partitioning the feature space into regions: R_1 and R_2 (see **Figure 3**), all values of x in R_1 are classified as w_1 , and all values of x in R_2 are classified as w_2 . It is obvious that decision errors are unavoidable. The total probability, P_e , of committing a decision error is given by

$$P_e = \frac{1}{2} \int_{-\infty}^{x_0} p(x / \omega_2) dx + \frac{1}{2} \int_{x_0}^{\infty} p(x / \omega_1) dx \quad (11)$$

which is equal to the total shaded area under the curves in **Figure 4**. So the error decision rate is calculated by

$$R_e = P_e \times 100\% \quad (12)$$

5. RESULT

Some WCE(n) were chosen to form WCE feature vector, which was used to distinguish FS surface EMG signals from FP surface EMG signals. It was found that the WCE feather vector consisted of WCE(7) (187.25Hz, 218.75Hz) and WCE(8) (218.75Hz, 250Hz) can more effectively recognize FS and FP patterns than other

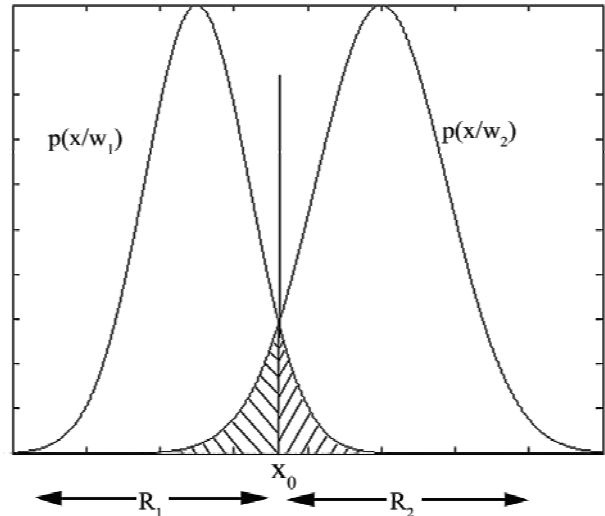


Figure 4. Example of the two regions R_1 and R_2 formed by the Bayesian classifier for the case of two classes. The straight line at x_0 is a threshold of R_1 and R_2 . $p(x/w_1)$ and $p(x/w_2)$ are respectively the class-conditional probability density function at regions: R_1 and R_2 .

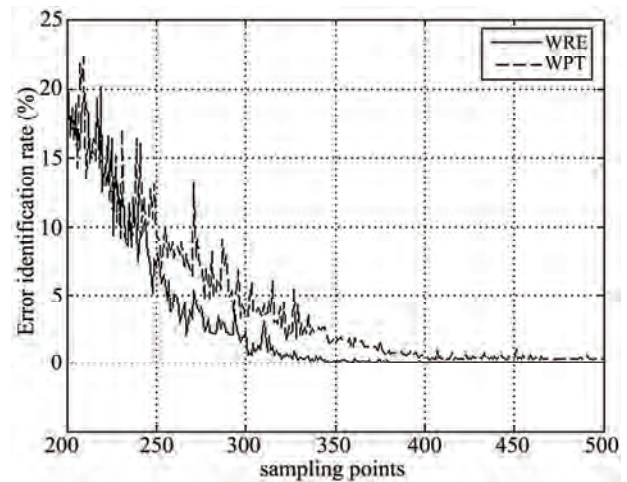


Figure 5. The error decision rate based on bayes decision VS the sampling points of initial signal.

WCE feature vector. Therefore, WCE(7) and WCE(8) were chosen to constitute a 2 dimensionality WCE feature. Based on Bayes decision, both WCE feature and WPT feature were employed to recognize FP and FS surface EMG signal. **Figure 5** depicted the error identification rate vs. initial signal sampling points. The curves on **Figure 5** were the real error decision rate to the sampling points. With the increasing of the sampling points, the signal undoubtedly included more and more feature information, so the error decision rate decreased with the increasing of the sampling points. However, from **Figure 5**, we found another result that the WCE feature performed better than the WPT feature. When the sampling points were between 200 and 500, the error decision rate by the WCE features was lower than by the

WPT features. Furthermore, when the sampling points was above 350, the error decision rate by the WCE features was almost 0.

6. DISCUSSION

In pattern recognition [19], a feature vector was insisted of some features. The number of the features in the feature vector was called as dimensionality. In general cases, whether one pattern of signal could be effectively and accurately identified depended much upon two important factors. One was a set of optimal features. A set of desired features not only contain the **characteristic information** which characterize one pattern of signals, but also ignore the **particular information**, which only existed in some individual signals or sometime might be the result of noisy measurements, and the **general information**, which exist in all pattern signals. From the results in this paper, both WCE feature and WPT feature could capture the characteristic information of one pattern of surface EMG signal.

In this paper, wavelet packet coefficients matrix D (see Eq.7) can be rewrote as a 16X63 matrix

$$D = \begin{bmatrix} d_1(1), d_1(2), \dots, d_1(63) \\ d_2(1), d_2(2), \dots, d_2(63) \\ \dots \\ d_{16}(1), d_{16}(2), \dots, d_{16}(63) \end{bmatrix}$$

Find some orthonormal matrix P in $Y = PD$ such that C_Y , the covariance matrix of Y , is a diagonal matrix.

$$C_Y = PC_D P^T = \begin{bmatrix} \lambda_1 & 0 & 0 & \dots & 0 \\ 0 & \lambda_2 & 0 & \dots & 0 \\ 0 & 0 & \lambda_3 & \dots & 0 \\ 0 & 0 & 0 & \dots & \lambda_{63} \end{bmatrix} \quad (13)$$

Here, the rows of P are the principal components of D . C_D is the covariance matrix of D . $\lambda_1 > \lambda_2 > \lambda_3 > \dots$

According to the following criterion, eight bigger λ_i form WPT feature vector.

$$TH = \frac{\sum_{i=1}^M \lambda_i}{\sum_{i=1}^{63} \lambda_i} > Threshold \quad (14)$$

When $M=8$, $TH > 0.934$. If $M \geq 9$, TH increase very weeny.

Obviously, WPT feature vector included the information about the whole frequency band (0Hz-500Hz).

At the other hand, the WCE features were got from only two narrower FBs, so the WCE features were rationally considered including less common information of surface EMG signal and noise than WPT features. The

other was dimensionality reduction. There was more than one reason for the necessity to reduce the number of features to a sufficient minimum [19]. Computational complexity was the obvious and important one. The computational complexity for pattern recognition was reduced as dealing with the features in a lower dimensional space. In this paper, WCE feature vector only needed two features, but in WPT feature vector, we used 8 features.

7. CONCLUSIONS

WCE was a more effective method to extract feature from surface EMG signal than the combination of WPT and principal components analysis. FS surface EMG signals could be successfully and rapidly distinguished from FP surface EMG signals by the WCE features.

8. ACKNOWLEDGEMENTS

The research was funded by the educational science program of Guangzhou during the 11th Five-Year Plan Period (No.07B171and 07B258) and Guangdong Natural Science Fund (No. 7301261).

REFERENCES

- [1] Stokes, I.A.F. (2005) Relationships of EMG to effort in the trunk under isometric conditions force-increasing and decreasing effects and temporal delays. *Clinical Biomechanics*, **20**, 9-15.
- [2] Wakeling, J.M. (2009) Patterns of motor recruitment can be determined using surface EMG. *Journal of Electromyography and Kinesiology*, **19**, 199-207.
- [3] Kaplanis, P.A., Pattichis, C.S., Hadjileontiadis, L.J., Roberts, V.C. (2009) Surface EMG analysis on normal subjects based on isometric voluntary contraction. *Journal of Electromyography and Kinesiology*, **19**, 157-171.
- [4] Lei, M., Wang, Z.Z., Feng, Z.J. (2001) Detecting nonlinearity of action surface EMG signal. *Physics Letters A*, **290**, 297-303.
- [5] Englehart, K., Hudgins, B., Parker, P.A., Stevenson, M. (1999) Classification of the myoelectric signal using time-frequency based representations. *Medical Engineering & Physics*, **21**, 431-438.
- [6] Hudgins, B., Parker, P., Scott, R.N. (1993) A new strategy for multifunction myoelectric control. *IEEE Trans. Biomed. Eng.*, **40**(1), 82-94.
- [7] Stashuk, D. (2001) EMG signal decomposition: how can it be accomplished and used? *Journal of Electromyography and Kinesiology*, **11**, 151-173.
- [8] Hu, X. and Wang, Z.Z. (2004) Detecting the motor unit action potential from surface EMG signals based on wavelet transform, 2004 IEEE International workshop on Biomedical circuits & system, S2, 6-15.
- [9] Farina, D. and Merletti, R. (2001) A novel approach for precise simulation of the EMG signal detected by surface electrodes. *IEEE Trans. Biomed. Eng.*, **48**(6), 637-646.
- [10] Merletti, R. and Torino, P.D. (1999) Standards for Re-

- porting EMG Data. *Journal of Electromyography and Kinesiology*.
- [11] Hu, X., Yu, P., Yu Q., Liu, W.X., Qin, J. (2008) Classification of Surface EMG Signal Based on Energy Spectra Change, 2008 International Conference on BioMedical Engineering and Informatics, 375-379.
- [12] Mallat, S.G. (1989) A theory for multiresolution signal decomposition: the wavelet representation. *IEEE Trans. Pattern Anal. Mach. Intell.*, **11**, 674-693.
- [13] Daubechies, I., Mallat, S., Willsky, A.S. (1992) Introduction to the special issue on wavelet transforms and multiresolution signal analysis. *IEEE Trans. Inform. Theory*, **38**, 529-531.
- [14] Coifman, R.R. and Wickerhauser, M.V. (1992) Entropy-based algorithms for best basis selection. *IEEE Trans. Inform. Theom*, **38**, 713-718.
- [15] Karlsson, S., Yu, J., Akay, M. (1999) Enhancement of spectral analysis of myoelectric signals during static contractions using wavelet methods. *IEEE Trans. Biomed. Eng.*, **46**, 670-684.
- [16] Flanders, M. (2002) Choosing a wavelet for single-trial EMG. *Journal of Neuroscience Methods*, **116**, 165 -177.
- [17] Englehart, K. and Hudgins, B. (2003) A robust, real-time control scheme for multi-function myoelectric control. *IEEE Trans. Biomed. Eng.*, **50(7)**, 848-854.
- [18] Flanders, M. (2002) Choosing a wavelet for single-trial EMG. *Journal of Neuroscience Methods*, **116**, 165-177.
- [19] Sameer, S., Nabeel, M., Walter, K. (2001) Advances in pattern recognition. *Springer*.